mgr Piotr Wojtyniak

Rola mitofuzyny 2 w uszkodzeniu i regeneracji komórek w modelach ischemii i reperfuzji mózgu.

Mitofusin 2 role in cell death and survival in brain ischemia-reperfusion models.

Rozprawa na stopień naukowy doktora
w dziedzinie nauk medycznych i nauk o zdrowiu
w dyscyplinie nauki medyczne
w formie monotematycznego zbioru publikacji

Promotor: Prof. dr hab. Barbara Zabłocka
Promotor pomocniczy: Dr Maria Kawalec

IMDiK
Polska Akademia Nauk

Obrona rozprawy doktorskiej przed Radą Naukową
Instytutu Medycyny Doświadczalnej i Klinicznej
im. Mirosława Mossakowskiego PAN

Warszawa, 2023

4

5

SPIS TREŚCI

8

WYKAZ SKRÓTÓW

CA1	region hipokampa wrażliwy na krótkotrwałe niedokrwienie mózgu
CA2-3, DG	regiony hipokampa mało wrażliwe na krótkotrwałe niedokrwienie mózgu
DND	opóźniona śmierć neuronów
Drp1	(*Dynamin related protein 1*) główne białko biorące udział w procesie fragmentacji mitochondriów
ER	siateczka śródplazmatyczna
ETC	łańcuch transportu elektronów
Hsp60	białko szoku cieplnego zlokalizowane w macierzy mitochondrialnej
I/R	model stresu niedokrwienno-reperfuzyjnego mózgu *in vivo*
LC3-I	białko związane z mikrotubulami
LC3-II	aktywna, lipidowana forma białka LC3
LDH	dehydrogenaza mleczanowa
L-Opa1	długa izoforma białka Opa1
MCAO	zamknięcie tętnicy środkowej mózgu
Mfn1	białko mitofuzyna 1
Mfn2	białko mitofuzyna 2
MPTP	megakanał mitochondrialny
mtDNA	mitochondrialne DNA
mTOR	białko docelowe dla rapamycyny występujące u ssaków
Nrf1	jądrowy czynnik transkrypcyjny 1
OGD	przejściowy brak tlenu i glukozy *in vitro*
Opa1	(*Optic atrophy 1*) białko odpowiedzialne za fuzję wewnętrznej błony mitochondrialnej
PARIS	białko substratowe dla parkiny
parkina	ligaza ubikwityny E3
PGC-1α	białkowy koaktywator receptorów aktywowanych proliferatorami peroksysomów 1α
PINK1	kinaza indukowana przez PTEN
ROS	reaktywne formy tlenu
shRNA	krótkie RNA o strukturze spinki do włosów

S-Opa1   krótka izoforma białka Opa1

SQSTM1/p62 (*Sequestosome-1*) białko adaptorowe w procesie autofagii

TEM   transmisyjna mikroskopia elektronowa

Tfam   mitochondrialny czynnik transkrypcyjny A

TIA   przemijający atak niedokrwienny

TOM20   białko, translokaza błony zewnętrznej o masie 20 kDa

$\Delta\Psi$m   mitochondrialny potencjał błonowy

STRESZCZENIE

Prawidłowe funkcjonowanie mitochondriów jest kluczowe dla wszystkich komórek ssaków, w tym dla neuronów, a w warunkach niedokrwienia i reperfuzji (I/R) mózgu może decydować o ich przeżyciu lub śmierci. Aktywność mitochondriów zależy od wielu procesów, wśród których szczególną rolę odgrywają zjawiska fuzji i podziału mitochondriów oraz eliminacji uszkodzonych organelli na drodze autofagii. Zapobiegają one nagromadzeniu uszkodzeń i sprzyjają utrzymaniu puli prawidłowych organelli. Ubytek mitochondriów może być natomiast uzupełniany na drodze ich biogenezy. Jednak szczegółowa rola tych kluczowych procesów oraz zależności pomiędzy nimi w przeżyciu neuronów po I/R nie jest w pełni poznana. Postawiono hipotezę, że mitofuzyna 2 (Mfn2), białko biorące udział w fuzji zewnętrznej błony mitochondrialnej, w neuronach w warunkach stresu może działać jako białko integrujące przebudowę sieci mitochondrialnej z mitofagią i biogenezą mitochondriów.

Zatem, głównym celem przeprowadzonych badań było poznanie roli Mfn2 w odpowiedzi neuronów na bodziec ischemiczno-reperfuzyjny ze szczególnym uwzględnieniem procesów odpowiadających za dynamikę sieci, zawartość i jakość mitochondriów (mitofagię i biogenezę mitochondriów).

Badania prowadzono w modelu *in vivo* przejściowego niedokrwienia mózgu suwaka mongolskiego, poddając analizie dwa obszary hipokampa: podatny (CA1) i oporny (CA2-3, DG) na epizod ischemiczno-reperfuzyjny oraz w modelu *in vitro* przejściowego niedoboru tlenu i glukozy (OGD) w hodowli pierwotnej neuronów kory mózgu szczura, prawidłowych (*wild type*) oraz z obniżoną ekspresją Mfn2.

Na podstawie przeprowadzonych badań wykazano, że w obszarze CA2-3, DG hipokampa w modelu *in vivo* oraz w hodowli neuronów prawidłowych *in vitro*, poischemiczne uszkodzenie mitochondriów jest naprawiane w pierwszej kolejności poprzez zwiększoną dynamikę sieci mitochondrialnej. Zaobserwowano nasilenie fuzji mitochondriów w odpowiedzi na bodziec i ich usunięcie za pomocą mitofagii, co ma miejsce w dłuższym czasie reperfuzji/reoksygenacji. Ponadto wykazano aktywację procesu biogenezy, objawiającą się m.in. zwiększeniem ilości białek kompleksów oddechowych. Jednocześnie istotnie przyrastała zawartość Mfn2, wobec czego sugeruje się, że Mfn2 jest niezbędna, aby opisane wyżej procesy mogły mieć miejsce i przebiegały prawidłowo.

Natomiast ubytek Mfn2, obserwowany w CA1 po epizodzie ischemiczo-reperfuzyjnym oraz obecny w neuronach o obniżonej ekspresji Mfn2, sprzyja znacznemu rozdrobnieniu mitochondriów. Co więcej, po epizodach I/R i OGD w neuronach obszaru CA1 oraz *in vitro* w neuronach o obniżonej ekspresji Mfn2, uszkodzenie mitochondriów było istotnie nasilone i nie obserwowano zwiększonej fuzji mitochondriów. Równolegle wykazano zwiększoną niespecyficzną autofagię (makroautofagię), która wystąpiła w krótkim czasie po niedokrwieniu/niedotlenieniu. W przeciwieństwie do neuronów obszaru CA2-3, DG oraz prawidłowych neuronów *in vitro* nie wykazano aktywacji procesu biogenezy mitochondriów. Taki typ odpowiedzi komórkowej nie ma charakteru neuroprotekcyjnego i w efekcie neurony CA1 *in vivo* ulegają opóźnionej degeneracji.

Zatem, przedstawione wyniki sugerują, że Mfn2 jest jednym z białek koniecznych do prawidłowej odpowiedzi neuronów na przejściowy bodziec niedokrwienno-reperfuzyjny, umożliwiającej ich przeżycie, poprzez regulowanie zależności pomiędzy eliminacją mitochondriów, a ich biogenezą. Zjawiska te mogą być elementami endogennej, naturalnej neuroprotekcji, która występuje w mało wrażliwych na krótkotrwały epizod ischemiczny regionach: CA2-3, DG i sprzyja przeżyciu neuronów w tych obszarach hipokampa.

SUMMARY

Proper mitochondrial functioning is crucial for the neuron and, under conditions of ischemia and reperfusion (I/R) can determine its survival or death. The activity of mitochondria depends on many processes, among which the phenomena of fusion and fission of mitochondria and elimination of damaged organelles by autophagy play a crucial role. These processes might prevent the accumulation of damaged mitochondria and support the maintenance of proper mitochondrial morphology and function. On the other hand, the loss of mitochondria can be supplemented by mitochondrial biogenesis. However, the precise role of these processes in the survival of the neuron after I/R and the relationships between them are not fully understood.

It has been hypothesized that mitofusin 2 (Mfn2), a protein involved in mitochondrial fusion, might integrate mitochondrial network remodeling with mitophagy and mitochondrial biogenesis in post-ischemic neurons. Therefore, the main aim of this study

12

was to investigate the role of Mfn2 in the neuronal response to ischemia-reperfusion injury, with particular focus on the mitochondrial network dynamics, mitochondrial content and quality.

Two experimental models were used. An *in vivo* studies were performed in the model of transient cerebral ischemia followed by reperfusion (I/R) in mongolian gerbils. Two areas of the hippocampus: ischemia-vulnerable (CA1) and ischemia-resistant (CA2-3, DG) were analyzed. Secondly, a primary culture of rat cortical neurons, wild type and Mfn2-knock down, were subjected to transient oxygen and glucose deprivation.

It was shown that in the CA2-3, DG neurons and wild-type neurons *in vitro*, post-ischemic damage of the mitochondria is initially repaired by the enhanced dynamics of the mitochondrial network. An increase in mitochondrial fusion and in mitochondrial elimination at later stage of reoxygenation have been observed. Furthermore, the activation of the mitochondrial biogenesis and subsequent increase in the amount of respiratory complexes proteins has been shown. Meanwhile, the content of Mfn2 increased significantly.

On the other hand, the reduction of the Mfn2 protein level, as observed in CA1 after I/R and induced in Mfn2-knock down neurons, promotes a significant fragmentation of mitochondria. In CA1 neurons after I/R episode and in Mfn2-knock down neurons after OGD mitochondrial damage was significantly enhanced. An increased mitochondrial fusion was not observed. In parallel, an increased macroautophagy has been demonstrated shortly after the insult. In contrast to the hippocampal CA2-3, DG *in vivo* and wild-type neurons *in vitro*, activation of mitochondrial biogenesis was not observed. This type of cellular response is not neuroprotective and, as a result, CA1 neurons *in vivo* undergo delayed degeneration.

Thus, presented results suggest that Mfn2 is one of the key proteins conditioning pro-survival response of neurons to transient ischemic injury, enabling their survival, by regulating the relationship between mitochondrial elimination and biogenesis. These phenomena might contribute to the mechanism of the endogenous neuroprotection observed in CA2-3, DG and promote neuronal survival in these areas of the hippocampus.

13

14

INNOWACYJNOŚĆ ROZPRAWY

Rozprawa dotyczy procesów dynamiki (fuzji i podziału), usuwania i biogenezy mitochondriów w modelach *in vivo* i *in vitro*, a jej oryginalność i nowatorstwo wynikają z przedstawienia danych doświadczalnych na poparcie koncepcji o występowaniu zależności pomiędzy tymi procesami w modelach przejściowego niedokrwienia mózgu. Co więcej, praca proponuje Mfn2 jako jedno z kluczowych białek regulujących zależność pomiędzy dynamiką, eliminacją i biogenezą mitochondriów w kontekście przeżycia neuronów w odpowiedzi na przejściowy bodziec niedokrwienny, co nie zostało opisane do tej pory. Po raz pierwszy pokazano następujące zależności:

- Uszkodzenie mitochondriów poprzedza zmiany morfologiczne oraz śmierć neuronów wywołane przejściowym bodźcem ischemicznym.

- Zwiększoną dynamikę sieci mitochondrialnej, aktywację mitofagii i biogenezy po krótkotrwałym niedokrwieniu i reperfuzji mózgu *in vivo* w obszarach CA2-3, DG hipokampa, w przeciwieństwie do sektora CA1. Postresowa aktywacja tych procesów może promować względną oporność rejonów CA2-3, DG na bodziec niedokrwienno-reperfuzyjny.

- Skutkiem eksperymentalnego obniżenia ekspresji Mfn2 w neuronach jest nasilenie autofagii, zahamowanie biogenezy mitochondriów i zwiększone uszkodzenie neuronów w odpowiedzi na przejściowy brak tlenu i glukozy w modelu *in vitro*.

Niniejsza rozprawa poszerza wiedzę na temat mechanizmów wewnątrzkomórkowych sprzyjających naprawie mitochondriów, co jest konieczne do przeżycia neuronów po bodźcu ischemiczno-reperfuzyjnym i wykazuje, że białko Mfn2 jest ich ważnym elementem.

16

WSTĘP

Udar mózgu jest istotnym problemem klinicznym. Chociaż właściwe zarządzanie czynnikami ryzyka naczyniowego i coraz częstsze stosowanie środków profilaktycznych od lat 70 do początku XXI wieku spowodowało roczny spadek częstości występowania udarów mózgu o 1–1,5% w krajach rozwiniętych [1] to jednak schorzenie to nadal jest trzecią przyczyną niepełnosprawności fizycznej i intelektualnej dorosłych, i pozostaje drugą przyczyną śmierci w krajach rozwiniętych. Co więcej, rosnąca częstość występowania cukrzycy [2] i otyłości [3] wraz ze starzeniem się społeczeństwa prawdopodobnie zwiększy częstość występowania udarów mózgu oraz przemijających ataków niedokrwiennych (TIA) w nadchodzących dekadach [4]. TIA definiuje się jako przejściowy epizod dysfunkcji neurologicznej spowodowany ogniskowym lub globalnym niedokrwieniem mózgu, gdzie objawy ustępują do 24 godzin, jednak może poprzedzać pełnoobjawowy udar mózgu. Obecnie terapia udarów jest bardzo ograniczona (tPA i trombektomia wewnątrznaczyniowa) i nie może być stosowana u wszystkich chorych, ze względu na wąskie okno terapeutyczne [5]. Tak więc niezbędne jest lepsze zrozumienie podstaw mechanizmów uszkodzenia oraz naturalnej regeneracji neuronów aby opracować nowe metody leczenia [6,7]. Śmierć neuronów po przejściowym niedokrwieniu globalnym rozwija się stopniowo i selektywnie uszkadza komórki w określonych obszarach mózgu ze względu na ich wewnętrzną wrażliwość. W szczególności za poważny problem uznaje się wywołane globalnym niedokrwieniem uszkodzenie hipokampa, głównej struktury mózgu związanej z uczeniem się i pamięcią [8], które obejmuje różne zmiany neurologiczne i behawioralne, w tym upośledzenia funkcji poznawczych [9].

Hipokamp jest jedną ze struktur mózgu podatnych na przejściowe niedokrwienie, a badania pokazują, że ta wrażliwość jest różna dla każdego obszaru hipokampa (CA1–3). W modelach uszkodzenia niedokrwienno-reperfuzyjnego mózgu gryzoni eliminacja dotyczy neuronów w obszarze CA1, podczas gdy neurony w obszarach CA2-3 i komórkach ziarnistych zakrętu zębatego (DG) są stosunkowo odporne [10-13]. W modelu *in vivo* u suwaka mongolskiego (dawniej: myszoskoczek) w CA1 neurony piramidowe umierają 3–5 dni po przejściowym niedokrwieniu przodomózgowia trwającym 5 minut (model ischemii i reperfuzji, I/R), a ten proces śmierci komórek piramidowych określa się mianem opóźnionej śmierci neuronów (DND, ang. *delayed neuronal death*) [10,12]. Mechanizm śmierci komórek nerwowych po I/R jest bardzo

17

złożony i związany przede wszystkim z: neurotoksycznością glutaminianu i Ca^{2+} [14,15], zmianami w wewnątrzkomórkowym przekazywaniu sygnału wapniowego [16], stresem oksydacyjny [17], uszkodzeniem DNA i stanami zapalnymi [18], metabolizmem lipidów i ich rolą w transdukcji sygnału [19,20], co w efekcie prowadzi do apoptozy. Niemniej jednak nie wszystkie mechanizmy DND zostały w pełni wyjaśnione. Natomiast w rejonach CA2-3, DG ten sam bodziec I/R nie wywołuje eliminacji neuronów, a wzbudzane procesy skutkują przeżyciem komórek i są określane jako mechanizmy endogennej neuroprotekcji.

Mitochondria odgrywają kluczową rolę w homeostazie energetycznej komórki i są szczególnie zaangażowane w śmierć neuronów po udarze niedokrwiennym. Podczas krótkotrwałego niedokrwienia mózgu dochodzi do zaburzenia równowagi energetycznej neuronów na skutek zmniejszenia dopływu krwi oraz wyczerpania zasobów i zahamowania syntezy adenozynotrójfosforanu (ATP). Oprócz swojej zasadniczej roli w syntezie ATP, mitochondria biorą udział w regulacji różnych szlaków śmierci komórki, w tym apoptozy [21]. Wykazano, że mitochondria przyczyniają się do patologii udaru niedokrwiennego poprzez: wzmożoną produkcję reaktywnych form tlenu (ROS, reactive oxidative species), akumulację jonów wapnia, indukowanie apoptozy czy zaburzoną biogenezę. Nadmierne stężenie Ca^{2+} w mitochondriach dodatkowo aktywuje spiralę uszkodzeń poprzez rozproszenie potencjału błony mitochondrialnej ($\Delta\Psi m$), wzrost produkcji ROS i otwarcia MPTP [22]. Produkcja ROS w kompleksie I mitochondrialnego łańcucha oddechowego prowadzi do uszkodzenia oksydacyjnego oraz zaburzenia funkcji mitochondriów [23]. Jest czynnikiem inicjującym kaskadę różnych uszkodzeń tkanki w fazie reperfuzji [24].

Mitochondria to niezwykle dynamiczne organelle komórkowe charakteryzujące się zdolnością do zmiany wielkości, kształtu i położenia poprzez precyzyjnie regulowane procesy podziału (rozdzielenia pojedynczego mitochondrium na dwa lub więcej organelli potomnych) i fuzji (reakcja przeciwstawna) [25]. Podział i fuzja to aktywne procesy, koordynowane przez wyspecjalizowane białka o aktywności GTPazy. Białko Drp1 (ang. *Dynamin-related protein*) jest niezbędne do podziałów mitochondriów; za fuzję zewnętrznej błony mitochondrialnej odpowiadają mitofuzyna 1 (Mfn1) i mitofuzyna 2 (Mfn2), a Opa1 (ang. *Optic atrophy 1*) za fuzję wewnętrznej błony mitochondrialnej [26-29]. Obecnie wiadomo, że procesy te odgrywają kluczową rolę w utrzymaniu integralności mitochondriów i funkcji neuronów zarówno w warunkach prawidłowych,

18

jak i w sytuacjach stresów metabolicznych lub środowiskowych, a ich zaburzenia prowadzą do upośledzenia ruchliwości i aktywności mitochondriów [30]. Fuzja umożliwia szybką wymianę fragmentów błon mitochondrialnych, mitochondrialnego DNA (mtDNA) i metabolitów mitochondrialnych w obrębie sieci mitochondrialnej; uszkodzone mitochondria mogą ulec naprawie poprzez fuzję z prawidłowymi mitochondriami w celu zintegrowania zawartości obu, co sprzyjania przeżyciu komórki. Z drugiej strony podział mitochondriów umożliwia segregację uszkodzonych mitochondriów, a w konsekwencji ich późniejszą eliminację poprzez selektywną autofagię mitochondriów [31].

Autofagia mitochondriów, określana jako mitofagia, to kataboliczny proces, w którym dysfunkcyjne mitochondria są zamykane w dwubłonowej strukturze zwanej autofagosomem i dostarczane do lizosomu lub peroksysomu w celu degradacji [32,33]. Mitofagia odgrywa ważną rolę w fizjologii komórki i organizmu oraz reguluje homeostazę i biogenezę mitochondriów, a także kontroluje liczbę i jakość mitochondriów [34]. Upośledzenie mitofagii może powodować akumulację mitochondriów, zwiększone zużycie tlenu i nadmierne tworzenie ROS, co ostatecznie może prowadzić do degeneracji i śmierci komórki [35]. Z drugiej strony, nadmierne tworzenie ROS, otwarcie MPTP, utrata $\Delta\Psi$m, podział mitochondriów mogą wyzwalać proces mitofagii w neuronach. Badania wykazały, że MPTP ma zasadnicze znaczenie dla inicjacji mitofagii [36]. Najlepiej scharakteryzowaną ścieżką tego procesu jest mitofagia zależna od kinazy indukowanej przez PTEN - PINK1 (PTEN-induced kinase 1) i parkiny, ligazy ubikwityny E3 (Parkin, E3 ubiquitin ligase) [37,38]. W neuronach kory mózgu wykazano, ze zmniejszenie potencjału wewnętrznej błony mitochondrialnej i nadmierny napływ jonów wapnia aktywują szlak mitofagii zależnej od PINK1 oraz parkiny [39,40]. Na zewnętrznej błonie mitochondriów o obniżonym $\Delta\Psi$m dochodzi do akumulacji kinazy PINK1, która w prawidłowo funkcjonujących mitochondriach ulega degradacji [41]. Aktywowana przez autofosforylację PINK1 rekrutuje do uszkodzonych mitochondriów ligazę ubikwityny, parkinę i poprzez kolejne reakcje fosforylacji parkiny potęguje jej aktywność. Aktywowana w ten sposób parkina ubikwitynyluje białka zewnętrznej błony mitochondrialnej, w tym Mfn2, co natychmiast prowadzi do utraty funkcji fuzji mitochondriów, charakterystycznej dla mitofagii [42-44]. Następnie łańcuchy poliubikwityny na białkach zewnętrznej błony mitochondrialnej wiążą się z aktywnymi lipidowanymi formami białka LC3 (microtubule-associated protein 1A/1B light chain 3)

19

za pośrednictwem białka adaptorowego SQSTM1/p62 [45,46], co pozwala na wiązanie i zamknięcie uszkodzonego i tak naznaczonego mitochondrium przez autofagosom i degradację jego zawartości po połączeniu z lizosomem [45].

Procesem umożliwiającym wzrost i odbudowę istniejącej sieci mitochondrialnej, zwłaszcza po usunięciu określonej puli mitochondriów przez mitofagię, jest biogeneza mitochondriów. Ten złożony proces zależy od skoordynowanej ekspresji jądrowego i mitochondrialnego DNA (mtDNA), by w efekcie dostosować pulę mitochondriów do zapotrzebowania energetycznego komórki [47]. W rzeczywistości, w odpowiedzi na różne warunki fizjologiczne i środowiskowe, funkcje metaboliczne komórki wymagają zmiennych ilości energii, w dużej mierze zapewnianej przez mitochondrialny metabolizm oksydacyjny. Taki metabolizm energetyczny jest zwykle wydajny również dzięki stałej modulacji transkrypcji mtDNA. Kluczowym i nadrzędnym regulatorem w tym procesie jest koaktywator receptorów aktywowanych proliferatorami peroksysomów 1α (PGC-1α, Peroxisome proliferator-activated receptor gamma coactivator 1-alpha), tworzący kompleksy z DNA i innymi czynnikami transkrypcyjnymi, takimi jak jądrowe czynniki oddechowe 1/2 (Nrf1/2, Nuclear Respiratory Factor 1/2) [48,49]. Czynniki te regulują transkrypcję genów jądrowych kodujących białka mitochondrialne. Dodatkowo, mitochondrialny czynnik transkrypcyjny A (Tfam, Mitochondrial transcription factor A) ulega ekspresji z jądrowego DNA, a następnie translacji w cytoplazmie i jest transportowany do mitochondriów [50]. Tfam jest zaangażowany w wiele procesów takich jak: transkrypcja mtDNA [51], stabilizowanie mtDNA [52] i replikacja, a także prawdopodobnie naprawa mtDNA [53]. Dlatego poprzez regulację ilości Tfam, koaktywator PGC-1α wydaje się kontrolować ekspresję białek kodowanych przez mtDNA [54]. Tfam kieruje transkrypcją 13 podjednostek czterech mitochondrialnych kompleksów oddechowych, kodowanych w genomie mitochondrialnym, wraz z RNA potrzebnym do ich translacji [55]. W neuronach, w stosunku do innych typów komórek, PGC-1 α ulega nasilonej ekspresji ze względu na ich wysokie zapotrzebowanie na energię [56].

Mfn2 to GTPaza zewnętrznej błony mitochondrialnej zaangażowana w utrzymanie i przebudowę sieci mitochondrialnej. U ssaków, występują dwa typy mitofuzyny, Mfn1 i Mfn2, wykazujące znaczny stopień homologii sekwencji DNA i białka [57], podobieństwa budowy i funkcji [58] [57]. Jednak pomimo wielu podobieństw szereg badań dowodzi, że Mfn2 pełni również inne funkcje niezwiązane bezpośrednio z

20

jej aktywnością fuzyjną [59,60]. Mfn2 pośredniczy w tworzeniu i regulacji połączeń pomiędzy mitochondriami a siateczką śródplazmatyczną (ER) [61,62], przez co kontroluje wymianę jonów wapnia [63] oraz transfer fosfolipidów [64] między obydwoma organellami. Wykazano, że Mfn2 zapobiega inicjacji mitofagii zależnej od PINK1 i parkiny, poprzez utrzymywanie połączeń mitochondriów z ER [65,66]. Jak wykazano w badaniach na komórkach *in vitro* na skutek obniżenia ΔΨm Mfn2 oddziałuje z parkiną w sposób zależny od PINK1, tzn. ufosforylowana przez PINK1 Mfn2 pełni rolę receptora dla parkiny [67]. Dodatkowo, ubikwitynylacja mitofuzyny 2 przez parkinę, prowadzi do utraty jej właściwości fuzyjnych [42,66]. Ubikwitynylowana Mfn2 ulega degradacji w proteasomie, co ułatwia dysocjację mitochondriów od ER, umożliwiając usuwanie uszkodzonych lub starzejących się mitochondriów [44,66]. Ponadto uważa się, że Mfn2 może być pośrednio zaangażowana w metabolizm i procesy energetyczne mitochondriów, co jest sugerowane poprzez jej udział w zaburzeniach metabolicznych, takich jak otyłość i cukrzyca [68-70]. Ubytek Mfn2 prowadzi do zmniejszenia ΔΨm, tempa zużycia tlenu i mitochondrialnego wycieku protonów oraz upośledza utlenianie glukozy, pirogronianu i kwasów tłuszczowych [71-73]. Co ważne, utrata funkcji Mfn2 znacząco obniża syntezę kodowanych jądrowo białek podjednostek kompleksów łańcucha oddechowego I, II, III i V, niezależnie od jej właściwości fuzyjnych [72,74]. Dodatkowo wykazano, że Mfn2 jest wymagana do replikacji i zachowania stabilności mtDNA. Ponadto badania sugerują związek Mfn2 i biogenezy mitochondriów polegający na tym, że PGC-1α indukuje biogenezę mitochondriów poprzez nasilenie transkrypcji i translacji Mfn2, tak więc wydaje się, że PGC-1α może być istotnym regulatorem ekspresji Mfn2 [75-77].

Mając na uwadze powyższy stan wiedzy w prezentowanych badaniach weryfikowano **hipotezę, że Mfn2 w neuronach może działać jako białko integrujące przebudowę sieci mitochondrialnej z mitofagią i biogenezą mitochondriów. Ponadto założono, że zależności miedzy dynamiką, eliminacją i biogenezą mitochondriów mogą być kluczowe dla zachowania homeostazy mitochondriów, a tym samym przeżycia neuronów w warunkach stresu niedokrwienno-reperfuzyjnego**.

21

22

CEL PRACY

Cel ogólny

Poznanie roli Mfn2 w odpowiedzi neuronów na bodziec ischemiczno-reperfuzyjny ze szczególnym uwzględnieniem procesów odpowiadających za dynamikę sieci, zawartość i jakość mitochondriów.

Cele szczegółowe

1. Porównanie dynamiki fuzji i podziału, eliminacji oraz biogenezy mitochondriów w odpowiedzi na przejściowe niedokrwienie mózgu w sektorach hipokampa suwaka mongolskiego (*Meriones unguiculatus*) charakteryzujących się różną przeżywalnością neuronów po bodźcu ischemiczno-reperfuzyjnym (publikacja I).

2. Zbadanie roli Mfn2 w przebudowie sieci mitochondrialnej, eliminacji i biogenezie mitochondriów w neuronach *in vitro* w odpowiedzi na przejściowy brak tlenu i glukozy (OGD) poprzez ocenę przebiegu tych procesów w neuronach prawidłowych oraz z obniżoną ekspresją Mfn2 (publikacja II).

24

MATERIAŁY I METODY

W badaniach wykorzystano dwa dobrze scharakteryzowane modele stresu niedokrwienno – reperfuzyjnego:

1. *In vivo* polegający na przejściowym, 5-minutowym globalnym niedokrwieniu mózgu (I/R) suwaka mongolskiego (*Meriones unguiculatus*) poprzez zaciśnięcie tętnic szyjnych wspólnych, które skutkuje różną przeżywalnością neuronów hipokampa [10,12,13,78-80], co przedstawiono również w publikacji I, rycina 1A. Mózgi izolowano w wybranych punktach czasowych od 3 do 96 godzin po przywróceniu krążenia, a hipokampy dzielono na regiony CA1 i CA2-3, DG do badania przebiegu zmian w obecności białek odpowiedzialnych za dynamikę sieci mitochondrialnej, eliminację i biogenezę mitochondriów za pomocą techniki Western blot oraz obserwacji w mikroskopie elektronowym.

W celu oceny zmian dynamiki mitochondriów analizowano charakterystyczne białka związane z fuzją (Mfn1, Mfn2, Opa1) oraz podziałem mitochondriów (Drp1 oraz jego forma ufosforylowana na Ser616). Do oceny ogólnej i specyficznej autofagii wykorzystano białka markerowe takie jak LC3, SQSTM1/p62, PINK1 i parkina. Biogenezę badano na podstawie zmian w obecności czynników transkrypcyjnych PGC-1α, Nrf1, Tfam oraz białek podjednostek kompleksów łańcucha oddechowego. Zawartość mitochondriów oznaczano pośrednio, przy pomocy pomiarów aktywności syntazy cytrynianowej, poziomu białka macierzy mitochondrialnej Hsp60 oraz pomiar stosunku DNA mitochondrialnego do jądrowego (mtDNA/nDNA).

Mikroskopia elektronowa pozwoliła na dokładną obserwację ultrastruktury i morfologii mitochondriów przed i po I/R. Za pomocą programu ImageJ przeprowadzono analizę następujących parametrów opisujących zawartość, kształt oraz obrzmienie mitochondriów: *mitochondrial content* [%] (obszar w ciele komórki zajmowany przez mitochondria), *mitochondrial elongation* (współczynnik wydłużenia mitochondriów) oraz *mitochondrial swelling* (współczynnik obliczany jako stosunek powierzchnia/obwód znormalizowany do parametru kolistości mitochondriów) opisane w pracy Dagda i wsp. (2009) [81] oraz Lam i wsp. (2021) [82]. Ponadto, technika TEM posłużyła do zweryfikowania obecności różnych struktur autofagowych w neuronach hipokampa.

25

Materiały i metody wykorzystane w badaniach *in vivo* zostały szczegółowo opisane w publikacji I.

2.   Model *in vitro* stanowiła hodowla pierwotna neuronów kory mózgu szczura, która była poddawana przejściowemu (1 godzina) niedoborowi tlenu i glukozy (OGD). Czas trwania bodźca OGD został dobrany eksperymentalnie, tak aby śmiertelność neuronów po 24 godzinach po bodźcu nie przekraczała 20%, umożliwiając tym samym śledzenie zmian po przywróceniu prawidłowych warunków hodowli.

Badania prowadzono na neuronach prawidłowych (*wild type*) oraz z obniżoną ekspresją Mfn2. W celu obniżenia ekspresji Mfn2 zastosowano dostępne komercyjnie konstrukty krótkiego RNA o strukturze spinki do włosów (*short hairpin* RNA, shRNA) (Origene) w wektorach lentiwirusowych. Do eksperymentów wybrano dwa konstrukty, sh-Mfn2 B i sh-Mfn2 D, w oparciu o zadowalającą skuteczność wyciszania Mfn2 przy stosunkowo niskiej toksyczności. Jako kontrolę dla komórek transdukowanych zastosowano konstrukt zawierający niefunkcjonalną sekwencję shRNA (scrambled RNA, scrRNA). Wszystkie neurony były poddawane procedurze 1-godzinnego OGD, a próbki analizowano po 3 i 24 godzinach po przywróceniu tlenu i glukozy, jak przedstawiono na rycinach 1A i 2A w publikacji II.

Do oceny śmiertelności neuronów po eksperymencie OGD wykonano pomiary uwalniania dehydrogenazy mleczanowej (LDH) do pożywki hodowlanej przy użyciu komercyjnego testu CytoTox-ONE (Promega) oraz przy użyciu mikroskopu fluorescencyjnego wyznaczono liczbę jąder pyknotycznych znakowanych Hoechst 33342.

Aby śledzić w czasie zmiany dynamiki mitochondriów analizowano charakterystyczne białka związane z fuzją (Mfn1, Mfn2, Opa1) oraz podziałem mitochondriów (Drp1). Do oceny mitofagii wykorzystano białko markerowe takie jak parkina oraz poziom białek TOM22 i Hsp60.

Ponadto, w celu przeanalizowania dynamiki i morfologii sieci mitochondrialnej mitochondria wybarwiano znacznikiem fluorescencyjnym Mitotracker Red (Thermo Scientific), a uzyskane obrazy analizowano przy użyciu rozszerzenia Mito-Morphology jak opisano w pracy Dagda i wsp. (2009) [81] opracowanego dla programu ImageJ. Do scharakteryzowania morfologii sieci mitochondrialnej wykorzystano następujące parametry: *mito-count* (liczba obiektów w komórce), *mitochondrial content* [%] (obszar w ciele komórki zajmowany przez mitochondria), *mitochondrial Avg. Area*

26

[Avg. Size, μm^2] (średnia powierzchnia mitochondrium), *mitochondria elongation* (współczynnik wydłużenia mitochondriów), *mitochondrial interconnectivity* [Area/Perimeter] (rozgałęzienie sieci mitochondrialnej) [81].

Postęp mitofagii analizowano z wykorzystaniem sondy fluorescencyjnej Mitophagy Dye (Dojindo) specyficznej dla mitochondriów i pozwalającej uwidaczniać mitofagosomy w żywych komórkach. Metoda charakteryzuje się zmianą intensywności fluorescencji znacznika/sondy w odpowiedzi na zmianę pH spowodowaną fuzją autofagosomów (zawierających mitochondria) z lizosomami. Aby zwiększyć specyficzność obserwacji dojrzałych mitofagosomów, lizosomy znakowano sondą Lysoview 633 (Biotium), a liczbę kolokalizujących punktów mitochondrialnych (Mitophagy Dye - pozytywnych) i lizosomalnych (LysoView - pozytywnych) określono ilościowo za pomocą programu ImageJ (publikacja II, rycina 4A).

Dodatkowo w barwieniu immunocytochemicznym oceniano akumulację parkiny na mitochondriach. Zwiększona rekrutacja parkiny do mitochondriów jest uważana za jedną z cech charakterystycznych uszkodzenia mitochondriów i kluczowy etap w selektywnej eliminacji mitochondriów. Białko parkina było znakowane specyficznymi przeciwciałami, a mitochondria wybarwiano sondą Mitotracker Red, na podstawie metody opisanej przez Van Laar i wsp. (2015) [83].

Biogenezę mitochondriów badano analogicznie jak w modelu *in vivo*, wykorzystując analizę Western blot czynników transkrypcyjnych PGC-1α i Nrf1 oraz białek podjednostek kompleksów mitochondrialnego łańcucha oddechowego. Dodatkowo, przeprowadzono reakcję łańcuchową polimerazy w czasie rzeczywistym (Real-time qPCR) do pomiaru ilości mtDNA w stosunku do DNA jądrowego. Względną liczbę kopii obliczono stosując analizę różnicy w cyklu granicznym (Ct, treshold cycle) między mtDNA i DNA jądrowym.

Materiały i metody wykorzystane w badaniach *in vitro* zostały szczegółowo opisane w publikacji II.

PODSUMOWANIE NAJWAŻNIEJSZYCH WYNIKÓW

Ad. Cel szczegółowy 1

W odpowiedzi na 5-minutowe globalne niedokrwienie i reperfuzję mózgu (I/R) w komórkach rejonu CA1 hipokampa, w których ilość Mfn2 ulega obniżeniu po I/R (publikacja I, rycina 2) dochodzi do poważnego uszkodzenia mitochondriów objawiającego się m.in.: ich obrzmieniem i zaburzeniem struktury grzebieni mitochondrialnych widocznych na obrazach z mikroskopu elektronowego (publikacja I, ryciny 1B i 3A), rozmieszczenia mitochondriów głównie w pobliżu jądra komórkowego oraz istotnego wzrostu wybranych parametrów morfologicznych po 24 godzinach reperfuzji w stosunku do CA2-3, DG (publikacja I, rycina 3A-C). Co więcej, zaobserwowano również nasilenie podziałów mitochondriów, o czym świadczy statystycznie istotny, utrzymujący się wzrost stosunku p-Drp1/Drp1 (ponad dwukrotny wzrost w stosunku do kontroli w 3 godziny po I/R) przy równoczesnym, postępującym w czasie obniżeniu poziomu białek odpowiedzialnych za fuzję mitochondriów tj. Mfn1, Mfn2 i Opa1 (publikacja I, rycina 2). Uszkodzone organella są usuwane na drodze ogólnej, nieselektywnej autofagii, rozpoczynającej się krótko po bodźcu, na co wskazuje niemal trzykrotny wzrost stosunku lipidowanej formy białka LC3 czyli LC3-II do LC3-I w trzeciej godzinie reperfuzji oraz obecność struktur autofagowych obserwowanych przy pomocy mikroskopu elektronowego, już 24 godziny po niedokrwieniu (publikacja I, rycina 4). Skutkuje to obniżeniem zawartości mitochondriów przedstawionej jako około 20 % obniżenie ilości białka macierzy mitochondrialnej Hsp60, zmniejszeniem aktywności enzymatycznej syntazy cytrynianowej (publikacja I, rycina 1C i 1D) oraz obniżeniem zawartości białek kompleksów łańcucha oddechowego (publikacja I, rycina 6). Zjawiska te obserwowane w sektorze CA1 towarzyszą postępującej degeneracji neuronów, co pokazano w publikacji I , rycina 1.

Tymczasem w CA2-3, DG uszkodzenie mitochondriów nie jest tak dotkliwe, jak w CA1 (publikacja I, rycina 1). Zaobserwowano równomierne rozmieszczenie mitochondriów w ciałach neuronów oraz istotny wzrost liczby wydłużonych mitochondriów po 24 godzinach reperfuzji w stosunku do CA1 mierzone za pośrednictwem parametru określającego wydłużenie mitochondriów (publikacja I, rycina 3A i 3D). Nasilona dynamika sieci mitochondrialnej, opisana zwiększoną obecnością białek pro-fuzyjnych (Mfn1, Mfn2, Opa1) i pro-podziałowych (p-Drp1/Drp1), wydaje się sprzyjać złagodzeniu uszkodzenia sieci mitochondrialnej i segregacji wadliwych

29

mitochondriów (publikacja I, rycina 2), które są usuwane poprzez selektywną autofagię, mitofagię zależną od PINK1 i parkiny. Proces ten jest widoczny od 48 godzin po niedokrwieniu jako zmiany w stosunku LC3-II do LC3-I (ponad trzykrotny po 72 godzinach reperfuzji (publikacja I, rycina 4B). Uwagę zwraca białko Mfn2, którego charakter zmian wyróżniał się na tle innych białek zaangażowanych w dynamikę mitochondriów: znaczny i dosyć wczesny wzrost od 6 godziny reperfuzji w obszarze CA2-3, DG oraz wyraźne, długotrwałe obniżenie w CA1 (publikacja I, rycina 2). Dodatkowo w rejonach niewrażliwych hipokampa, aktywowana wydaje się być biogeneza mitochondriów, przedstawiona jako wzrost występowania czynników transkrypcyjnych: PGC-1α, Nrf1 i Tfam, prowadząca do zwiększonej biosyntezy białek mitochondrialnych, takich jak Hsp60, Mfn2 oraz białek kompleksów łańcucha oddechowego, nie tylko w celu zrekompensowania puli utraconych mitochondriów, ale również zwiększenia ilości kluczowych białek odpowiedzialnych za syntezę ATP w fazie reperfuzji (publikacja I, rycina 5B i 6). Współwystępowanie tych procesów wewnątrzkomórkowych wydaje się być jedną z cech komórek w rejonach CA2-3, DG hipokampa, które promują przeżycie neuronów po przejściowym niedokrwieniu.

Badania *in vivo* przedstawione w publikacji I sugerują, że wzrost ilości Mfn2 występujący po epizodzie I/R wraz z aktywacją pozostałych białek związanych z dynamiką sieci mitochondrialnej, kontrolowaną mitofagią oraz biogenezą mitochondriów w sektorach CA2-3, DG hipokampa odpornych na stres krótkotrwałego niedokrwienia i reperfuzji może mieć istotną rolę w zjawisku tzw. endogennej neuroprotekcji.

Ad. Cel szczegółowy 2

W neuronach prawidłowych (*wild type*) *in vitro* wymodelowany bodziec krótkotrwałego, 1-godzinnego OGD nie wpływał negatywnie na żywotność neuronów aczkolwiek znacząco i długotrwale (po 3 i 24 godzinach) obniżał obecność Mfn2, bez szczególnego wpływu w dłuższym czasie na inne badane białka mitochondrialne: Mfn1, Opa1, Drp1, TOM22 i Hsp60 (publikacja II, rycina 1D). W odpowiedzi na bodziec OGD neurony wykazywały wzmożoną fuzję mitochondriów i zwiększone rozgałęzienie sieci mitochondrialnej wciąż obserwowane 24 godziny od zadziałania bodźca mierzone za pośrednictwem wybranych parametrów morfologicznych (publikacja II, rycina 3). W neuronach prawidłowych po bodźcu OGD obserwowano, że wczesny i przejściowy

30

wzrost liczby mitofagosomów (publikacja II, rycina 4) współwystępował ze wzrostem akumulacji parkiny na mitochondriach przy jednoczesnym obniżeniu ilości tego białka (publikacja II, rycina 5), co wskazuje na selektywną aktywację procesu eliminacji uszkodzonych mitochondriów. Co więcej, obserwowano aktywację kompensacyjnej biogenezy mitochondriów poprzez wzrost poziomu nadrzędnego czynnika transkrypcyjnego PGC-1α, zwiększony stosunek mitochondrialnego do jądrowego DNA (mtDNA/nDNA), jak i podwyższony poziom białek wybranych podjednostek kompleksów łańcucha oddechowego w neuronach po 24 godzinach po bodźcu OGD (publikacja II, rycina 6).

Natomiast, obniżenie ekspresji Mfn2 (sh-Mfn2 B, D) w neuronach *in vitro* prowadziło do zaburzeniem równowagi fuzji i podziałów mitochondriów, co skutkowało zmianami w morfologii sieci mitochondrialnej, sprzyjając jej fragmentacji, co stwierdzono na podstawie wybranych parametrów morfologicznych (publikacja II, rycina 3). Co więcej, obniżeniu ekspresji Mfn2 towarzyszyła zwiększona akumulacja parkiny na mitochondriach wraz ze zmniejszonym poziomem tego białka, sugerując łagodne uszkodzenie mitochondriów w takich neuronach długo przed zadziałaniem bodźca OGD (publikacja II, rycina 5). Pomimo, że samo obniżenie ekspresji Mfn2 nie miało wpływu na żywotność neuronów mierzoną poziomem uwolnionego z komórek LDH oraz odsetkiem jąder pyknotycznych, to jednak takie neurony wykazywały zwiększoną wrażliwość na łagodny niedobór tlenu i glukozy (publikacja II, rycina 2D, E). Co więcej, zaobserwowano, że obniżeniu ekspresji Mfn2 towarzyszyła zwiększona ekspresja Mfn1, niemniej jednak wydaje się, że utrata funkcji Mfn2 nie została w pełni skompensowana przez Mfn1 (publikacja II, rycina 2 B).

Obniżenie ekspresji Mfn2 w neuronach zahamowało przebudowę sieci mitochondrialnej w odpowiedzi na bodziec OGD: nie obserwowano wzrostu fuzji i usieciowania, ani w krótkim ani w długim czasie po OGD (3 i 24 godziny) (publikacja II, rycina 3), co prawdopodobnie ograniczało regenerację mitochondriów. Ponadto w takich neuronach obserwowano przedłużoną w czasie eliminację mitochondriów, o czym świadczyła wciąż wysoka liczba mitofagosomów oceniana 24 godziny po bodźcu OGD (publikacja II, rycina 4). W przeciwieństwie do neuronów prawidłowych (*wild type*), nie wykazano wzrostu stosunku mtDNA/nDNA jak również nie zaobserwowano wzrostu poziomu wybranych podjednostek kompleksów łańcucha oddechowego w neuronach ze zmniejszoną ekspresją Mfn2 po bodźcu OGD, pomimo wzrostu poziomu nadrzędnego czynnika transkrypcyjnego PGC-1α obserwowanego 24

godziny po bodźcu OGD. Te wyniki sugerują ograniczoną odbudowę zdolności oddechowej mitochondriów w neuronach pozbawionych Mfn2 po bodźcu OGD (publikacja II, rycina 6).

Badania *in vitro* przedstawione w publikacji II wskazują, że w odpowiedzi na łagodny stres OGD mitochondria w neuronach prawidłowych (*wild type*) są naprawiane poprzez wzmożoną fuzję, selektywną i kontrolowaną mitofagię oraz zwiększoną biosyntezę białek łańcucha oddechowego, co prowadzi do przeżycia tych neuronów. Natomiast obniżenie ekspresji Mfn2 zarówno uszkadza mitochondria w warunkach kontrolnych, jak i uniemożliwia przebudowę sieci mitochondrialnej, prowadzi do zaburzenia równowagi eliminacji i biogenezy mitochondriów w odpowiedzi neuronów na stres OGD, co skutkuje większą śmiertelnością komórek.

DYSKUSJA

Prezentowane badania podkreślają, że przeżycie neuronów po stresie niedokrwienno-reperfuzyjnym nie jest determinowane przez pojedynczy proces wewnątrzkomórkowy, ale zależy od złożonych relacji pomiędzy wszystkimi cząsteczkami i organellami w komórce, włączając w to mechanizmy dynamiki, eliminacji i biogenezy mitochondriów.

Wykazaliśmy, że uszkodzenie mitochondriów może być naprawione w pierwszej kolejności poprzez zwiększoną dynamikę sieci mitochondrialnej, jak w CA2-3, DG w modelu *in vivo* oraz neuronach prawidłowych *in vitro*, kiedy obserwuje się nasilenie fuzji mitochondriów w odpowiedzi na bodziec. Sugerujemy, że w dłuższym czasie reperfuzji mitochondria, które mimo fuzji uległy uszkodzeniu zostają oddzielone od sieci mitochondrialnej i usunięte za pomocą mitofagii. Jednocześnie wydaje się, że Mfn2 jest niezbędna, aby takie procesy mogły mieć miejsce i przebiegały prawidłowo.

Molekularne podstawy procesów dynamiki mitochondriów i mitofagii zostały dobrze zbadane i opisane w niezależnych modelach, ale badania mające na celu wyjaśnienie wzajemnych zależności między tymi dwoma procesami znacząco wpływającymi na jakość i zawartość mitochondriów są ograniczone. Dotychczasowe badania wykazały, że mitochondria w neuronach obszaru CA1 hipokampa szczura ulegają wzmożonej fragmentacji rozpoczynającej się już 2 godziny po I/R [84], co zostało również pokazane w naszych badaniach (publikacja I). Podobnie, fragmentację mitochondriów opisano w CA3 i zakręcie zębatym (DG) w modelu globalnego przejściowego niedokrwienia mózgu myszy; jednak, w przeciwieństwie do CA1, mitochondria w neuronach tych obszarów zaczęły ulegać fuzji po 24 h reperfuzji, co wykazano także w naszych badaniach w modelu I/R suwaka mongolskiego (publikacja I). Te dane sugerują, że w neuronach odpornych na niedokrwienie po rozległej i nasilonej fragmentacji dynamika mitochondrialna została przesunięta w kierunku fuzji [85]. W związku z tym można przypuszczać, że zwiększony i długotrwały podział mitochondriów sprzyja śmierci neuronów po niedokrwieniu mózgu [86] i ponadto może przyczyniać się do nasilenia mitofagii [31]. Dostępne dane nie są jednoznaczne. W modelach 2-godzinnego zamknięcia tętnicy środkowej mózgu (MCAO) szczura oraz 4-godzinnego OGD na pierwotnych neuronach kory mózgu szczura wykazano, że zahamowanie aktywności Drp1, białka związanego z podziałem, ograniczało fragmentację mitochondriów i prowadziło do zachowania prawidłowej morfologii

i funkcji mitochondriów w neuronach narażonych na niedokrwienie [87-89]. Natomiast w modelu 10-minutowego globalnego niedokrwienia mózgu szczura w neuronach CA3 hipokampa nasileniu procesu mitofagii towarzyszył wzrost poziomu Drp1 po I/R [90]. Tymczasem wydaje się, że równowaga przesunięta w stronę fuzji mitochondriów chroni komórki przed uszkodzeniem [91,92] i nadmierną aktywacją mitofagii [93], co sugerują badania w modelach 90-minutowego MACO u 12-dniowych szczurów oraz ogniskowego niedokrwienia mózgu u samców myszy (C57BL/6) indukowanego przez MACO. Podobne zależności zaobserwowaliśmy także w naszym modelu, gdzie w obszarze CA2-3, DG po I/R przyrasta obecność białek związanych z fuzją mitochondriów, zwłaszcza Mfn2, a czego nie wykazaliśmy w CA1 (publikacja I).

Dotychczas, w modelach *in vivo* i *in vitro* niedokrwienia mózgu wykazano, że obniżenie ekspresji Mfn2 prowadziło do dysfunkcji mitochondriów, zaburzenia homeostazy jonów wapnia i aktywacji białek proapoptotycznych, co skutkowało opóźnioną śmiercią neuronów. Pokazano, że nadekspresja Mfn2 ograniczała apoptozę wywołaną hipoksją, zmniejszała obrzęk mózgu po udarze niedokrwiennym u szczurów [91,92], jak również ograniczała uszkodzenie i przywracała prawidłową morfologię mitochondriów w modelu ogniskowego niedokrwienia mózgu myszy [91]. Wyniki te są zgodne z naszymi obserwacjami: trwałym obniżeniem Mfn2 we wrażliwym na I/R CA1 oraz wzrostem w obszarach CA2-3, DG, co może świadczyć o roli Mfn2 w endogennej neuroprotekcji obserwowanej w tych rejonach hipokampa (publikacja I). Co ważne, Mfn2 może łagodzić skutki uszkodzenia I/R poprzez zwiększenie tworzenia autofagosomów i promowanie fuzji autofagosomów i lizosomów [90], co ponownie potwierdza ważną rolę Mfn2 w procesie selektywnego usuwaniu mitochondriów wykraczającą poza jej właściwości fuzyjne.

Nasze badania w modelach przejściowego niedokrwienia mózgu wykazały, że w przypadku znacznego uszkodzenia mitochondriów (obserwowanego w CA1 *in vivo*) oraz w neuronach o obniżonej ekspresji Mfn2 *in vitro*, odpowiedź polegająca na zwiększeniu dynamiki sieci mitochondrialnej wydaje się nie występować, co jest zgodnie z obecnym stanem wiedzy. Co więcej, ubytek białka zaangażowanego w fuzję mitochondriów, jakim jest Mfn2, obserwowany w CA1 oraz obecny w neuronach o obniżonej ekspresji Mfn2, sprzyja znacznemu rozdrobnieniu mitochondriów. Równolegle obserwowana jest nasilona autofagia. Wydaje się, że taki typ odpowiedzi nie ma jednoznacznego charakteru neuroprotekcyjnego.

34

W związku z powyższym można powiedzieć, że nadal istnieją kontrowersje dotyczące tego, czy nasilenie procesu mitofagii w warunkach I/R jest korzystne, czy szkodliwe dla przeżycia neuronów. Właściwsze może być rozważenie mitofagii jako wieloetapowego procesu prowadzącego do utrzymania równowagi w neuronach, uwzględniającego także dynamikę i biogenezę mitochondriów, zwłaszcza po I/R [94]. Większość badań potwierdza hipotezę, że mitofagia jest niezbędna do usunięcia dysfunkcyjnych mitochondriów po I/R i przeżycia neuronów [95]. Natomiast przy znacznie ograniczonej mitofagii lub jej braku – uszkodzone mitochondria nie zostaną usunięte, co może przyczynić się do nadmiernego tworzenia ROS, nasilenia dysfunkcji mitochondriów, a ostatecznie do śmierci komórki. Z drugiej strony, nadmierna mitofagia w połączeniu z zwiększoną fragmentacją mitochondriów, zahamowaniem biogenezy mitochondriów i globalnym spadkiem syntezy białek [96,97] powoduje zmniejszenie masy mitochondrialnej, a w konsekwencji deficyt syntezy ATP i śmierć komórki [98].

Co więcej, na podstawie przeprowadzonych przez nas badań można wnioskować, że wystąpienie biogenezy mitochondriów, prowadzącej do zwiększenia ilości białek kompleksów oddechowych wydaje się ważnym elementem endogennego mechanizmu neuroprotekcyjnego. Proces ten nie występuje jednak przy obniżeniu Mfn2, obserwowanym w CA1 w modelu I/R oraz indukowanym eksperymentalnie w neuronach *in vitro*. Jednak nasze dotychczasowe badania ani dostępne źródła nie pozwalają w pełni opisać mechanizmu tej zależności, dlatego dalsze badania są konieczne.

Podobnie jak w przypadku mitofagii, biogeneza mitochondrialna jest wysoce złożonym i zmiennym procesem oraz jest ściśle regulowana w odpowiedzi na różne bodźce, takie jak zapotrzebowanie na energię czy stres komórkowy [99]. Stres oksydacyjny wywołuje fragmentację mitochondriów i powoduje zaburzenia biogenezy mitochondriów [100]. Z kolei zaburzenia dynamiki i biogenezy mitochondriów prowadzą do zwiększonej produkcji ROS [101]. Jak wykazano, ROS mogą również aktywować szlak sygnałowy PGC-1α, a w konsekwencji biogenezę mitochondriów i ekspresję genów zaangażowanych w ekspresje białek kompleksów oddechowych [102]. Co więcej, jony wapnia są również ważnym regulatorem biogenezy mitochondriów. Wzrastające stężenie wolnych Ca^{2+} indukuje ekspresję PGC-1α i Tfam [103,104] oraz prowadzi do aktywacji jądrowych czynników transkrypcyjnych Nrf [103].

Wiele komórkowych szlaków sygnałowych łączy się w celu regulacji zarówno mitofagii, jak i biogenezy mitochondriów, jednym z nich jest szlak sygnałowy kinazy mTOR, (ang. mammalian target of rapamycin kinase), który reguluje m.in. homeostazę

35

związków wysokoenergetycznych w warunkach stresu spowodowanego ograniczeniem lub brakiem substancji odżywczych [105]. Szlak sygnałowy kinazy mTOR może wpływać na biogenezę mitochondriów, mitofagię i metabolizm mitochondriów poprzez regulację czynnika transkrypcyjnego PGC-1α [106]. Co ciekawe, parkina jest także zaangażowana w regulację biogenezy mitochondriów [107]. Degradacja białka PARIS (parkin interacting substrate), substratu parkiny, zwiększa ekspresję genów zależnych od PGC-1α i biogenezę mitochondriów [108]. Co więcej, utrata funkcji parkiny blokuje biogenezę mitochondriów poprzez akumulację PARIS [109]. W naszych badaniach *in vitro* zaobserwowaliśmy, że obniżeniu ekspresji Mfn2 w neuronach towarzyszył zmniejszony poziom białka parkiny niezależnie od OGD oraz ograniczona lub brak biogenezy mitochondriów po zadziałaniu bodźca OGD. Zatem wydaje się, ze istnieje ścisła relacja pomiędzy Mfn2 a parkiną i biogenezą mitochondriów, chociaż szczegóły molekularne tego zjawiska wymagają dalszych badań,

Wydaje się zatem prawdopodobne, że mechanizmy kontrolujące biogenezę mitochondriów są ściśle powiązane z procesami fuzji mitochondriów. Wykazano, że wzrost ekspresji Mfn2 przyczynia się do zwiększonej ekspresji PGC-1α [76], co sugeruje związek między tymi białkami. Sugestia ta została potwierdzona obserwacjami, że PGC-1α indukował biogenezę mitochondriów poprzez nasilenie transkrypcji i translacji Mfn2 w mięśniach szkieletowych i brązowej tkance tłuszczowej. Dlatego też prawdopodobnie PGC-1α jest kluczowym regulatorem aktywności Mfn2, zwłaszcza podczas wysokiego zapotrzebowania energetycznego komórki [76,110].

Mając na uwadze aktualny stan wiedzy, przeprowadzone przez nas badania podkreślają, że wzajemne zależności miedzy dynamiką, eliminacją i biogenezą mitochondriów mogą być kluczowe dla zachowania homeostazy mitochondriów, a tym samym przeżycia neuronów w warunkach niedokrwienia. Co więcej, Mfn2 w neuronach może działać nie tylko jako białko odpowiedzialne za fuzję mitochondriów czy tworzenie połączeń z ER, ale także integrujące przebudowę sieci mitochondrialnej z mitofagią i biogenezą mitochondriów.

36

PODSUMOWANIE

- W neuronach przeżywających przejściowe niedokrwienie dochodzi do wzrostu dynamiki mitochondriów objawiającej się wzmożoną fuzją.

- Selektywna i kontrolowana autofagia, w tym szczególnie mitofagia zależna od PINK1 i parkiny, sprzyja przeżyciu neuronów po bodźcu ischemiczno-reperfuzyjnym *in vivo* i krótkotrwałym OGD *in vitro*.

- Równowaga między procesami eliminacji i biogenezy mitochondriów jest kluczowa dla przeżycia neuronów po łagodnym/przejściowym bodźcu I/R i OGD.

- Mfn2 bierze szczególny udział w kształtowaniu i utrzymaniu prawidłowej sieci mitochondrialnej w neuronach oraz jej przebudowie po bodźcu I/R i OGD.

- Mfn2 moduluje stopień eliminacji wadliwych mitochondriów i pozytywnie wpływa na ich regenerację poprzez wzmożoną fuzję i odbudowę w procesie biogenezy.

WNIOSEK

Mfn2 jest białkiem koniecznym do prawidłowej odpowiedzi neuronów na przejściowy bodziec niedokrwienny, umożliwiając ich przeżycie, poprzez regulowanie zależności pomiędzy eliminacją mitochondriów, a ich biogenezą.

38

LITERATURA

1. Feigin, V.L.; Lawes, C.M.; Bennett, D.A.; Barker-Collo, S.L.; Parag, V. Worldwide stroke incidence and early case fatality reported in 56 population-based studies: a systematic review. *Lancet Neurol* 2009, *8*, 355-369, doi:10.1016/S1474-4422(09)70025-0.

2. Danaei, G.; Finucane, M.M.; Lu, Y.; Singh, G.M.; Cowan, M.J.; Paciorek, C.J.; Lin, J.K.; Farzadfar, F.; Khang, Y.H.; Stevens, G.A.; et al. National, regional, and global trends in fasting plasma glucose and diabetes prevalence since 1980: systematic analysis of health examination surveys and epidemiological studies with 370 country-years and 2·7 million participants. *Lancet* 2011, *378*, 31-40, doi:10.1016/S0140-6736(11)60679-X.

3. (NCD-RisC), N.R.F.C. Trends in adult body-mass index in 200 countries from 1975 to 2014: a pooled analysis of 1698 population-based measurement studies with 19·2 million participants. *Lancet* 2016, *387*, 1377-1396, doi:10.1016/S0140-6736(16)30054-X.

4. Li, L.; Scott, C.A.; Rothwell, P.M.; Study, O.V. Trends in Stroke Incidence in High-Income Countries in the 21st Century: Population-Based Study and Systematic Review. *Stroke* 2020, *51*, 1372-1380, doi:10.1161/STROKEAHA.119.028484.

5. Jauch, E.C.; Saver, J.L.; Adams, H.P.; Bruno, A.; Connors, J.J.; Demaerschalk, B.M.; Khatri, P.; McMullan, P.W.; Qureshi, A.I.; Rosenfield, K.; et al. Guidelines for the early management of patients with acute ischemic stroke: a guideline for healthcare professionals from the American Heart Association/American Stroke Association. *Stroke* 2013, *44*, 870-947, doi:10.1161/STR.0b013e318284056a.

6. Yang, S.H.; Lou, M.; Luo, B.; Jiang, W.J.; Liu, R. Precision Medicine for Ischemic Stroke, Let Us Move Beyond Time Is Brain. *Transl Stroke Res* 2018, *9*, 93-95, doi:10.1007/s12975-017-0566-y.

7. Feigin, V.L.; Krishnamurthi, R. Public health strategies could reduce the global stroke epidemic. *Lancet Neurol* 2010, *9*, 847-848, doi:10.1016/S1474-4422(10)70190-3.

8. Izquierdo, I.; Medina, J.H. Memory formation: the sequence of biochemical events in the hippocampus and its connection to activity in other brain structures. *Neurobiol Learn Mem* 1997, *68*, 285-316, doi:10.1006/nlme.1997.3799.

9. Schaapsmeerders, P.; van Uden, I.W.; Tuladhar, A.M.; Maaijwee, N.A.; van Dijk, E.J.; Rutten-Jacobs, L.C.; Arntz, R.M.; Schoonderwaldt, H.C.; Dorresteijn, L.D.; de Leeuw, F.E.; et al. Ipsilateral hippocampal atrophy is associated with long-term memory dysfunction after ischemic stroke in young adults. *Hum Brain Mapp* 2015, *36*, 2432-2442, doi:10.1002/hbm.22782.

10. Kirino, T. Delayed neuronal death in the gerbil hippocampus following ischemia. *Brain Res* 1982, *239*, 57-69, doi:10.1016/0006-8993(82)90833-2.

11. Pulsinelli, W.A. Selective neuronal vulnerability: morphological and molecular characteristics. *Prog Brain Res* 1985, *63*, 29-37, doi:10.1016/S0079-6123(08)61973-1.

12. Dluzniewska, J.; Sarnowska, A.; Beresewicz, M.; Johnson, I.; Srai, S.K.; Ramesh, B.; Goldspink, G.; Górecki, D.C.; Zabłocka, B. A strong neuroprotective effect of the autonomous C-terminal peptide of IGF-1 Ec (MGF) in brain ischemia. *FASEB J* 2005, *19*, 1896-1898, doi:10.1096/fj.05-3786fje.

13. Beręsewicz-Haller, M.; Krupska, O.; Bochomulski, P.; Dudzik, D.; Chęcińska, A.; Hilgier, W.; Barbas, C.; Zablocki, K.; Zablocka, B. Mitochondrial Metabolism behind Region-Specific Resistance to Ischemia-Reperfusion Injury in Gerbil Hippocampus. Role of PKCβII and Phosphate-Activated Glutaminase. *Int J Mol Sci* 2021, *22*, doi:10.3390/ijms22168504.

14. Ankarcrona, M.; Dypbukt, J.M.; Bonfoco, E.; Zhivotovsky, B.; Orrenius, S.; Lipton, S.A.; Nicotera, P. Glutamate-induced neuronal death: a succession of necrosis or apoptosis depending on mitochondrial function. *Neuron* 1995, *15*, 961-973.

15. Aarts, M.M.; Tymianski, M. Molecular mechanisms underlying specificity of excitotoxic signaling in neurons. *Current molecular medicine* 2004, *4*, 137-147.

16. Lazarewicz, J.W. Calcium transients in brain ischemia: role in neuronal injury. *Acta Neurobiol Exp (Wars)* 1996, *56*, 299-311.

17. Lee, C.H.; Park, J.H.; Yoo, K.Y.; Choi, J.H.; Hwang, I.K.; Ryu, P.D.; Kim, D.H.; Kwon, Y.G.; Kim, Y.M.; Won, M.H. Pre- and post-treatments with escitalopram protect against experimental ischemic neuronal damage via regulation of BDNF expression and oxidative stress. *Exp Neurol* 2011, *229*, 450-459, doi:10.1016/j.expneurol.2011.03.015.

18. Hwang, I.K.; Yoo, K.Y.; Suh, H.W.; Kim, Y.S.; Kwon, D.Y.; Kwon, Y.G.; Yoo, J.H.; Won, M.H. Folic acid deficiency increases delayed neuronal death, DNA damage, platelet endothelial cell adhesion molecule-1 immunoreactivity, and gliosis in the hippocampus after transient cerebral ischemia. *J Neurosci Res* 2008, *86*, 2003-2015, doi:10.1002/jnr.21647.

19. Strosznajder, J.; Zambrzycka, A.; Kacprzak, M.D.; Kopczuk, D.; Strosznajder, R.P. Alteration of phosphoinositide degradation by cytosolic and membrane-bound phospholipases after forebrain ischemia-reperfusion in gerbil: effects of amyloid beta peptide. *Neurochem Res* 1999, *24*, 1277-1284, doi:10.1023/a:1020929208038.

20. Cristea, I.M.; Degli Esposti, M. Membrane lipids and cell death: an overview. *Chem Phys Lipids* 2004, *129*, 133-160, doi:10.1016/j.chemphyslip.2004.02.002.

21. Bakthavachalam, P.; Shanmugam, P.S.T. Mitochondrial dysfunction - Silent killer in cerebral ischemia. *J Neurol Sci* 2017, *375*, 417-423, doi:10.1016/j.jns.2017.02.043.

22. Szydlowska, K.; Tymianski, M. Calcium, ischemia and excitotoxicity. *Cell Calcium* 2010, *47*, 122-129, doi:10.1016/j.ceca.2010.01.003.

23. Hu, F.; Liu, F. Mitochondrial stress: a bridge between mitochondrial dysfunction and metabolic diseases? *Cell Signal* 2011, *23*, 1528-1533, doi:10.1016/j.cellsig.2011.05.008.

24. Lesnefsky, E.J.; Chen, Q.; Tandler, B.; Hoppel, C.L. Mitochondrial Dysfunction and Myocardial Ischemia-Reperfusion: Implications for Novel Therapies. *Annu*

40

Rev Pharmacol Toxicol 2017, *57*, 535-565, doi:10.1146/annurev-pharmtox-010715-103335.

25. Legros, F.; Lombès, A.; Frachon, P.; Rojo, M. Mitochondrial fusion in human cells is efficient, requires the inner membrane potential, and is mediated by mitofusins. *Mol Biol Cell* 2002, *13*, 4343-4354, doi:10.1091/mbc.e02-06-0330.

26. Youle, R.J.; van der Bliek, A.M. Mitochondrial fission, fusion, and stress. *Science* 2012, *337*, 1062-1065, doi:10.1126/science.1219855.

27. van der Bliek, A.M.; Shen, Q.; Kawajiri, S. Mechanisms of mitochondrial fission and fusion. *Cold Spring Harb Perspect Biol* 2013, *5*, doi:10.1101/cshperspect.a011072.

28. Farmer, T.; Reinecke, J.B.; Xie, S.; Bahl, K.; Naslavsky, N.; Caplan, S. Control of mitochondrial homeostasis by endocytic regulatory proteins. *J Cell Sci* 2017, *130*, 2359-2370, doi:10.1242/jcs.204537.

29. Burté, F.; Carelli, V.; Chinnery, P.F.; Yu-Wai-Man, P. Disturbed mitochondrial dynamics and neurodegenerative disorders. *Nat Rev Neurol* 2015, *11*, 11-24, doi:10.1038/nrneurol.2014.228.

30. Bereiter-Hahn, J.; Vöth, M. Dynamics of mitochondria in living cells: shape changes, dislocations, fusion, and fission of mitochondria. *Microsc Res Tech* 1994, *27*, 198-219, doi:10.1002/jemt.1070270303.

31. Twig, G.; Elorza, A.; Molina, A.J.; Mohamed, H.; Wikstrom, J.D.; Walzer, G.; Stiles, L.; Haigh, S.E.; Katz, S.; Las, G.; et al. Fission and selective fusion govern mitochondrial segregation and elimination by autophagy. *EMBO J* 2008, *27*, 433-446, doi:10.1038/sj.emboj.7601963.

32. Nakatogawa, H.; Suzuki, K.; Kamada, Y.; Ohsumi, Y. Dynamics and diversity in autophagy mechanisms: lessons from yeast. *Nat Rev Mol Cell Biol* 2009, *10*, 458-467, doi:10.1038/nrm2708.

33. Yang, Z.; Klionsky, D.J. Eaten alive: a history of macroautophagy. *Nat Cell Biol* 2010, *12*, 814-822, doi:10.1038/ncb0910-814.

34. Guan, R.; Zou, W.; Dai, X.; Yu, X.; Liu, H.; Chen, Q.; Teng, W. Mitophagy, a potential therapeutic target for stroke. *J Biomed Sci* 2018, *25*, 87, doi:10.1186/s12929-018-0487-4.

35. Palikaras, K.; Tavernarakis, N. Mitochondrial homeostasis: the interplay between mitophagy and mitochondrial biogenesis. *Exp Gerontol* 2014, *56*, 182-188, doi:10.1016/j.exger.2014.01.021.

36. Rodriguez-Enriquez, S.; Kai, Y.; Maldonado, E.; Currin, R.T.; Lemasters, J.J. Roles of mitophagy and the mitochondrial permeability transition in remodeling of cultured rat hepatocytes. *Autophagy* 2009, *5*, 1099-1106, doi:10.4161/auto.5.8.9825.

37. Narendra, D.P.; Jin, S.M.; Tanaka, A.; Suen, D.F.; Gautier, C.A.; Shen, J.; Cookson, M.R.; Youle, R.J. PINK1 is selectively stabilized on impaired mitochondria to activate Parkin. *PLoS Biol* 2010, *8*, e1000298, doi:10.1371/journal.pbio.1000298.

38. Matsuda, N.; Sato, S.; Shiba, K.; Okatsu, K.; Saisho, K.; Gautier, C.A.; Sou, Y.S.; Saiki, S.; Kawajiri, S.; Sato, F.; et al. PINK1 stabilized by mitochondrial

depolarization recruits Parkin to damaged mitochondria and activates latent Parkin for mitophagy. *J Cell Biol* 2010, *189*, 211-221, doi:10.1083/jcb.200910140.

39. Ashrafi, G.; Schwarz, T.L. The pathways of mitophagy for quality control and clearance of mitochondria. *Cell Death Differ* 2013, *20*, 31-42, doi:10.1038/cdd.2012.81.

40. Narendra, D.; Tanaka, A.; Suen, D.F.; Youle, R.J. Parkin is recruited selectively to impaired mitochondria and promotes their autophagy. *J Cell Biol* 2008, *183*, 795-803, doi:10.1083/jcb.200809125.

41. Pickrell, A.M.; Youle, R.J. The roles of PINK1, parkin, and mitochondrial fidelity in Parkinson's disease. *Neuron* 2015, *85*, 257-273, doi:10.1016/j.neuron.2014.12.007.

42. Gegg, M.E.; Cooper, J.M.; Chau, K.Y.; Rojo, M.; Schapira, A.H.; Taanman, J.W. Mitofusin 1 and mitofusin 2 are ubiquitinated in a PINK1/parkin-dependent manner upon induction of mitophagy. *Hum Mol Genet* 2010, *19*, 4861-4870, doi:10.1093/hmg/ddq419.

43. Poole, A.C.; Thomas, R.E.; Yu, S.; Vincow, E.S.; Pallanck, L. The mitochondrial fusion-promoting factor mitofusin is a substrate of the PINK1/parkin pathway. *PLoS One* 2010, *5*, e10054, doi:10.1371/journal.pone.0010054.

44. Tanaka, A.; Cleland, M.M.; Xu, S.; Narendra, D.P.; Suen, D.F.; Karbowski, M.; Youle, R.J. Proteasome and p97 mediate mitophagy and degradation of mitofusins induced by Parkin. *J Cell Biol* 2010, *191*, 1367-1380, doi:10.1083/jcb.201007013.

45. Geisler, S.; Holmström, K.M.; Skujat, D.; Fiesel, F.C.; Rothfuss, O.C.; Kahle, P.J.; Springer, W. PINK1/Parkin-mediated mitophagy is dependent on VDAC1 and p62/SQSTM1. *Nat Cell Biol* 2010, *12*, 119-131, doi:10.1038/ncb2012.

46. Narendra, D.; Kane, L.A.; Hauser, D.N.; Fearnley, I.M.; Youle, R.J. p62/SQSTM1 is required for Parkin-induced mitochondrial clustering but not mitophagy; VDAC1 is dispensable for both. *Autophagy* 2010, *6*, 1090-1106, doi:10.4161/auto.6.8.13426.

47. Scarpulla, R.C. Metabolic control of mitochondrial biogenesis through the PGC-1 family regulatory network. *Biochim Biophys Acta* 2011, *1813*, 1269-1278, doi:10.1016/j.bbamcr.2010.09.019.

48. Wu, Z.; Puigserver, P.; Andersson, U.; Zhang, C.; Adelmant, G.; Mootha, V.; Troy, A.; Cinti, S.; Lowell, B.; Scarpulla, R.C.; et al. Mechanisms controlling mitochondrial biogenesis and respiration through the thermogenic coactivator PGC-1. *Cell* 1999, *98*, 115-124, doi:10.1016/S0092-8674(00)80611-X.

49. Huss, J.M.; Kopp, R.P.; Kelly, D.P. Peroxisome proliferator-activated receptor coactivator-1alpha (PGC-1alpha) coactivates the cardiac-enriched nuclear receptors estrogen-related receptor-alpha and -gamma. Identification of novel leucine-rich interaction motif within PGC-1alpha. *J Biol Chem* 2002, *277*, 40265-40274, doi:10.1074/jbc.M206324200.

50. Attardi, G.; Schatz, G. Biogenesis of mitochondria. *Annu Rev Cell Biol* 1988, *4*, 289-333, doi:10.1146/annurev.cb.04.110188.001445.

51. Fisher, R.P.; Clayton, D.A. Purification and characterization of human mitochondrial transcription factor 1. *Mol Cell Biol* 1988, *8*, 3496-3509, doi:10.1128/mcb.8.8.3496-3509.1988.

52. Ekstrand, M.I.; Falkenberg, M.; Rantanen, A.; Park, C.B.; Gaspari, M.; Hultenby, K.; Rustin, P.; Gustafsson, C.M.; Larsson, N.G. Mitochondrial transcription factor A regulates mtDNA copy number in mammals. *Hum Mol Genet* 2004, *13*, 935-944, doi:10.1093/hmg/ddh109.

53. Canugovi, C.; Maynard, S.; Bayne, A.C.; Sykora, P.; Tian, J.; de Souza-Pinto, N.C.; Croteau, D.L.; Bohr, V.A. The mitochondrial transcription factor A functions in mitochondrial base excision repair. *DNA Repair (Amst)* 2010, *9*, 1080-1089, doi:10.1016/j.dnarep.2010.07.009.

54. Scarpulla, R.C. Transcriptional paradigms in mammalian mitochondrial biogenesis and function. *Physiol Rev* 2008, *88*, 611-638, doi:10.1152/physrev.00025.2007.

55. Larsson, N.G.; Wang, J.; Wilhelmsson, H.; Oldfors, A.; Rustin, P.; Lewandoski, M.; Barsh, G.S.; Clayton, D.A. Mitochondrial transcription factor A is necessary for mtDNA maintenance and embryogenesis in mice. *Nat Genet* 1998, *18*, 231-236, doi:10.1038/ng0398-231.

56. Andersson, U.; Scarpulla, R.C. Pgc-1-related coactivator, a novel, serum-inducible coactivator of nuclear respiratory factor 1-dependent transcription in mammalian cells. *Mol Cell Biol* 2001, *21*, 3738-3749, doi:10.1128/MCB.21.11.3738-3749.2001.

57. Zorzano, A.; Pich, S. What is the biological significance of the two mitofusin proteins present in the outer mitochondrial membrane of mammalian cells? *IUBMB Life* 2006, *58*, 441-443, doi:10.1080/15216540600644838.

58. Zorzano, A.; Liesa, M.; Sebastián, D.; Segalés, J.; Palacín, M. Mitochondrial fusion proteins: dual regulators of morphology and metabolism. *Semin Cell Dev Biol* 2010, *21*, 566-574, doi:10.1016/j.semcdb.2010.01.002.

59. Filadi, R.; Pendin, D.; Pizzo, P. Mitofusin 2: from functions to disease. *Cell Death Dis* 2018, *9*, 330, doi:10.1038/s41419-017-0023-6.

60. Dorn, G.W. Mitofusins as mitochondrial anchors and tethers. *J Mol Cell Cardiol* 2020, *142*, 146-153, doi:10.1016/j.yjmcc.2020.04.016.

61. de Brito, O.M.; Scorrano, L. Mitofusin-2 regulates mitochondrial and endoplasmic reticulum morphology and tethering: the role of Ras. *Mitochondrion* 2009, *9*, 222-226, doi:10.1016/j.mito.2009.02.005.

62. de Brito, O.M.; Scorrano, L. Mitofusin 2 tethers endoplasmic reticulum to mitochondria. *Nature* 2008, *456*, 605-610.

63. Rizzuto, R.; Pinton, P.; Carrington, W.; Fay, F.S.; Fogarty, K.E.; Lifshitz, L.M.; Tuft, R.A.; Pozzan, T. Close contacts with the endoplasmic reticulum as determinants of mitochondrial Ca2+ responses. *Science* 1998, *280*, 1763-1766, doi:10.1126/science.280.5370.1763.

64. Hernández-Alvarez, M.I.; Sebastián, D.; Vives, S.; Ivanova, S.; Bartoccioni, P.; Kakimoto, P.; Plana, N.; Veiga, S.R.; Hernández, V.; Vasconcelos, N.; et al. Deficient Endoplasmic Reticulum-Mitochondrial Phosphatidylserine Transfer

Causes Liver Disease. *Cell* 2019, *177*, 881-895.e817, doi:10.1016/j.cell.2019.04.010.

65.   Basso, V.; Marchesan, E.; Peggion, C.; Chakraborty, J.; von Stockum, S.; Giacomello, M.; Ottolini, D.; Debattisti, V.; Caicci, F.; Tasca, E.; et al. Regulation of ER-mitochondria contacts by Parkin via Mfn2. *Pharmacol Res* 2018, *138*, 43-56, doi:10.1016/j.phrs.2018.09.006.

66.   McLelland, G.L.; Goiran, T.; Yi, W.; Dorval, G.; Chen, C.X.; Lauinger, N.D.; Krahn, A.I.; Valimehr, S.; Rakovic, A.; Rouiller, I.; et al. Mfn2 ubiquitination by PINK1/parkin gates the p97-dependent release of ER from mitochondria to drive mitophagy. *Elife* 2018, *7*, doi:10.7554/eLife.32866.

67.   Chen, Y.; Dorn, G.W. PINK1-phosphorylated mitofusin 2 is a Parkin receptor for culling damaged mitochondria. *Science (New York, N.Y.)* 2013, *340*, 471-475.

68.   Bach, D.; Naon, D.; Pich, S.; Soriano, F.X.; Vega, N.; Rieusset, J.; Laville, M.; Guillet, C.; Boirie, Y.; Wallberg-Henriksson, H.; et al. Expression of Mfn2, the Charcot-Marie-Tooth neuropathy type 2A gene, in human skeletal muscle: effects of type 2 diabetes, obesity, weight loss, and the regulatory role of tumor necrosis factor alpha and interleukin-6. *Diabetes* 2005, *54*, 2685-2693.

69.   Sebastián, D.; Hernández-Alvarez, M.I.; Segalés, J.; Sorianello, E.; Muñoz, J.P.; Sala, D.; Waget, A.; Liesa, M.; Paz, J.C.; Gopalacharyulu, P.; et al. Mitofusin 2 (Mfn2) links mitochondrial and endoplasmic reticulum function with insulin signaling and is essential for normal glucose homeostasis. *Proc Natl Acad Sci U S A* 2012, *109*, 5523-5528, doi:10.1073/pnas.1108220109.

70.   Schneeberger, M.; Dietrich, M.O.; Sebastián, D.; Imbernón, M.; Castaño, C.; Garcia, A.; Esteban, Y.; Gonzalez-Franquesa, A.; Rodríguez, I.C.; Bortolozzi, A.; et al. Mitofusin 2 in POMC neurons connects ER stress with leptin resistance and energy imbalance. *Cell* 2013, *155*, 172-187, doi:10.1016/j.cell.2013.09.003.

71.   Bach, D.; Pich, S.; Soriano, F.X.; Vega, N.; Baumgartner, B.; Oriola, J.; Daugaard, J.R.; Lloberas, J.; Camps, M.; Zierath, J.R.; et al. Mitofusin-2 determines mitochondrial network architecture and mitochondrial metabolism. A novel regulatory mechanism altered in obesity. *J Biol Chem* 2003, *278*, 17190-17197, doi:10.1074/jbc.M212754200.

72.   Pich, S.; Bach, D.; Briones, P.; Liesa, M.; Camps, M.; Testar, X.; Palacín, M.; Zorzano, A. The Charcot-Marie-Tooth type 2A gene product, Mfn2, up-regulates fuel oxidation through expression of OXPHOS system. *Hum Mol Genet* 2005, *14*, 1405-1415, doi:10.1093/hmg/ddi149.

73.   Chen, H.; Chomyn, A.; Chan, D.C. Disruption of fusion results in mitochondrial heterogeneity and dysfunction. *J Biol Chem* 2005, *280*, 26185-26192, doi:10.1074/jbc.M503062200.

74.   Kawalec, M.; Boratyńska-Jasińska, A.; Beręsewicz, M.; Dymkowska, D.; Zabłocki, K.; Zabłocka, B. Mitofusin 2 Deficiency Affects Energy Metabolism and Mitochondrial Biogenesis in MEF Cells. *PLoS One* 2015, *10*, e0134162, doi:10.1371/journal.pone.0134162.

75.   Puigserver, P.; Wu, Z.; Park, C.W.; Graves, R.; Wright, M.; Spiegelman, B.M. A cold-inducible coactivator of nuclear receptors linked to adaptive thermogenesis. *Cell* 1998, *92*, 829-839, doi:10.1016/s0092-8674(00)81410-5.

44

76. Soriano, F.X.; Liesa, M.; Bach, D.; Chan, D.C.; Palacin, M.; Zorzano, A. Evidence for a mitochondrial regulatory pathway defined by peroxisome proliferator-activated receptor-gamma coactivator-1 alpha, estrogen-related receptor-alpha, and mitofusin 2. *Diabetes* 2006, *55*, 1783-1791.

77. Liesa, M.; Borda-d'Agua, B.; Medina-Gómez, G.; Lelliott, C.J.; Paz, J.C.; Rojo, M.; Palacín, M.; Vidal-Puig, A.; Zorzano, A. Mitochondrial fusion is increased by the nuclear coactivator PGC-1beta. *PLoS One* 2008, *3*, e3613, doi:10.1371/journal.pone.0003613.

78. Kirino, T.; Sano, K. Selective vulnerability in the gerbil hippocampus following transient ischemia. *Acta Neuropathol.* 1984, *62*, 201-208.

79. Gadamski, R.; Mossakowski, M.J. Asymatric demage of the CA1 sector of ammon's horn after short-term forebrain ischemia in Mongolian gerbils. *Neropatologia Polska* 1992, *30*, 209-219.

80. Domañska-Janik, K.; Buzañska, L.; Dłuzniewska, J.; Kozłowska, H.; Sarnowska, A.; Zabłocka, B. Neuroprotection by cyclosporin A following transient brain ischemia correlates with the inhibition of the early efflux of cytochrome C to cytoplasm. *Brain Res Mol Brain Res* 2004, *121*, 50-59, doi:10.1016/j.molbrainres.2003.11.006.

81. Dagda, R.K.; Cherra, S.J.; Kulich, S.M.; Tandon, A.; Park, D.; Chu, C.T. Loss of PINK1 function promotes mitophagy through effects on oxidative stress and mitochondrial fission. *J Biol Chem* 2009, *284*, 13843-13855, doi:10.1074/jbc.M808515200.

82. Lam, J.; Katti, P.; Biete, M.; Mungai, M.; AshShareef, S.; Neikirk, K.; Garza Lopez, E.; Vue, Z.; Christensen, T.A.; Beasley, H.K.; et al. A Universal Approach to Analyzing Transmission Electron Microscopy with ImageJ. *Cells* 2021, *10*, doi:10.3390/cells10092177.

83. Van Laar, V.S.; Roy, N.; Liu, A.; Rajprohat, S.; Arnold, B.; Dukes, A.A.; Holbein, C.D.; Berman, S.B. Glutamate excitotoxicity in neurons triggers mitochondrial and endoplasmic reticulum accumulation of Parkin, and, in the presence of N-acetyl cysteine, mitophagy. *Neurobiol Dis* 2015, *74*, 180-193, doi:10.1016/j.nbd.2014.11.015.

84. Kumar, R.; Bukowski, M.J.; Wider, J.M.; Reynolds, C.A.; Calo, L.; Lepore, B.; Tousignant, R.; Jones, M.; Przyklenk, K.; Sanderson, T.H. Mitochondrial dynamics following global cerebral ischemia. *Mol Cell Neurosci* 2016, *76*, 68-75, doi:10.1016/j.mcn.2016.08.010.

85. Kislin, M.; Sword, J.; Fomitcheva, I.V.; Croom, D.; Pryazhnikov, E.; Lihavainen, E.; Toptunov, D.; Rauvala, H.; Ribeiro, A.S.; Khiroug, L.; et al. Reversible Disruption of Neuronal Mitochondria by Ischemic and Traumatic Injury Revealed by Quantitative Two-Photon Imaging in the Neocortex of Anesthetized Mice. *J Neurosci* 2017, *37*, 333-348, doi:10.1523/JNEUROSCI.1510-16.2016.

86. Zhao, Y.X.; Cui, M.; Chen, S.F.; Dong, Q.; Liu, X.Y. Amelioration of ischemic mitochondrial injury and Bax-dependent outer membrane permeabilization by Mdivi-1. *CNS Neurosci Ther* 2014, *20*, 528-538, doi:10.1111/cns.12266.

87. Zhang, N.; Wang, S.; Li, Y.; Che, L.; Zhao, Q. A selective inhibitor of Drp1, mdivi-1, acts against cerebral ischemia/reperfusion injury via an anti-apoptotic

pathway in rats. *Neurosci Lett* 2013, *535*, 104-109, doi:10.1016/j.neulet.2012.12.049.

88. Tang, Y.; Liu, X.; Zhao, J.; Tan, X.; Liu, B.; Zhang, G.; Sun, L.; Han, D.; Chen, H.; Wang, M. Hypothermia-induced ischemic tolerance is associated with Drp1 inhibition in cerebral ischemia-reperfusion injury of mice. *Brain Res* 2016, *1646*, 73-83, doi:10.1016/j.brainres.2016.05.042.

89. Grohm, J.; Kim, S.W.; Mamrak, U.; Tobaben, S.; Cassidy-Stone, A.; Nunnari, J.; Plesnila, N.; Culmsee, C. Inhibition of Drp1 provides neuroprotection in vitro and in vivo. *Cell Death Differ* 2012, *19*, 1446-1458, doi:10.1038/cdd.2012.18.

90. Zuo, W.; Yang, P.F.; Chen, J.; Zhang, Z.; Chen, N.H. Drp-1, a potential therapeutic target for brain ischaemic stroke. *Br J Pharmacol* 2016, *173*, 1665-1677, doi:10.1111/bph.13468.

91. Peng, C.; Rao, W.; Zhang, L.; Wang, K.; Hui, H.; Wang, L.; Su, N.; Luo, P.; Hao, Y.L.; Tu, Y.; et al. Mitofusin 2 ameliorates hypoxia-induced apoptosis via mitochondrial function and signaling pathways. *Int J Biochem Cell Biol* 2015, *69*, 29-40, doi:10.1016/j.biocel.2015.09.011.

92. Martorell-Riera, A.; Segarra-Mondejar, M.; Muñoz, J.P.; Ginet, V.; Olloquequi, J.; Pérez-Clausell, J.; Palacín, M.; Reina, M.; Puyal, J.; Zorzano, A.; et al. Mfn2 downregulation in excitotoxicity causes mitochondrial dysfunction and delayed neuronal death. *EMBO J* 2014, *33*, 2388-2407, doi:10.15252/embj.201488327.

93. Barsoum, M.J.; Yuan, H.; Gerencser, A.A.; Liot, G.; Kushnareva, Y.; Gräber, S.; Kovacs, I.; Lee, W.D.; Waggoner, J.; Cui, J.; et al. Nitric oxide-induced mitochondrial fission is regulated by dynamin-related GTPases in neurons. *EMBO J* 2006, *25*, 3900-3911, doi:10.1038/sj.emboj.7601253.

94. Anzell, A.R.; Maizy, R.; Przyklenk, K.; Sanderson, T.H. Mitochondrial Quality Control and Disease: Insights into Ischemia-Reperfusion Injury. *Mol Neurobiol* 2018, *55*, 2547-2564, doi:10.1007/s12035-017-0503-9.

95. Zhang, X.; Yan, H.; Yuan, Y.; Gao, J.; Shen, Z.; Cheng, Y.; Shen, Y.; Wang, R.R.; Wang, X.; Hu, W.W.; et al. Cerebral ischemia-reperfusion-induced autophagy protects against neuronal injury by mitochondrial clearance. *Autophagy* 2013, *9*, 1321-1333, doi:10.4161/auto.25132.

96. Racay, P.; Tatarková, Z.; Drgová, A.; Kaplan, P.; Dobrota, D. Ischemia-reperfusion induces inhibition of mitochondrial protein synthesis and cytochrome c oxidase activity in rat hippocampus. *Physiol Res* 2009, *58*, 127-138, doi:10.33549/physiolres.931383.

97. DeGracia, D.J.; Kumar, R.; Owen, C.R.; Krause, G.S.; White, B.C. Molecular pathways of protein synthesis inhibition during brain reperfusion: implications for neuronal survival or death. *J Cereb Blood Flow Metab* 2002, *22*, 127-141, doi:10.1097/00004647-200202000-00001.

98. Shi, R.Y.; Zhu, S.H.; Li, V.; Gibson, S.B.; Xu, X.S.; Kong, J.M. BNIP3 interacting with LC3 triggers excessive mitophagy in delayed neuronal death in stroke. *CNS Neurosci Ther* 2014, *20*, 1045-1055, doi:10.1111/cns.12325.

99. Zhang, Y.; Xu, H. Translational regulation of mitochondrial biogenesis. *Biochem Soc Trans* 2016, *44*, 1717-1724, doi:10.1042/BST20160071C.

46

100. Wu, S.; Zhou, F.; Zhang, Z.; Xing, D. Mitochondrial oxidative stress causes mitochondrial fragmentation via differential modulation of mitochondrial fission-fusion proteins. *FEBS J* 2011, *278*, 941-954, doi:10.1111/j.1742-4658.2011.08010.x.

101. Bhat, A.H.; Dar, K.B.; Anees, S.; Zargar, M.A.; Masood, A.; Sofi, M.A.; Ganie, S.A. Oxidative stress, mitochondrial dysfunction and neurodegenerative diseases; a mechanistic insight. *Biomed Pharmacother* 2015, *74*, 101-110, doi:10.1016/j.biopha.2015.07.025.

102. Valerio, A.; Bertolotti, P.; Delbarba, A.; Perego, C.; Dossena, M.; Ragni, M.; Spano, P.; Carruba, M.O.; De Simoni, M.G.; Nisoli, E. Glycogen synthase kinase-3 inhibition reduces ischemic cerebral damage, restores impaired mitochondrial biogenesis and prevents ROS production. *J Neurochem* 2011, *116*, 1148-1159, doi:10.1111/j.1471-4159.2011.07171.x.

103. Ojuka, E.O.; Jones, T.E.; Han, D.H.; Chen, M.; Holloszy, J.O. Raising Ca2+ in L6 myotubes mimics effects of exercise on mitochondrial biogenesis in muscle. *FASEB J* 2003, *17*, 675-681, doi:10.1096/fj.02-0951com.

104. Wright, D.C.; Geiger, P.C.; Han, D.H.; Jones, T.E.; Holloszy, J.O. Calcium induces increases in peroxisome proliferator-activated receptor gamma coactivator-1alpha and mitochondrial biogenesis by a pathway leading to p38 mitogen-activated protein kinase activation. *J Biol Chem* 2007, *282*, 18793-18799, doi:10.1074/jbc.M611252200.

105. Dibble, C.C.; Cantley, L.C. Regulation of mTORC1 by PI3K signaling. *Trends Cell Biol* 2015, *25*, 545-555, doi:10.1016/j.tcb.2015.06.002.

106. LaGory, E.L.; Wu, C.; Taniguchi, C.M.; Ding, C.C.; Chi, J.T.; von Eyben, R.; Scott, D.A.; Richardson, A.D.; Giaccia, A.J. Suppression of PGC-1α Is Critical for Reprogramming Oxidative Metabolism in Renal Cell Carcinoma. *Cell Rep* 2015, *12*, 116-127, doi:10.1016/j.celrep.2015.06.006.

107. Kuroda, Y.; Mitsui, T.; Kunishige, M.; Shono, M.; Akaike, M.; Azuma, H.; Matsumoto, T. Parkin enhances mitochondrial biogenesis in proliferating cells. *Hum Mol Genet* 2006, *15*, 883-895, doi:10.1093/hmg/ddl006.

108. Pilsl, A.; Winklhofer, K.F. Parkin, PINK1 and mitochondrial integrity: emerging concepts of mitochondrial dysfunction in Parkinson's disease. *Acta Neuropathol* 2012, *123*, 173-188, doi:10.1007/s00401-011-0902-3.

109. Shin, J.H.; Ko, H.S.; Kang, H.; Lee, Y.; Lee, Y.I.; Pletinkova, O.; Troconso, J.C.; Dawson, V.L.; Dawson, T.M. PARIS (ZNF746) repression of PGC-1α contributes to neurodegeneration in Parkinson's disease. *Cell* 2011, *144*, 689-702, doi:10.1016/j.cell.2011.02.010.

110. Cartoni, R.; Léger, B.; Hock, M.B.; Praz, M.; Crettenand, A.; Pich, S.; Ziltener, J.L.; Luthi, F.; Dériaz, O.; Zorzano, A.; et al. Mitofusins 1/2 and ERRalpha expression are increased in human skeletal muscle after physical exercise. *J Physiol* 2005, *567*, 349-358, doi:10.1113/jphysiol.2005.092031.

48

WSKAŹNIK ODDZIAŁYWANIA

Wskaźnik oddziaływania (IF) publikacji wchodzących w skład rozprawy doktorskiej:

Publikacja I

Kawalec M, Wojtyniak P, Bielska E, Lewczuk A, Boratyńska-Jasińska A, Beręsewicz-Haller M, Frontczak-Baniewicz M, Gewartowska M, Zabłocka B. Mitochondrial dynamics, elimination and biogenesis during post-ischemic recovery in ischemia-resistant and ischemia-vulnerable gerbil hippocampal regions. *Biochim Biophys Acta Mol Basis Dis.* 2022 Dec 22:166633. doi: 10.1016/j.bbadis.2022.166633 (**IF = 6.633**)

Publikacja II

Wojtyniak P., Boratynska-Jasinska A., Serwach K., Gruszczynska-Biegala J., Zablocka B., Jaworski J., Kawalec K. Mitofusin 2 Integrates Mitochondrial Network Remodelling, Mitophagy and Renewal of Respiratory Chain Proteins in Neurons after Oxygen and Glucose Deprivation. *Mol Neurobiol* 59, 6502–6518 (2022). doi: 10.1007/s12035-022-02981-6 (**IF = 5.686**)

PUBLIKACJA I

Kawalec M, <u>Wojtyniak P</u>, Bielska E, Lewczuk A, Boratyńska-Jasińska A, Beręsewicz-Haller M, Frontczak-Baniewicz M, Gewartowska M, Zabłocka B. Mitochondrial dynamics, elimination and biogenesis during post-ischemic recovery in ischemia-resistant and ischemia-vulnerable gerbil hippocampal regions. *Biochim Biophys Acta Mol Basis Dis*. 2022 Dec 22:166633. doi: 10.1016/j.bbadis.2022.166633.

51

Mitochondrial dynamics, elimination and biogenesis during post-ischemic recovery in ischemia-resistant and ischemia-vulnerable gerbil hippocampal regions

Maria Kawalec [a,*,1], Piotr Wojtyniak [a,1], Ewelina Bielska [a], Anita Lewczuk [a], Anna Boratyńska-Jasińska [a], Małgorzata Beręsewicz-Haller [a], Małgorzata Frontczak-Baniewicz [b], Magdalena Gewartowska [b], Barbara Zabłocka [a]

[a] Molecular Biology Unit, Mossakowski Medical Research Institute, Polish Academy of Sciences, Warsaw, Poland
[b] Electron Microscopy Research Unit, Mossakowski Medical Research Institute, Polish Academy of Sciences, Warsaw, Poland

ARTICLE INFO

ABSTRACT

Transient ischemic attacks (TIA) result from a temporary blockage in blood circulation in the brain. As TIAs cause disabilities and often precede full-scale strokes, the effects of TIA are investigated to develop neuroprotective therapies. We analyzed changes in mitochondrial network dynamics, mitophagy and biogenesis in sections of gerbil hippocampus characterized by a different neuronal survival rate after 5-minute ischemia-reperfusion (I/R) insult.

Our research revealed a significantly greater mtDNA/nDNA ratio in CA2–3, DG hippocampal regions (5.8 ± 1.4 vs 3.6 ± 0.8 in CA1) that corresponded to a neuronal resistance to I/R. During reperfusion, an increase of pro-fission (phospho-Ser616-Drp1/Drp1) and pro-fusion proteins (1.6 ± 0.5 and 1.4 ± 0.3 for Mfn2 and Opa1, respectively) was observed in CA2–3, DG. Selective autophagy markers, PINK1 and SQSTM1/p62, were elevated 24-96 h after I/R and accompanied by significant elevation of transcription factors proteins PGC-1α and Nrf1 (1.2 ± 0.4, 1.78 ± 0.6, respectively) and increased respiratory chain proteins (e.g., 1.5 ± 0.3 for complex IV at I/R 96 h).

Contrastingly, decreased enzymatic activity of citrate synthase, reduced Hsp60 protein level and electron transport chain subunits (0.88 ± 0.03, 0.74 ± 0.1 and 0.71 ± 0.1 for complex IV at I/R 96 h, respectively) were observed in I/R-vulnerable CA1. The phospho-Ser616-Drp1/Drp1 was increased while Mfn2 and total Opa1 reduced to 0.88 ± 0.1 and 0.77 ± 0.17, respectively. General autophagy, measured as LC3-II/I ratio, was activated 3 h after reperfusion reaching 2.37 ± 0.9 of control.

This study demonstrated that enhanced mitochondrial fusion, followed by late and selective mitophagy and mitochondrial biogenesis might together contribute to reduced susceptibility to TIA.

1. Introduction

Transient brain ischemic attacks (TIAs) are becoming more and more frequent in aging and post-Covid-19 society [1,2]. TIA is a temporary blockage of blood flow to the brain. Since it does not always cause extensive but only regional permanent damage, it is often ignored. TIAs may signal a full-blown stroke ahead [3]. Therefore, intracellular mechanisms of neuronal death and protection have been studied to elaborate on therapeutic approaches that enhance functional recovery of damaged neurons in TIA patients [4].

Mitochondria have been established the key mediators in neuronal survival. More and more evidence demonstrates that neuronal survival under the ischemic stress is not determined by a single molecular pathway but it depends on a range of complex relations between mechanisms which regulate mitochondrial content and quality.

Mitochondria are organized in a dynamic network which may be remodeled in response to various intra- and extracellular stimuli by continued mitochondrial fusion and fission events [5]. Proper

---

mitochondrial fusion involves the sequential merge of the outer (OMM) and inner (IMM) mitochondrial membranes of two distinct mitochondria. Large GTPases: mitofusin 1 (Mfn1) and mitofusin 2 (Mfn2) are required for OMM fusion [6], while dynamin-like 120 kDa protein (Opa1) mediates the fusion of IMM [7]. Furthermore, the dynamin-related protein 1 (Drp1) is a key regulator of the counteracting process of mitochondrial fission with the activity being regulated by its phosphorylation [8].

A role of mitochondrial network dynamics in response to ischemia-reperfusion injury has already been studied and various relationships have been described [9–13,87]. Enhanced mitochondrial fission is observed as a frequent consequence of ischemic injury preceding apoptotic neuronal death [10,15] while increased mitochondrial fusion emerges as a pro-survival response of post-ischemic neurons, supporting the maintenance of normal mitochondrial morphology and function [12,13]. An inhibition of mitochondrial fission was observed to produce a protective effect in I/R neuronal injury in both, in vitro and in vivo models [9,16–18]. As observed later on, maintained phosphorylation of Drp1 at Ser637 improved mitochondrial respiratory capacity, Ca^{2-} homeostasis, and it attenuated superoxide production in response to ischemia and excitotoxicity in vitro and ex vivo [11], thereby demonstrating that the status of mitochondrial connectivity and Drp1 phosphorylation play a critical role in determining the severity of cerebral ischemic injury. Accordingly, an overexpression of pro-fusion agents, like Mfn2 or Opa1, also exerts a neuroprotective effect in I/R injury [14,19], pointing to pro-survival effects of mitochondrial fusion and providing further support for the existing link between mitochondrial network dynamics and neuronal survival.

The neuronal dependence on proper mitochondrial dynamics is also reflected by the fact that mutations in genes that code the key proteins mediating mitochondrial fusion and fission were reported to lead to neurodegenerative diseases, like Charcot-Marie-Tooth 2A for Mfn2 [5], dominant optic atrophy for Opa1 [20,21] and progressive paroxysmal dystonia for Drp1 [22]. As shown by Kandimalla et al., Drp1 is also implicated in pathogenesis of Alzheimer's disease and reduced Drp1 is beneficial in a symptomatic-transgenic Tau mice [23].

Mitochondrial fission is considered to be a form of a quality control mechanism, as it enables the segregation and elimination of damaged mitochondria, while mitochondrial fusion supports the restoration of the mitochondrial function leading to content exchange and the maximization of the oxidative capacities of the cell [24]. Enhanced mitochondrial dynamics may mitigate mild mitochondrial damage, while severely damaged mitochondria undergo proteolytic elimination. Mitochondria may be eliminated through general autophagy when the whole cytoplasmic region may be engulfed and degraded. A drop in mitochondrial membrane potential caused by blood flow cessation and adenosine triphosphate (ATP) depletion may cause PINK1 accumulation and Parkin recruitment to mitochondria, leading to selective mitochondrial elimination. By means of the electron microscopy, it was shown that ischemia induced synaptic autophagy which may contribute to the neuronal death in the CA1 area in the model of transient global ischemia [25]. Furthermore, in neonatal hypoxia-ischemia model (HI), mitophagy was upregulated immediately after the HI episode and then followed by a second mitophagic wave 7 days later [26]. As shown by western blot, both PINK1/Parkin-dependent and -independent mechanisms were upregulated immediately after HI, whereas a PINK1/Parkin-dependent mechanism predominated 7 days after HI. It was further hypothesized that excessive mitophagy in the early phase contributed to pathologic secondary energy depletion, whereas late mitophagy might be involved in post-HI regeneration and repair [26], presenting divergent effects of mitochondria elimination on neuronal survival.

Mitochondrial biogenesis constitutes an opposite mechanism, complementary to mitochondrial elimination. PGC-1α, a master regulator of mitochondria biogenesis, regulates Nrf1 and Tfam expression and together with PINK1 and Parkin contributes to up- or downregulation of mitochondrial proteins, respectively. Unbalanced mitophagy/

autophagy may have detrimental effects on neurons, while increased mitochondria biogenesis may ameliorate neuronal damage thereby preventing bioenergetic failure [27]. Activation of PGC-1α, and the subsequent mitochondrial biogenesis, are neuroprotective mechanisms in brain injury caused by systemic prenatal HI, thus, PGC-1α promotion might be a potential treatment applied as protection against hippocampal injury and cognitive defects after intrauterine HI [28]. Moreover, activation of PGC-1α-mediated mitochondrial biogenesis proved to be neuroprotective also in ischemia-preconditioning model and subsequent middle cerebral artery occlusion (MCAO) [29]. Additionally, Al Rahim et al. [30] measured the increase in mitochondrial DNA content and up-regulation of mitochondrial proteins COXIV and Hsp60 and observed that proper regulation of mitochondrial biogenesis was necessary for neuronal survival in HI model [30]. Therefore, the promotion of PGC-1α appears promising as a potential treatment solution to prevent hippocampal injury and cognitive defects after intrauterine HI [28].

Still, the precise role and relation between these molecular events in neuronal survival is not fully elucidated, nor is the mechanism underlying higher TIA tolerance in particular brain regions.

Therefore, the main goal of this study was to further elucidate the role of mitochondrial elimination and renewal in neuronal survival after transient brain ischemia. To address this issue we used a unique model elaborated by Kirino et al., where the same ischemia-reperfusion insult resulted in different rates of neuronal death in particular hippocampal regions [31,32]. We presumed that, in response to I/R, damaged mitochondria were supposed to be eliminated via autophagy and/or rescued by mitochondrial content mixing caused by intensified mitochondrial fusion and fission. Mitochondrial biogenesis may be needed to maintain sufficient pool of proper mitochondria and ATP production. We further hypothesized that different susceptibility of neurons in hippocampal CA1 and CA2–3, DG to I/R might result from different implications of these phenomena in neuronal response.

2. Materials and methods

2.1. Ethical statement and animals

Mongolian gerbils (*Meriones unguiculatus*) were obtained from the Animal House of the Mossakowski Medical Research Institute of the Polish Academy of Sciences. Animal care was in accordance with the European Communities Council Directive (86/609/EEC). The experimental procedures were approved by the Local Commission for the Ethics of Animal Experimentation no. 2 in Warsaw (385/2017 and WAW2/032/2021) and every effort was made to minimize animal suffering and to reduce the number of specimens used. Animals were randomized for the experiments.

2.2. Transient cerebral ischemia in gerbils

Male adult gerbils weighing 60–70 g were subjected to transient cerebral ischemia by 5-min bilateral ligation of common carotid arteries under isoflurane anesthesia, in strictly controlled normothermic conditions as described previously [31,33]. Sham animals, which underwent the same surgical procedure, but without the actual ligation, served as controls. The animals recovered for 3–96 h after ischemia. Then brains were isolated to obtain CA1 and CA2–3, DG regions of hippocampus for further processing or animals were perfused for histological evaluation. Hippocampi from sham operated animals served as controls. Tissues intended for DNA extraction were stored at −20 °C.

2.3. Hematoxylin and eosin staining

Histological examination was performed on gerbils' brain from control and ischemic individuals (24, 48, 72 and 96 h of reperfusion) as describes earlier [34]. After perfusion with 4 % paraformaldehyde, the

2

54

isolated brains were dehydrated in a series of ethanol and xylene baths and embedded in paraffin wax. Sections of 5–7 μm were stained with hematoxylin and eosin (HE). The microscopic evaluation was performed with Axiolab light microscope at 40× and 400× magnification with Axiocam and ZEN 3.0 software for photographic documentation.

2.4. Transmission Electron Microscopy (TEM)

The specimens were sequentially fixed in 2 % paraformaldehyde, 2.5 % glutaraldehyde in cacodylate buffer, and 1 % osmium tetraoxide with potassium ferricyanide for 2 h. Then, the samples were dehydrated in a series of ethanol baths and embedded in resin. The ultra-thin sections were stained with uranyl acetate and lead citrate. The images were acquired in randomized way using JEM-1011 EX (Jeol, Tokyo, Japan) transmission electron microscope equipped with MORADA camera and iTEM 1233 software.

Series of images from different conditions were analyzed with ImageJ software and mitochondria in the cells' soma were quantified morphometrically. The inverse of circularity was used as a measure of mitochondrial elongation and the area/perimeter normalized to circularity parameter was used to calculate mitochondrial swelling, as validated elsewhere [35–37] while mitochondrial content was represented by the total area occupied by mitochondria normalized to the area of the measured cell. 28–43 neurons per condition and at least 22 mitochondria per cell body (907–1165 mitochondria per time point) were quantified.

2.5. Immunoblotting

For western blotting, isolated hippocampal sectors were homogenized in Cell Lysis Buffer (Cell Signalling Technology, Danvers, USA; #9803) containing 1 mM PMSF (Sigma-Aldrich, Poznań, Poland) and kept on ice for additional 5 min for lysis. The samples were sonicated and centrifuged at 14,000 ×g for 10 min at 4 °C. The supernatants were collected, and a Modified Lowry Protein Assay (Thermo Fisher Scientific, Grand Island, NY, USA; #23240) was performed to determine the total protein concentration. Samples were diluted in a reducing sample buffer and boiled at 100 °C for 5 min. Following manufacturer guidelines, the samples were not boiled for western blotting with anti-OXPHOS antibody cocktail.

Equal amounts of protein, 50 μg (for anti-LC3 and anti-OXPHOS) or 20 μg (others) were loaded onto SDS-PAGE gels (self-prepared or gradient Mini-PROTEAN TGX Precast Protein Gels, Bio-Rad Laboratories, Hercules, CA, USA), electro-transferred onto nitrocellulose (Amersham, Sigma-Aldrich) membrane [38] and stained for total protein with 0.1 % Ponceau S (Sigma-Aldrich). Following imaging of the total protein, the membranes were blocked with 5 % non-fat milk in Tris-buffered saline (TBS) with 0.1 % Tween 20 (TBST) for 1 h at room temperature. Thereafter, membranes were incubated with the appropriate primary antibodies diluted in TBST or 2.5 % milk/TBST at 4 °C overnight, including anti-Mfn1 (1:1000, Novus Biologicals, Centennial, CO, USA, NBP1-71775), anti-Mfn2 (1:1000, Sigma-Aldrich, M6319), anti-OPA1 (1:1000, Cell Signaling Technology, 80471), anti-Phospho-Drp1 (1:1000, Thermo Fisher Scientific, PA5-64821), anti-Drp1 (1:1000, Cell Signaling Technology,14647S), anti-PINK1(1:250, Santa Cruz Biotechnology, Santa Cruz, CA, USA, sc-517353), anti-Parkin (1:1000, Cell Signaling Technology, 4211), anti- SQSTM1/p62 (1:1000, Cell Signaling Technology,23214S), anti-LC3 (1:1000, Cell Signaling Technology, 12741S), anti-PGC-1α (1:250, Santa Cruz Biotechnology, sc-518025), anti-Nrf1 (1:250; Santa Cruz Biotechnology, sc-28379), anti-Tfam (1:500, Genway Biotech, San Diego, CA, USA, GWB-22C6C2), anti-Hsp60 (1:1000, Cell Signaling Technology, 12165S), anti-TOM20 (1:1000, Cell Signaling Technology, 42406S), anti-OXPHOS (1:500; Abcam, Cambridge, UK, ab110413). The membranes were washed and incubated with the following peroxidase-conjugated secondary antibodies: anti-mouse (Sigma-Aldrich, A9044) or anti-

rabbit (Sigma-Aldrich, A0545) diluted in 5 % non-fat dried milk in TBST for 30 min at room temperature. Bound antibodies were visualized by Amersham ECL Western Blotting Detection Reagent (Sigma-Aldrich, RPN2106). Blots were imaged and quantified using the Fusion FX imaging system (Vilber Lourmat, Marne-la-Vallée, France). The band intensities of the proteins of interest were normalized to the total protein optic densities corresponding to the same lane and quantified using ImageJ software with gel analyzer feature (NIH, Bethesda, MD, USA) as shown by Thacker et al. [39] and discussed by Moritz [40].

2.6. DNA extraction and Real-Time qPCR

Total DNA was purified using E.Z.N.A. MicroElute Genomic DNA Kit (Omega Bio-tek, Norcross, GA, USA; D3096-02). Tissues were processed according to the manufacturer's instructions. Purity (absorbance ratio at 260/280) and concentration of DNA samples were determined spectroscopically using DeNovix DS-11 FX+ (DeNovix Inc., Wilmington, DE, USA).

A singleplex TaqMan RT-qPCR assay was established to measure the amount of gerbil mtDNA relative to the nuclear DNA (nDNA). This assay targets the mitochondrial ND1 gene (18129817) and the nuclear single-copy gene, glucagon [Gcg] (110548637) Primers and probes were designed using the Primer3web (https://primer3.ut.ee/) [41], based on the available DNA sequences of selected genes of *Meriones unguiculatus* in the National Center for Biotechnology Information (Bethesda, MD, USA) database. Primers and probes were synthesized by DNA Sequencing and Synthesis Facility (IBB PAN, Warsaw, Poland). Primers and probes are listed in Table 1.

The GCG probe was labeled at the 5′-end with 6-Carboxyfluorescein (6-FAM), while ND-1 probe was labeled with Hexachlorofluorescein (Hex) at the 5′-end. A quencher dye, Black Hole Quencher-1 (BHQ-1), was linked to the 3′-end of both probes. Primer amplification efficiencies were determined by construction of a standard curve using 5-fold serial dilutions of gerbil DNA template. Real-time PCR was performed in a MicroAmp EnduraPlate optical 96-well reaction plate (Applied Biosystems, Foster City, CA, USA) sealed with MicroAmp optical adhesive film (Applied Biosystems) on the ABI 7500 FAST Real-time PCR System (Applied Biosystems). The reaction mix (total volume 20 μl) consisted of: 10 μl TaqMan Fast Advanced Master Mix (Applied Biosystems, #4444963), 4 μl Nuclease-Free Water (Applied Biosystems), 2 μl mtDNA or nDNA primers (900 nM each), 2 μl mtDNA or nDNA probe (250 nM), 2 μl DNA (50 ng). The real-time PCR reactions were performed in triplicates for both genes. The temperature program was initiated with a polymerase activation at 95 °C for 2 min, followed by 40 cycles at 95 °C for 3 s and 60 °C for 30 s. Cycle threshold (Ct) values were determined using SDS 2.3 software (Applied Biosystems). Relative copy number was calculated using analysis of the difference in Ct between mtDNA and nDNA. Relative quantification was performed by the ΔΔCt method [42] and expressing the ratio as a fold-change of the calibrator – DNA from gerbil brain cortex – set as 1. RQ values were efficiency corrected by the software.

2.7. Citrate synthase activity assay

Enzymatic activity was measured using the Citrate Synthase Activity

Table 1
Primers and probes.

Target	Primer/probe name	Sequence (5′–3′)
mtDNA primers	ND1GerF	AGCAGTCGCTCAAACCATCT
	ND1GerR	CAGGCGGGAAGAACTAATCA
mtDNA probe	ND1613TM	AGCGGCTCCCTTTCCCTCCA
nDNA primers	GCG4820F	TTAACGGGTGGAGCATTAGG
	GCG5027R	GCATTGATTAAGCAGCGTCA
nDNA probe	GCG4983TM	AGAGCGCTTGCTCCTGCGGT

3

Assay Kit (Sigma-Aldrich, MAK193). The absorbance measurements were taken at 412 nm on microplate reader, Tecan INFINITE M1000 PRO with dedicated software (Tecan Group Ltd., Männedorf, Switzerland) with 6 readings over the 5 min time span and these readings were in the linear range of enzymatic activity. The total protein concentration was determined using a Modified Lowry Protein Assay (Thermo Fisher Scientific). Arbitrary enzymatic activity units were calculated according to the manual and normalized to the total protein concentration. Enzymatic activity is expressed in μmol/min/mg protein.

2.8. Statistical analysis

Statistical analysis was performed using GraphPad Prism (GraphPad Software, San Diego, CA, USA). Normally distributed data are presented as means ± standard deviation. Differences between three or more groups were analyzed using one-way ANOVA with Dunnett's post-hoc test (for comparisons to controls). Student's t-test was used to detect differences between two groups.

For the data with non-normal distribution (data based on TEM microphotographs: mitochondrial content, swelling and elongation) Kruskal-Wallis test followed by Dunn's multiple comparisons test was used and the results are presented as median (Q1 – Q3). p-Values <0.05 were considered significant. The distribution of data was analyzed by Shapiro-Wilk normality test.

3. Results

3.1. Ultrastructural and biochemical changes precede neuronal loss in CA1 triggered by ischemia-reperfusion

As shown by eosin/hematoxylin staining, 5-minute brain ischemia and subsequent reperfusion (I/R) in gerbils resulted in a selective and delayed reduction in the number of neurons in CA1 region (Fig. 1A), which is consistent with previously reported outcomes [31,32]. 24 and 48 h after I/R insult, the dense layout of pyramidal neurons in CA1 became more chaotic and looser, however, the morphology of neurons was still preserved as described earlier [43]. The first morphological signs of neuronal damage in CA1 were observed 72 h post ischemia, as neuronal shrinkage occurred as showed elsewhere [44]. At that time point a few cells with proper morphology were still present. Then, after 96 h, CA1 neurons showed a highly eosinophilic and shrunken architecture and condensed nuclei (red arrows).

Meanwhile, the morphology of CA2–3, DG after I/R was preserved. Even at 400× magnification, no significant changes in the morphology of this hippocampal sectors were observed. The morphological description is consistent with previous observations [43,45] and confirms the validity of the model.

By contrast, changes in the ultrastructure of hippocampal neurons were detected earlier, i.e., 24 h after I/R (Fig. 1B). In control groups, mitochondria showed an unchanged structure both in CA1 and CA2–3, DG neurons. Outer and inner mitochondrial membranes were consistent, mitochondrial cristae were preserved and mitochondrial matrix remained electron-dense. No signs of endoplasmic reticulum (ER) and Golgi Apparatus swelling were observed. However, in CA1 24 h after I/R, a great number of mitochondria lacked mitochondrial cristae. Mitochondrial matrix became lighter than in the control group. Morphological features of swelling of mitochondria, endoplasmic reticulum and Golgi apparatus occurred. Unbound ribosomes, detached from the ER, were detected in the cytoplasm. At the same time, ultrastructural changes in the CA2–3, DG region were not as pronounced as in CA1 and were manifested 48 h after I/R, as the structure of mitochondrial membranes and cristae in CA2–3, DG region became slightly blurred. Morphological features of swelling of the Golgi apparatus were not observed either. The ribosomes remained attached to the ER.

Mitochondrial damage caused by I/R in CA1-neurons was further confirmed by the analysis of the enzymatic activity of the citrate synthase (CS) in CA1 and CA2–3, DG homogenates (Fig. 1C). Citrate synthase is abundant in mitochondrial matrix and its enzymatic activity has already been analyzed to evaluate mitochondrial content [46]. The determined CS activity value in control CA1 reached 6 ± 1.1 μmol/min/mg, while in control CA2–3, DG: 5.3 ± 0.6 μmol/min/mg and no significant difference was observed between these hippocampal regions. A statistically significant decrease (0.88 ± 0.03 of control value, p < 0.01, n = 5) of CS enzymatic activity was observed in CA1 after I/R, while in CA2–3, DG this parameter was sustained.

Changes in mitochondrial content after I/R in CA1 were further demonstrated by a significant reduction of mitochondrial matrix Hsp60 immunodetection (0.74 ± 0.14, p < 0.001, n = 5), starting as early as at 3 h after the insult. Meanwhile, Hsp60 significantly increased in the ischemia-resistant hippocampal sectors reaching 1.6 ± 0.12 of control value (p < 0.001, n = 5) (Fig. 1D). Therefore, the loss of neurons in CA1, observed 72 h post I/R, was preceded by the severe damage of the mitochondrial ultrastructure and deterioration of the mitochondrial parameters represented by the citrate synthase enzymatic activity and Hsp60 protein level. Contrastingly, in CA2–3, DG mitochondrial damage was much less pronounced and manifested itself by a slightly blurred presentation of outer mitochondrial membrane. The internal structure of mitochondria was predominantly preserved, and it was not followed by the decrease in CS activity, nor in the immunodetection of mitochondrial protein marker.

3.2. Mitochondrial fission predominates in CA1, whereas in CA2–3 DG, both mitochondrial fusion and fission are enhanced in response to I/R

To analyze changes in the mitochondrial dynamics evoked by the transient ischemic insult and reperfusion western blot analysis of key proteins mediating mitochondrial fusion (Mfn1/2, Opa1) and mitochondrial fission (Drp1) were performed, as shown in Fig. 2.

In I/R-sensitive CA1, protein level of Mfn1 was sustained whereas Mfn2 and total Opa1 decreased in the time course of reperfusion (0.74 ± 0.16; p < 0.05 and 0.72 ± 0.12, p < 0.001, respectively). Meanwhile, in I/R-resistant regions of CA2–3, DG, an increase in all considered fusion proteins: Mfn1, Mfn2 and total Opa1 was observed (1.67 ± 0.61; p < 0.05, 1.63 ± 0,52; p < 0.001 and 1.33 ± 0.21, p < 0.001, respectively). For reference, protein levels of TOM20, another OMM protein, uninvolved in mitochondrial fusion and fission, were not altered (data not shown).

In addition to the analysis of total Opa1, changes in its long (L-Opa1) and short (S-Opa1) form were also investigated, as these two forms of Opa1 are involved in IMM fusion differently [47,48]. The values of L/S-Opa1 ratio did not change significantly in the course of reperfusion in any considered hippocampal regions, as both forms were reduced in CA1 and increased in CA2–3, DG. The L/S-Opa1 ratio for control CA1 and 96 h after I/R were: 9.9 ± 4.3 and 10.8 ± 4.8, respectively, while 11.0 ± 4.5 and 12.5 ± 5.1 for CA2–3, DG, pointing at the predominance of L-Opa1 over S-Opa1. The protein level of L-Opa1 in CA1 was significantly reduced 72 and 96 h after I/R (0.63 ± 0.15; p < 0.001 and 0.71 ± 0.17; p < 0.05). In CA2–3, DG the amount of L-Opa1 was increased at the same time points reaching: 1.26 ± 0.28; p < 0.05 and 1.30 ± 0.39; p < 0.01, respectively.

To investigate mitochondrial fission, phosphorylation of Drp1 protein at Ser 616 was measured. The results were expressed in relation to total Drp1. The phospho-Drp1/Drp1 ratio in control CA2–3, DG was half the level recorded in CA1 (0.41 ± 0.21; p < 0.01), however, a significant increase in phosphorylated Drp1 protein after I/R was observed in both hippocampal regions. In CA1 the maximal value of phospho-Drp1/Drp1 ratio was reached at 3 h after I/R (2.08 ± 0.49; p < 0.001) while in CA2–3, DG the highest values were observed later after the insult, reaching 4.14 ± 2.4 (p < 0.001).

Western blot analysis was followed by TEM observation on ultrastructure and intracellular distribution of mitochondria. As shown in Fig. 3A, mitochondria presented round or elongated shapes and could be

4
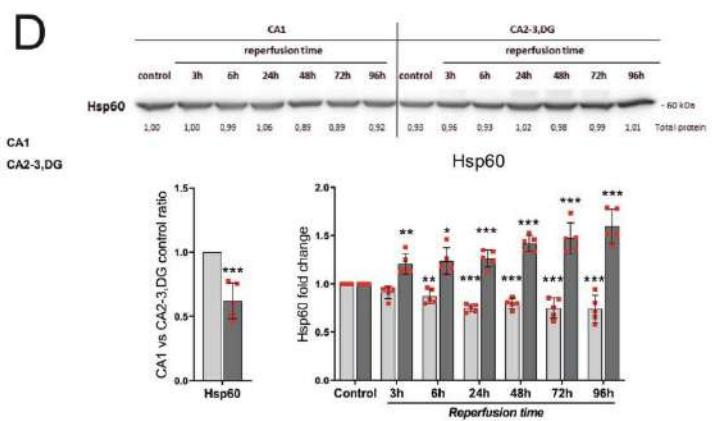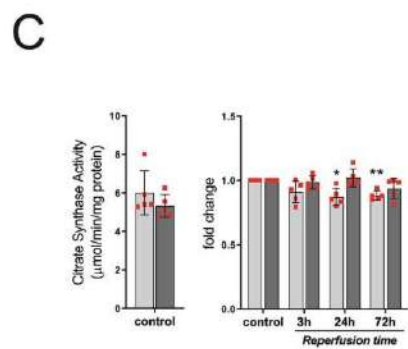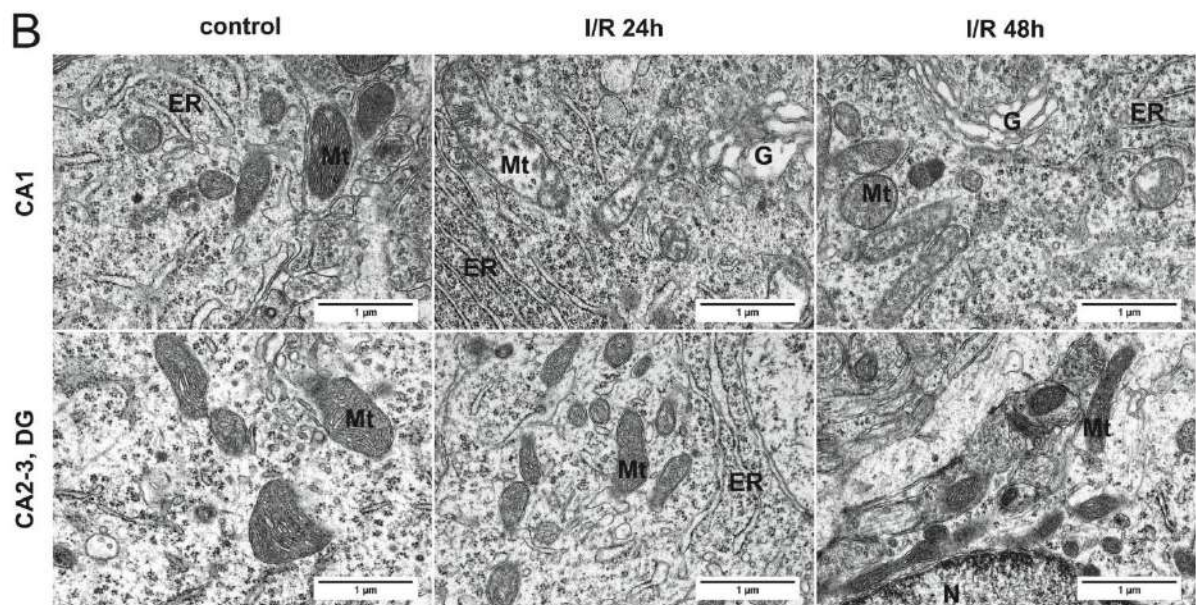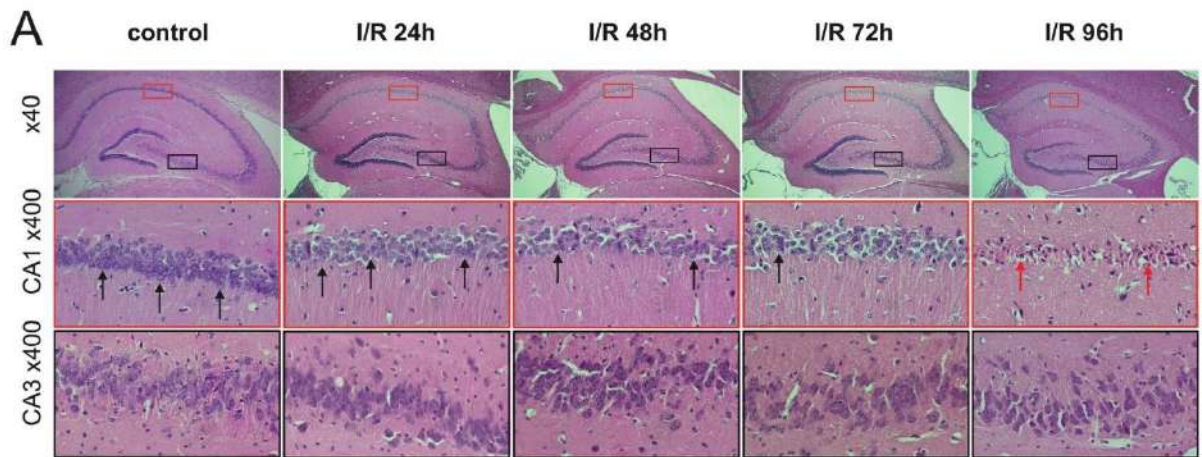
(caption on next page)

Fig. 1. Mitochondrial damage is more pronounced in CA1 over CA2–3, DG. Ultrastructural changes precede neuronal loss in CA1.

A. Hematoxylin and eosin staining of gerbil hippocampus in 40× and 400× magnifications. Black arrows - normal neurons, red arrows - highly eosinophilic and shrunken neurons with condensed nuclei.

B. Representative TEM images presenting the ultrastructure of mitochondria in I/R-sensitive (CA1) and I/R-resistant (CA2–3, DG) hippocampal regions. Mt. – mitochondria, ER- endoplasmic reticulum, G – Golgi apparatus.

C. Mean enzymatic activity of citrate synthase in CA1 and CA2–3, DG homogenates in controls and after I/R. Charts present mean values with standard deviation. Points represent biological replicates of the experiment. Student's t-test was applied for the comparison of CA1 and CA2–3, DG controls. One-way ANOVA followed by Dunnett's multiple comparisons test was applied for post-ischemia values for each part of hippocampus separately; n = 5; *p < 0.05, **p < 0.01 vs CA1 control.

D. Representative western blot and densitometric analysis of Hsp60 in CA1 and CA2–3, DG homogenates in controls and after I/R. Charts present mean values with standard deviation. Points represent biological replicates of the experiment. One Sample t-test was applied for the comparison of CA1 and CA2–3, DG controls. One-way ANOVA followed by Dunnett's multiple comparisons test was applied for post-ischemia values for each part of hippocampus separately; n = 5; *p < 0.05, **p < 0.01, ***p < 0.001 vs CA1 control or CA2–3, DG control, respectively. The optical density of the particular bands was normalized to the total protein in line stained with Ponceau S. Normalization factors are shown under representative western blot image.
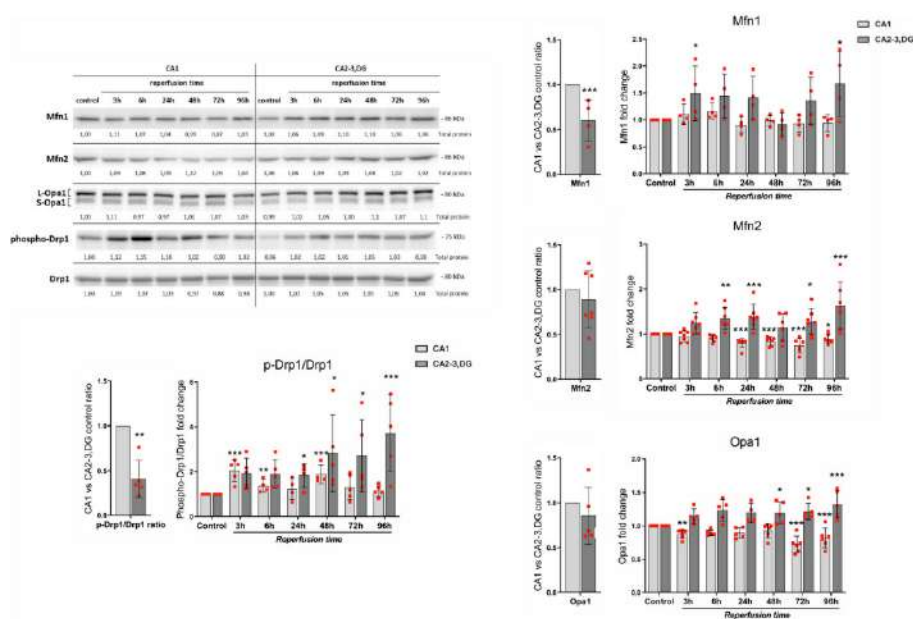

Fig. 2. Mitochondrial fission prevails in CA1 while in CA2–3, DG both, mitochondrial fission and fusion are enhanced after I/R.

Representative western blots and densitometric analysis of Mfn1, Mfn2, total Opa1 and phospho-Drp1/Drp1 ratio in CA1 and CA2–3, DG homogenates. Charts present mean values with standard deviation. Points represent biological replicates of the experiment. One Sample t-test was applied for the comparison of CA1 and CA2–3, DG controls. One-way ANOVA followed by Dunnett's multiple comparisons test was applied for post-ischemia values for each part of hippocampus separately; n = 6; *p < 0.05, **p < 0.01, ***p < 0.001 vs CA1 control or CA2–3, DG control, respectively. The optical density of the bands was normalized to the total protein in line stained with Ponceau S. Normalization factors are shown under representative western blot image.

easily spotted in the cell bodies and dendrites of control neurons. The signs of altered mitochondrial morphology were observed 24 h after I/R episode (Fig. 3A).

In CA1 the hallmarks of mitochondrial impairment, as damaged cristae and light mitochondrial matrix, were prominent and the mitochondria were mainly localized near the cell nucleus (Fig. 3A). This was accompanied by temporarily increased mitochondrial content (p < 0.01), as median (Q1-Q3) values were as follows: 5.1 (3.6–6.0) at 24 h post I/R versus 3.2 (2.7–3.8) for CA1 controls (Fig. 3B). Such change in this mitochondrial parameter might result from mitochondrial swelling, as was observed at TEM micrographs (Fig. 1B and 3A) and as further confirmed by significantly elevated parameter of mitochondrial area/perimeter normalized to circularity, reaching median value: 0.13 (0.10–0.19) in comparison to 0.09 (0.07–0.12) in control cells; p < 0.001 (Fig. 3C).

In CA2–3, DG mitochondria remained evenly located in the neuronal bodies, but an increasing number of elongated mitochondria was observed in reperfusion phase (Fig. 3 A). It was confirmed by a statistically significant rise of mitochondrial elongation parameter (Fig. 3 D), reaching median value at 24 and 48 I/R: 1.26 (1.08–1.67), p < 0.001 and 1.21 (1.07–1.62), p < 0.05, and was in agreement with elevated levels of fusion proteins in this hippocampal region (Fig. 2). Mitochondrial content also increased during reperfusion and 48 h after I/R a significant difference (p < 0.001) between CA1 and CA2–3, DG was observed: 2.60 (1.70–3.27) versus 4.69 (3.69–5.99), respectively (Fig. 3

B). Mitochondrial swelling was not observed and the parameter of area/perimeter normalized to circularity was even reduced during reperfusion to the value: 0.10 (0.08–0.14) in comparison to 0.11 (0.08–0.16) in control cells, p < 0.001 (Fig. 3 C).

Thus, in the course of reperfusion the predominance of the mitochondrial fission over mitochondrial fusion may be considered in CA1, while in CA2–3, DG an increased mitochondrial dynamics with signs of simultaneous activation of both mitochondrial fusion and fission might be observed together with an increase in mitochondrial content.

3.3. Postischemic mitochondrial elimination occurs in all hippocampal regions, but at different post-injury time points and via different intracellular mechanisms

It is considered that mitochondrial dynamics, especially mitochondrial fission, can facilitate mitochondrial degradation via autophagy. Here we used TEM observation together with the western blot analysis of key autophagy-involved proteins, mediating early (LC3-II/I ratio and SQSTM1/p62) stages of autophagic flux. Specific markers of selective autophagy of mitochondria, PINK1 and Parkin, were also analyzed.

According to TEM, hardly any autophagic structures were observed in CA1 and CA2–3, DG regions in control groups (Fig. 4A). A few single lysosomes could be spotted. The autophagic structures with clearly visible mitochondrial remnants were present in the CA1 24 h after the ischemic episode. Additionally, morphological features of swelling of
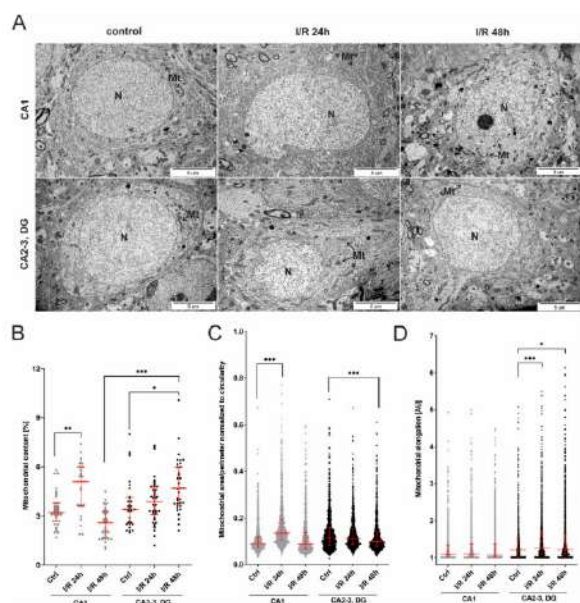
58

Fig. 3. Morphological features of mitochondria in CA1 and CA2–3, DG after I/R.

A. Representative TEM images presenting pyramidal neurons in CA1 and in CA2–3, DG. Mt. – mitochondria, N- nucleus.

B. Morphometric data on mitochondrial content (total area of mitochondria per cell soma area [%]). Points indicate number of neurons counted per time point (n = 28–43). Bars represent median with interquartile range (Q1 – Q3). Statistical significance was analyzed by Kruskal-Wallis Test followed by Dunn's Multiple Comparison Test: *p < 0.05, **p < 0.01, ***p < 0.001.

C, D. Morphometric quantification of mitochondrial swelling calculated as area/perimeter normalized to circularity and mitochondrial elongation [AU]. Points represent individual mitochondria quantified per time point (n = 907–1165). Bars represent median with interquartile range (Q1 – Q3). Statistical significance was analyzed by Kruskal-Wallis Test followed by Dunn's Multiple Comparison Test: *p < 0.05, **p < 0.01, ***p < 0.001.

Golgi apparatus were also present. At 48 h of reperfusion, the presentation of autophagic structures at different stages was even further enhanced in this region. Meanwhile, in CA2–3, DG autophagic structures were also observed, both 24 and 48 h after the ischemic episode, but not as abundant as in the CA1 region. Swelling of Golgi apparatus was not observed either.

In accordance with TEM analysis, rapid, statistically significant increase of LC3-II/I ratio was found in CA1 (Fig. 4B). This phenomenon was observed as soon as I/R 3 h reaching 2.37 ± 0.9 control value (p < 0.005, n = 6), it persisted throughout the experiment and was accompanied by a significant decrease of PINK1 protein (0.73 ± 0.2, p < 0.01, n = 6). The elevated LC3-II/I ratio was also present in CA2–3, DG but it was recorded further after the insult, starting from 48 h post I/R and reaching 3.5 ± 2.1 (p < 0.001, n = 7) 72 h after ischemia, together with a statistically significant increase of PINK1 (1.8 ± 0.3, p < 0.001, n = 7), Parkin (1.34 ± 0.2, p < 0.05, n = 7) and SQSTM1/p62 (1.29 ± 0.3, p < 0.05, n = 7) which was not observed in CA1.

Taken together, TEM and western blot analysis confirmed the implication of autophagy in the neuronal response to ischemia-reperfusion in our model. General autophagy was activated in CA1 shortly after I/R and persisted, while in CA2–3, DG, the activation of autophagy was delayed and less profound than in CA1. Furthermore, a selective, PINK1/Parkin-mediated elimination of mitochondria in CA2–3, DG might be involved.

3.4. mtDNA content in CA2–3, DG prevails over CA1 and this relation is preserved after I/R

To further examine mitochondrial quality and quantity, mtDNA content was analyzed by qPCR, calculated in relation to nuclear DNA (nDNA) and expressed as mtDNA/nDNA ratio (Fig. 5A). In control hippocampi the value of mtDNA/nDNA ratio in CA2–3, DG was significantly higher than the CA1 value and amounted to 5.81 ± 1.37 and 3.6 ± 0.78 (p < 0.001, n = 7), respectively. A transient drop in mtDNA/nDNA ratio was observed at 48 h in all hippocampal regions after ischemia. However, even after I/R, mtDNA content was higher in CA2–3, DG than in CA1 at 6 h, 24 h and 48 h time points.

3.5. Postischemic mitochondrial biogenesis is enhanced in CA2–3, DG but not in CA1

In the face of mitochondrial damage and elimination, a compensating mechanism is anticipated to regain cellular homeostasis and to restore intracellular ATP supply. As variations in mitochondrial mass can be subtle and challenging to follow, different approaches could be adopted. Here, we analyzed changes in the protein level of key transcriptional factors mediating mitochondrial biogenesis (PGC-1α, Nrf1, Tfam) together with selected proteins representing respiratory chain complexes by western blot.

Master regulator of mitochondrial biogenesis, PGC-1α, was not altered and the secondary transcriptional factor, Nrf1, was significantly decreased in CA1 in the course of reperfusion (Fig. 5 B). Transient and rapid, statistically significant increase in Tfam protein was observed at 3 h after I/R while the protein levels of representative subunits of electron transport chain (ETC) complexes: III, IV and V were reduced (Fig. 6). By contrast, the immunodetection of complex I subunit in CA1 was elevated at 48 h and 96 h after I/R (1.33 ± 0.1, 1.34 ± 0.2, p < 0.01, n = 4). Considering the decrease of citrate synthase enzymatic activity and Hsp60 protein, shown in Fig. 1C, D, no particular hallmarks of mitochondrial biogenesis in CA1 were detected, even though the protein level of PGC-1α in CA1 control was higher than in CA2–3, DG. An observed increase in Tfam protein did not result in an increased biosynthesis of the considered mitochondrial proteins, except for the complex I subunit of a ETC.

Contrastingly, in CA2–3, DG a statistically significant rise of PGC-1α protein level was observed as soon as 3 h after I/R with the maximum value reached at 24 h (1.87 ± 0.7, p < 0.001, n = 5) and 48 h post I/R (1.57 ± 0.4, p < 0.001, n = 5), despite a lower control value in relation to CA1 (Fig. 5B). It was accompanied by a significant increase in Nrf1 (reaching statistically significant values at 24 h, 72 h and 96 h after I/R, 1.4 ± 0.3, 1.5 ± 0.18, 1.77 ± 0.55, p < 0.05, p < 0.01, p < 0.001, respectively, n = 6)) and Tfam proteins observed at 6 h (1.43 ± 0.3, p < 0.05, n = 6) and 48 h (1.52 ± 0.6, p < 0.05, n = 6) after I/R. This was followed by enhanced immunodetection of representative subunits of ETC complexes: III, IV and V, except for complex I (Fig. 6).

Considering the above, the increased protein levels of all key transcriptional factors in CA2–3, DG after I/R may indicate the activation of mitochondrial biogenesis in this hippocampal region. An increased mitochondrial content in CA2–3, DG may be further considered as shown by the increased protein levels of mitochondrial marker, Hsp60 (Fig. 1D), and representative subunits of ETC (Fig. 6). The induction of mitochondrial biogenesis was not observed in CA1. The reduction in the protein level of particular ETC subunits, with the exception of complex I, may further reveal post-I/R mitochondrial loss in this hippocampal region.

4. Discussion

In this study we hypothesized that different neuronal sensitivity in hippocampal CA1 and CA2–3, DG to transient ischemic insult may result from a different regulation of mitochondrial content (by mitophagy and
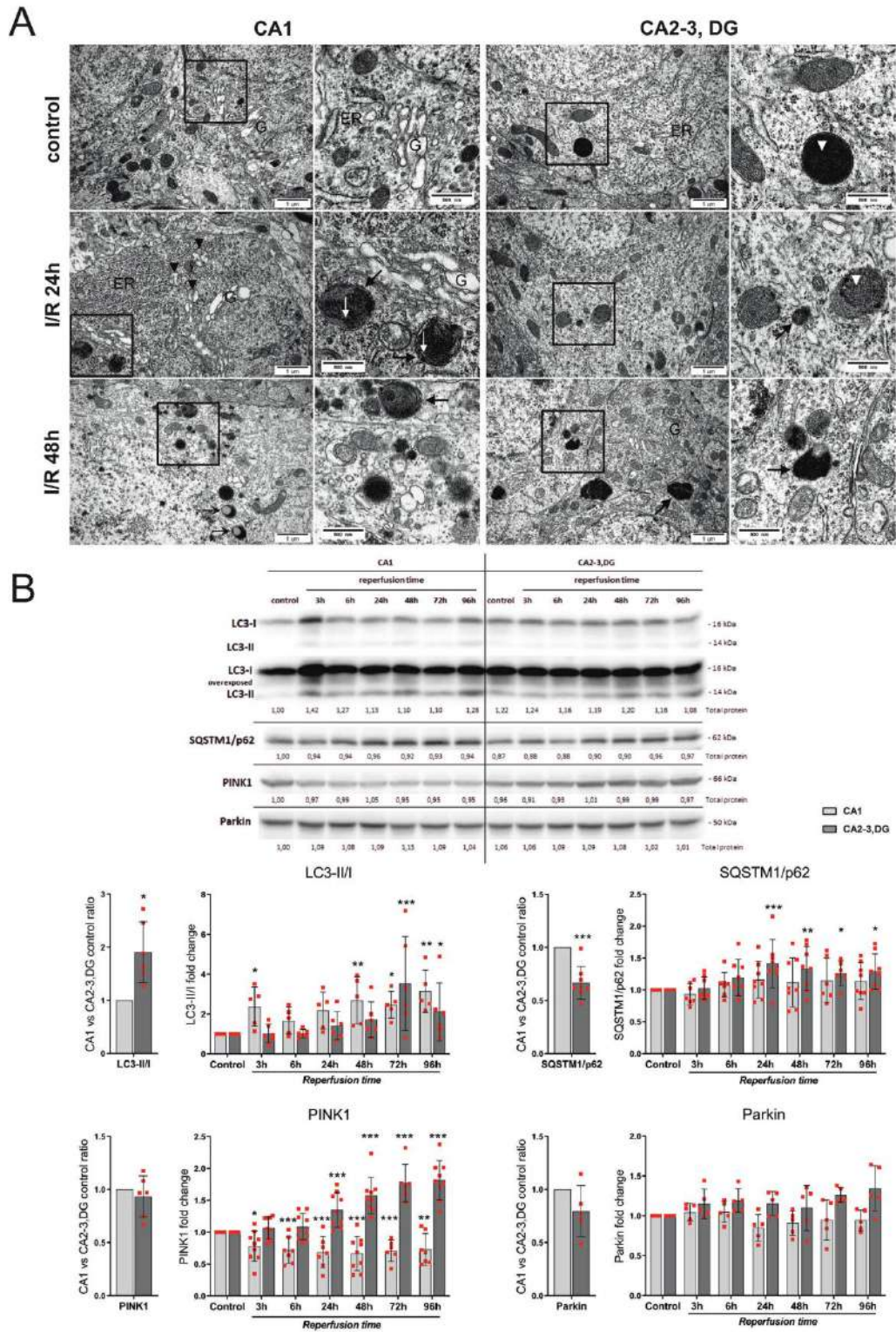
(caption on next page)

Fig. 4. General autophagy is activated shortly after I/R in CA1 while in CA2–3, DG autophagy markers are elevated further after I/R and involve PINK1 and SQSTM1/p62.

A. Representative TEM images presenting autophagic structures in CA1 and CA2–3, DG, 24 and 48 h after I/R. Mitochondrial remnants can be easily spotted (white arrows). ER – Endoplasmatic Reticulum, G – Golgi Complex, Black Arrowheads – disrupted mitochondria with damaged cristae and light mitochondrial matrix, White Arrowheads – lysosomes, White arrows – remnants of mitochondrial cristae, Black arrows – autolysosomes.

B. Representative western blots and densitometric analysis of LC3-II/I, SQSTM1/p62, PINK1 and Parkin in CA1 and CA2–3, DG homogenates before and after I/R. Charts present mean values with standard deviation. Points represent biological replicates of the experiment. One Sample t-test was applied for the comparison of CA1 and CA2–3, DG controls. One-way ANOVA followed by Dunnett's multiple comparisons test was applied for post-ischemia values for each part of hippocampus separately; n = 5–7; *p < 0.05, **p < 0.01, ***p < 0.001, vs CA1 control or CA2–3, DG control, respectively; The optical density of the particular bands was normalized to the total protein in line stained with Ponceau S. Normalization factors are shown under representative western blot image.
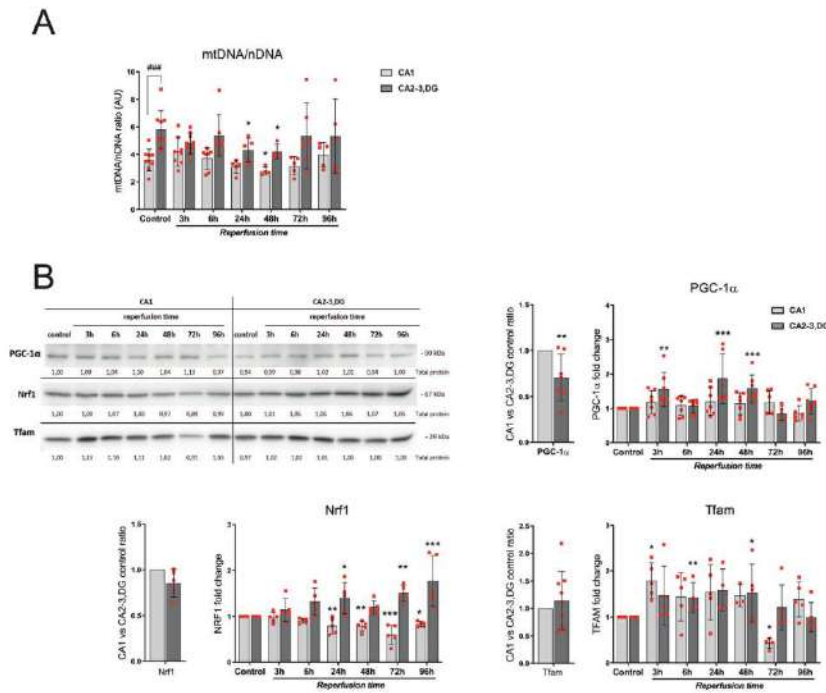

Fig. 5. Main mitochondrial biogenesis protein markers are elevated in CA2–3, DG but not in CA1. mtDNA content prevails in CA2–3, DG over CA1 and this relation is sustained after I/R.

A. Mean mitochondrial DNA content in CA1 and CA2–3, DG expressed as mtDNA/nDNA ratio. Charts present mean values with standard deviation. Points represent biological replicates of the experiment. One Sample t-test was applied for the comparison of CA1 and CA2–3, DG controls. One-way ANOVA followed by Dunnett's multiple comparisons test was applied for post-ischemia values for each part of hippocampus separately; n = 7; ### p < 0.001 vs CA1; *p < 0.05, **p < 0.01, vs CA1 control or CA2–3, DG control, respectively.

B. Representative western blots and densitometric analysis of PGC-1α, Nrf1 and Tfam in CA1 and CA2–3, DG homogenates before and after I/R. Charts present mean values with standard deviation. Points represent biological replicates of the experiment. One Sample t-test was applied for the comparison of CA1 and CA2–3, DG controls. One-way ANOVA followed by Dunnett's multiple comparisons test was applied for post-ischemia values for each part of hippocampus separately; n = 5–7; *p < 0.05, **p < 0.01, ***p < 0.001, vs CA1 control or CA2–3, DG control, respectively; The optical density of the particular bands was normalized to the total protein in line stained with Ponceau S. Normalization factors are shown under representative western blot image.

mitochondrial biogenesis) and mitochondrial quality (resulting from mitochondrial fusion, fission and mtDNA abundance) and that the proper relation between these processes may contribute to neuronal survival.

A well-established model of transient global ischemia of gerbil brain, [32,49–52] has already shown different neurodegeneration rates of hippocampal neurons after transient ischemic insult but the precise mechanism underlying various neuronal survival rates has not been fully described so far. Distinct differences between neurons located in particular hippocampal regions are evolutionarily conserved and may potentially result from different molecular mechanisms, including significant differences in gene expression profiles and mitochondrial activity [53–55]. This is especially true for CA1 neurons as their relatively high sensitivity is not only observed in ischemia but also in the aging process and neurodegenerative diseases [56,57].

In our study we used western blot analysis of homogenates obtained from CA1 and CA2–3, DG, thus representing changes in all cell types present in these hippocampal subregions This was supported by the analysis of transmission electron microscopy micrographs to observe post-ischemic changes in mitochondrial ultrastructure and localisation in the soma of neurons.

4.1. Mitochondrial ultrastructure and content

Using TEM, we showed that the morphological features of severe mitochondrial and cellular damage after I/R were much more pronounced in CA1 than in CA2–3, DG neurons and preceded neuronal loss in this region. This observation is in line with previous studies describing high vulnerability of CA1 neurons [52]. Post I/R ultrastructural disturbances in CA1 were accompanied by a reduced enzymatic activity of citrate synthase. This parameter is an accepted marker for the mitochondrial volume [46,58]. CA1 also demonstrated a reduced immunodetection of mitochondrial matrix marker, Hsp60, as well as other mitochondrial proteins: Mfn2, Opa1 and respiratory chain subunits III-IV-V. The consistent reduction of these parameters may point to reduced mitochondrial content in CA1 after I/R, which, in turn, may be the result of mitochondrial elimination. This assumption was further confirmed by increased autophagy markers (LC3-II/I, SQSTM1/p62) and ultrastructural presentation of autophagic figures which were abundant in CA1 after I/R, as discussed further below.

4.2. Mitochondrial fusion and fission

In our model, an enhanced post-ischemic mitochondrial fission was observed in ischemia-sensitive CA1. As demonstrated by TEM images, 24 h and 48 h after the insult, an elongated mitochondria in the soma of CA1 neurons were barely seen while mitochondrial swelling was evident. The observed mitochondrial fragmentation might result from a simultaneous activation of mitochondrial fission, demonstrated by an increased phoshpo-Ser616-Drp1/Drp1 ratio, and down-regulated
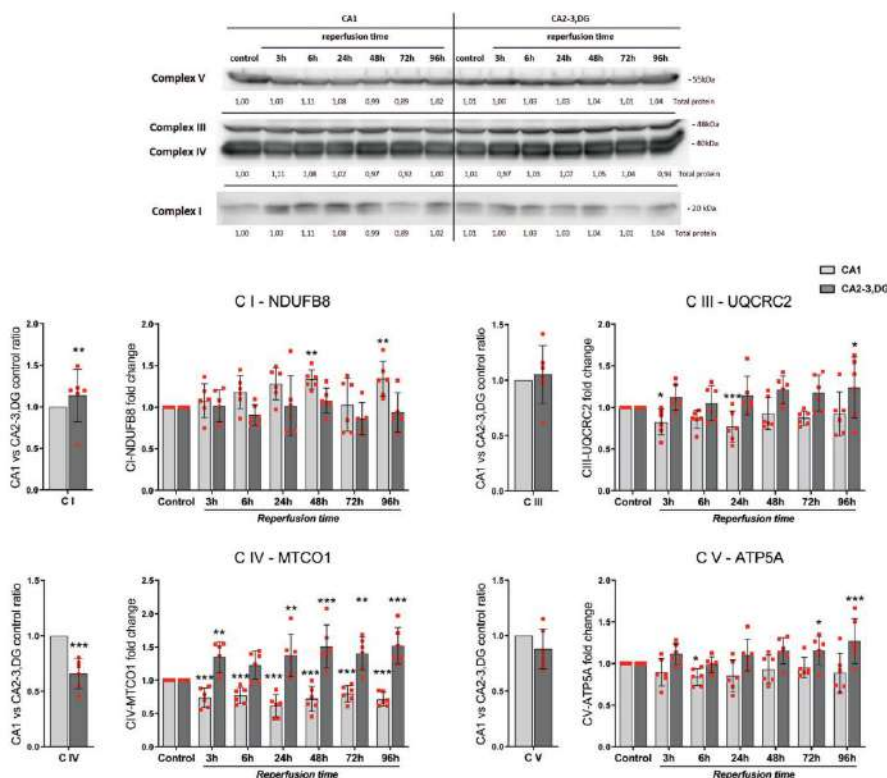
Fig. 6. Post-ischemic increase in selected subunits of the respiratory chain complexes is observed in CA2–3, DG but not in CA1, except for complex I.

Representative western blot and densitometric analysis of ETC subunits proteins in CA1 and CA2–3, DG tissue homogenates before and after I/R. Charts present mean values with standard deviation. Points represent biological replicates of the experiment. One Sample t-test was applied for the comparison of CA1 and CA2–3, DG controls. One-way ANOVA followed by Dunnett's multiple comparisons test was applied for post-ischemia values for each part of hippocampus separately; n = 4 biological replicates; $*p < 0.05$, $**p < 0.01$, $***p < 0.001$, vs CA1 control or CA2–3, DG control, respectively; The optical density of the particular bands was normalized to the total protein in line stained with Ponceau S. Normalization factors are shown under representative western blot image.

mitochondrial fusion, represented by a decreased Mfn2 and L-Opa1. Long, membrane-bound forms of Opa1 (L-Opa1) are required for mitochondrial fusion and cristae maintenance, but their processing to short, soluble forms (S-Opa1) can limit fusion and can facilitate mitochondrial fission [47,48]. However, as shown elsewhere, S-Opa1 is fully competent to maintain mitochondrial energetics and cristae structure [47]. Here, we did not observe a change in the ratio of L-Opa1 and S-Opa1 to total Opa1, as both forms of Opa1 were reduced in the ischemia-vulnerable hippocampus after the insult and so was the total Opa1. These observations are in line with previously reported outcomes presenting mitochondrial fission as an early and up-stream event in neurodegeneration [59,60]. Post-ischemic mitochondrial fragmentation in CA1 presented in this study is also consistent with previous reports on mitochondrial morphology in post-ischemic hippocampus [61]. An increased mitochondrial fission in hippocampus was also reported in neurodegeneration caused by mutant APP and amyloid beta in transgenic mice [62].

Accordingly, we observed an enhanced post-ischemic mitochondrial fusion in ischemia-resistant CA2–3, DG. An increased mitochondrial fusion in these hippocampal regions was manifested by the presence of elongated mitochondria, observed by TEM even at 48 h after the ischemic event and further demonstrated by mitochondrial elongation parameter and elevated protein levels of pro-fusion agents: Mfn1, Opa1 and, especially, Mfn2. The post-insult phospho-Ser616-Drp1/Drp1 ratio in CA2–3, DG was also increased, but it seems that mitochondrial fusion outweighed mitochondrial fragmentation in these hippocampal regions in reperfusion phase. In parallel, we observed significantly increased protein levels of respiratory chain subunits, confirming the positive effects of mitochondrial fusion on cellular oxidative capacities. Our observations on the neuroprotective effect of the increased mitochondrial fusion can be further supported by the data of neuronal protection by donepezil in the cardiac I/R injury model, where an increase in fusion-related mitochondrial proteins was observed in addition to BBB

protection, decreasing oxidative stress, mitochondrial dynamics imbalance and dendritic spine loss, among others [63]. In another study, Medala et al. [64] pointed that neurodegeneration in AD might be ameliorated by small molecular inhibitors of Drp1 which improve mitochondrial function and over-all neuronal health by restoring mitochondrial fusion and fission balance and improving mitochondrial biogenesis [64], which further supports the link between proper mitochondrial dynamics and neuroprotection.

4.3. Autophagy and mitochondrial elimination

Autophagy activation as a cellular response to an ischemic insult has been observed in various in vivo and in vitro models [65]. The effects of this phenomenon might be considered a double-edged sword [66]. General autophagy activation, as was observed here in CA1, may enable immediate separation and consequent elimination of damaged mitochondria and thus limit the release of pro-apoptotic agents. It may also serve as an attempt of energy retrieval under the oxygen and glucose shortage and thereby making further contribution to the neuronal survival, as discussed by Jiang et al. [67]. A common autophagy inducer, rapamycin, was shown to be neuroprotective in various in vivo models (MCAO or the four-vessel occlusion) as it prevented over-activation of mTOR signaling pathway reducing the infarct volume and ameliorating neurological functions [68,69]. However, in our research, we observed that even immediate endogenous activation of autophagy alone was not sufficient to prevent neuronal loss in CA1.

An increased protein level of autophagy markers, LC3-II and SQSTM1/p62, were present in all considered hippocampal regions. Generally, autophagy activation results in SQSTM1/p62 reduction, as this protein is degraded together with the other components of the autophagosomes, but exceptions have been described [70]. In our research, the accumulation of SQSTM1/p62 in the reperfusion might result from the imbalance between the degradation rate and a potential

increase in SQSTM1/p62 biosynthesis. The SQSTM1/p62 protein is also implicated in other molecular processes, e.g. ubiquitin-proteasome system and apoptosis, which may also affect its protein level [71,72].

Unlike in CA1, an increased LC3-II/I ratio in CA2–3, DG was accompanied by elevated PINK1 immunodetection. PINK1 is a key mediator of selective autophagy of damaged mitochondria [73]. However, according to Chen et al. [74], neuroprotective effects of PINK1 may also result from its counteracting effect on Drp1 translocation to mitochondria, as PINK1 may alter the phosphorylation of Drp1 at Ser616 [74]. The protective role of PINK1 via Drp1 phosphorylation was further presented in the intestinal I/R injury model [75]. In contrast with the reports by Chen et al. [74], we did not observe an increase in PINK1 protein in CA1 after I/R. Nonetheless, here we showed that this phenomenon occurred in CA2–3, DG and also corresponded with a higher neuronal survival rate and decreased mitochondrial fission. Thus, our data suggests that in I/R-resistant hippocampal regions PINK1 may contribute to neuronal survival by its role in selective elimination of damaged mitochondria but its impact on post-ischemic mitochondrial dynamics should not be excluded.

4.4. mtDNA content and Tfam

In contrast to the presumed changes in mitochondrial mass after I/R episode, mtDNA content was not significantly affected even in CA1 during the reperfusion. The number of mtDNA copies does not necessarily reflect the number of mitochondria, as the precise number of mtDNA particles varies according to the cell type and metabolic state [76,77]. However, it has been demonstrated that a relatively lower number of mtDNA copies in patients is associated with a higher risk of cardiovascular incidents [78] and the severity of outcomes after stroke [79]. Furthermore, the depletion of mtDNA was described to correspond with brain pathologies, like amyotrophic lateral sclerosis, and temporal lobe epilepsy with Ammon's horn sclerosis [80]. The accumulation of mtDNA deletion was observed in dopaminergic neurons of PD patients [81].

In our model, a significant difference in mtDNA between control CA1 and CA2–3, DG was observed, which was consistent with the data shown elsewhere [54]. A higher mtDNA content in CA2–3, DG corresponded with a higher ischemia resistance of this regions. As higher mtDNA content in CA2–3, DG was neither accompanied by a greater immunodetection of mitochondrial proteins nor the citrate synthase activity over the values in CA1, our findings are not sufficient to postulate a higher mitochondrial content in CA2–3, DG over CA1. What may be suggested, however, is a greater mtDNA copy density in CA2–3, DG than in CA1.

A relatively stable mtDNA content after I/R observed in our model is in line with an increased protein level of Tfam, detected as soon as 3 h after the insult in all hippocampal sections. In CA1 this phenomenon seems independent from PGC-1α and Nrf1, as the protein levels of these transcription factors were not changed after I/R. Tfam is a key player in mtDNA transcription, packaging, and maintenance and it is likely to encounter many types of mtDNA damage and secondary structures [82]. In the rat model of neonatal hypoxic-ischemic brain, the transient change in mtDNA content and proteins Hsp60 and COXIV, and citrate synthase activity together with expression of Nrf1 and Tfam were observed to increase in neurons in the cortical infarct border zone, whereas PGC-1α remained unaffected [83]. Consequently, the authors concluded that neonatal HI brain injury rapidly induced mitochondrial biogenesis, which may constitute a novel component of the endogenous repair mechanisms of the brain. Accordingly, the increase in Tfam protein level in CA1 at 3 h after ischemia shown here, together with the sustained mtDNA content, may also indicate an attempt of a rapid and PGC-1α-independent rescue.

4.5. Mitochondrial biogenesis and electron transport chain proteins

An increased level of PGC-1α after I/R insult, as observed here for CA2–3, DG, was previously described in various in vivo and in vitro models and also corresponded with higher neuronal survival [83]. It was further demonstrated that PGC-1α down-regulation sensitized neurons to ischemic/hypoxic insults while its overexpression resulted in neuroprotection [84]. The certain relationship between enhanced mitochondrial biogenesis and neuroprotection observed experimentally makes this molecular pathway a potent and potential target of post-ischemic treatment [85]. In our research, an activation of mitochondrial biogenesis in CA2–3, DG was manifested by increased protein levels of key transcriptional factors mediating mitochondrial biogenesis, PGC-1α, Nrf1 and Tfam, but also by an increase in mitochondrial proteins, like Hsp60 and particular subunits of electron transport chain complexes. The mitochondrial content parameter calculated from TEM images was also significantly higher in CA2–3, DG than in CA1 48 h after I/R. Furthermore, the enzymatic activity of citrate synthase, another marker of mitochondria quantity and quality, in ischemia-resistant regions was sustained during reperfusion despite the observed autophagy/mitophagy.

In CA2–3, DG, an elevated protein level of transcriptional factors was followed by increased immunodetection of ETC complexes III, IV and V but not complex I. As respiratory chain complex I is regarded to be the main source of reactive oxygen species, a relatively low expression of complex I would be beneficial under the oxygen deprivation and reoxygenation. As demonstrated before, PGC-1α contributes to neuronal protection also by its impact on ROS metabolism. Elevated PGC-1α was shown to activate ROS detoxifying enzymes [84]. However, further research is needed to investigate a regulatory effect of PGC-1α on complex I expression.

By contrast, we did not observe the activation of mitochondrial biogenesis in I/R-sensitive CA1. Although Tfam protein level during the reperfusion was increased and mtDNA content was sustained, it was not followed by biosynthesis of considered mitochondrial proteins, except for respiratory chain complex I. This was further accompanied by a decreased enzymatic activity of citrate synthase and reduced protein level of Hsp60 in CA1. One possible explanation is that increased complex I content in CA1 during the reperfusion, independent from transcription factors cascade, may serve as an attempt to gain ATP among bioenergetic crisis by rapid enhancement of electron supply onto the respiratory chain, even at the cost of ROS overproduction. However, as reviewed by Trushina et al. [86], partial reduction of the activity of the complexes involved in the oxidative phosphorylation and ETC machinery using genetic or pharmacological down modulation approaches has been shown to provide significant health benefits, improving mitochondrial function and cellular energetics in multiple model systems in vitro and in vivo [86]. In particular, partial inhibition of mitochondrial complex I using small molecules has emerged as a therapeutic strategy for multiple human conditions, including cancer and neurodegenerative diseases. Therefore, according to these observations, it is the down-regulation of protein complex I that may play a protective role, as we could see in CA2–3, DG, rather than its increase which correlated with neuronal damage in CA1.

5. Final conclusions

The I/R injury caused more severe damage to the mitochondria in CA1 neurons than in CA2–3, DG. I/R-induced impairment involved CA1 mitochondrial network division into round and swollen mitochondria. Damaged organelles were eliminated via general autophagy, starting shortly after the insult, which resulted in mitochondrial mass reduction. As this response was insufficient for neuronal survival, a neuronal loss was observed in CA1 after 72 h post I/R.

Meanwhile, in CA2–3, DG mitochondrial damage was not as severe as in CA1. An increased mitochondrial network dynamics appeared to alleviate the disruption in mitochondrial network. Damaged mitochondria underwent PINK1/Parkin-mediated mitophagy, which took place later after I/R episode. Additionally, mitochondrial biogenesis was

11

activated and led to increased biosynthesis of mitochondrial proteins, not only to compensate for the lost mitochondria but also to increase the amount of key proteins responsible for ATP synthesis in the reperfusion phase. The cooperation of these intracellular processes led to neuronal survival after transient ischemia.

The novelty of this study includes the demonstration of increased dynamics, selective mitophagy and mitochondrial biogenesis in the area of the hippocampus that is relatively insensitive to TIA. Such a post-TIA continuum may therefore ensure the preservation of proper mitochondrial quality and quantity and may be considered as part of a naturally occurring neuroprotection in a selected brain region.

Funding

Compliance with ethical standards

All procedures involving animals were performed in accordance with the ethical standards of the institution or practice at which the studies were conducted and EU Directive 2010/63/EU for animal experiments.

Institutional review board statement

The study was conducted according to the guidelines of the Declaration of Helsinki, and approved by Ethics Committee: IV Local Committee in Warsaw, and WAW2/032//2021.

CRediT authorship contribution statement

Maria Kawalec: Conceptualization, Validation, Formal analysis, Investigation, Data Curation, Writing - Original Draft, Visualization, Supervision, Project administration, Funding acquisition.

Piotr Wojtyniak: Investigation, Formal analysis, Writing - Original Draft (Materials & Methods), Writing - Review & Editing, Funding acquisition, Visualization.

Ewelina Bielska: Investigation.

Anita Lewczuk: Investigation, Resources, Writing - Original Draft (Materials & Methods).

Anna Boratynska-Jasinska: Formal analysis, Investigation, Writing - Original Draft (Materials & Methods), Writing - Review & Editing, Visualization.

Malgorzata Beresewicz-Haller: Investigation, Writing - Review & Editing,

Malgorzata Frontczak-Baniewicz: Formal analysis (TEM), Writing - Original Draft (Materials & Methods: TEM), Writing - Review & Editing.

Magdalena Gewartowska: Formal analysis (TEM).

Barbara Zablocka: Conceptualization, Validation, Writing - Original Draft, Writing - Review & Editing, Supervision, Funding acquisition.

Declaration of competing interest

The authors declare the following financial interests/personal relationships which may be considered as potential competing interests: Maria Kawalec reports financial support was provided by National Science Centre Poland. Piotr Wojtyniak reports financial support was provided by European Social Fund.

Data availability

Data will be made available on request.

References

[1] J. Finsterer, A. Wilfing, Anticoagulated de novo atrial flutter complicated by transitory ischemic attack in fatal COVID-19, Clin. Case Rep. 10 (2022), e05246.

[2] S.S. Shakil, S. Emmons-Bell, C. Rutan, J. Walchok, B. Navi, R. Sharma, K. Sheth, G. A. Roth, M.S.V. Elkind, Stroke among patients hospitalized with COVID-19: results from the American Heart Association COVID-19 cardiovascular disease registry, Stroke 53 (2022) 800–807.

[3] J.D. Easton, J.L. Saver, G.W. Albers, M.J. Alberts, S. Chaturvedi, E. Feldmann, T. S. Hatsukami, R.T. Higashida, S.C. Johnston, C.S. Kidwell, H.L. Lutsep, E. Miller, R. L. Sacco, AH Association, Council ASAS, Anesthesia CoCSa, Intervention CoCRa, Nursing CoC, Disease ICoPV, Definition and evaluation of transient ischemic attack: a scientific statement for healthcare professionals from the American Heart Association/American Stroke Association Stroke Council; Council on Cardiovascular Surgery and Anesthesia; Council on Cardiovascular Radiology and Intervention; Council on Cardiovascular Nursing; and the Interdisciplinary Council on Peripheral Vascular Disease. The American Academy of Neurology affirms the value of this statement as an educational tool for neurologists, Stroke 40 (2009) 2276–2293.

[4] D. Frank, A. Zlotnik, M. Boyko, B.F. Gruenbaum, The development of novel drug treatments for stroke patients: a review, Int. J. Mol. Sci. 23 (2022).

[5] Å.B. Gustafsson, G.W. Dorn 2nd, Evolving and expanding the roles of mitophagy as a homeostatic and pathogenic process, Physiol. Rev. 99 (2019) 853–892.

[6] A. Santel, M.T. Fuller, Control of mitochondrial morphology by a human mitofusin, J. Cell Sci. 114 (2001) 867–874.

[7] S. Cipolat, O. Martins de Brito, B. Dal Zilio, L. Scorrano, OPA1 requires mitofusin 1 to promote mitochondrial fusion, Proc. Natl. Acad. Sci. U. S. A. 101 (2004) 15927–15932.

[8] H. Otera, N. Ishihara, K. Mihara, New insights into the function and regulation of mitochondrial fission, Biochim. Biophys. Acta 1833 (2013) 1256–1268.

[9] M.J. Barsoum, H. Yuan, A.A. Gerencser, G. Liot, Y. Kushnareva, S. Gräber, I. Kovacs, W.D. Lee, J. Waggoner, J. Cui, A.D. White, B. Bossy, J.C. Martinou, R. J. Youle, S.A. Lipton, M.H. Ellisman, G.A. Perkins, E. Bossy-Wetzel, Nitric oxide-induced mitochondrial fission is regulated by dynamin-related GTPases in neurons, EMBO J. 25 (2006) 3900–3911.

[10] C. Duan, L. Kuang, X. Xiang, J. Zhang, Y. Zhu, Y. Wu, Q. Yan, L. Liu, T. Li, Drp1 regulates mitochondrial dysfunction and dysregulated metabolism in ischemic injury via Clec16a-, BAX-, and GSH- pathways, Cell Death Dis. 11 (2020) 251.

[11] K.H. Flippo, Z. Lin, A.S. Dickey, X. Zhou, N.A. Dhanesha, G.C. Walters, Y. Liu, R. A. Merrill, R. Meller, R.P. Simon, A.K. Chauhan, Y.M. Usachev, S. Strack, Deletion of a neuronal Drp1 activator protects against cerebral ischemia, J. Neurosci. 40 (2020) 3119–3129.

[12] R. Kumar, M.J. Bukowski, J.M. Wider, C.A. Reynolds, L. Calo, B. Lepore, R. Tousignant, M. Jones, K. Przyklenk, T.H. Sanderson, Mitochondrial dynamics following global cerebral ischemia, Mol. Cell. Neurosci. 76 (2016) 68–75.

[13] E.A. Wappler, A. Institoris, S. Dutta, P.V. Katakam, D.W. Busija, Mitochondrial dynamics associated with oxygen-glucose deprivation in rat primary neuronal cultures, PLoS One 8 (2013), e63206.

[14] L. Zhang, Z. He, Q. Zhang, Y. Wu, X. Yang, W. Niu, Y. Hu, J. Jia, Exercise pretreatment promotes mitochondrial dynamic protein OPA1 expression after cerebral ischemia in rats, Int. J. Mol. Sci. 15 (2014) 4453–4463.

[15] J.L. Yang, J. Mukda, S.D. Chen, Diverse roles of mitochondria in ischemic stroke, Redox Biol. 16 (2018) 263–275.

[16] J. Grohm, S.W. Kim, U. Mamrak, S. Tobaben, A. Cassidy-Stone, J. Nunnari, N. Plesnila, C. Culmsee, Inhibition of Drp1 provides neuroprotection in vitro and in vivo, Cell Death Differ. 19 (2012) 1446–1458.

[17] Y. Li, M. Wang, S. Wang, Effect of inhibiting mitochondrial fission on energy metabolism in rat hippocampal neurons during ischemia/reperfusion injury, Neurol. Res. 38 (2016) 1027–1034.

[18] Y.X. Zhao, M. Cui, S.F. Chen, Q. Dong, X.Y. Liu, Amelioration of ischemic mitochondrial injury and bax-dependent outer membrane permeabilization by Mdivi-1, CNS Neurosci. Ther. 20 (2014) 528–538.

[19] C. Peng, W. Rao, L. Zhang, K. Wang, H. Hui, L. Wang, N. Su, P. Luo, Y.L. Hao, Y. Tu, S. Zhang, Z. Fei, Mitofusin 2 ameliorates hypoxia-induced apoptosis via mitochondrial function and signaling pathways, Int. J. Biochem. Cell Biol. 69 (2015) 29–40.

[20] C. Alexander, M. Votruba, U.E. Pesch, D.L. Thiselton, S. Mayer, A. Moore, M. Rodriguez, U. Kellner, B. Leo-Kottler, G. Auburger, S.S. Bhattacharya, B. Wissinger, OPA1, encoding a dynamin-related GTPase, is mutated in autosomal dominant optic atrophy linked to chromosome 3q28, Nat. Genet. 26 (2000) 211–215.

[21] C. Delettre, G. Lenaers, J.M. Griffoin, N. Gigarel, C. Lorenzo, P. Belenguer, L. Pelloquin, J. Grosgeorge, C. Turc-Carel, E. Perret, C. Astarie-Dequeker, L. Lasquellec, B. Arnaud, B. Ducommun, J. Kaplan, C.P. Hamel, Nuclear gene OPA1, encoding a mitochondrial dynamin-related protein, is mutated in dominant optic atrophy, Nat.Genet. 26 (2000) 207–210.

[22] C.S. Ryan, A.L. Fine, A.L. Cohen, B.M. Schiltz, D.L. Renaud, E.C. Wirrell, M. C. Patterson, N.J. Boczek, R. Liu, D. Babovic-Vuksanovic, D.C. Chan, E.T. Payne, De novo DNM1L variant in a teenager with progressive paroxysmal dystonia and lethal super-refractory myoclonic status epilepticus, J. Child Neurol. 33 (2018) 651–658.

[23] R. Kandimalla, M. Manczak, J.A. Pradeepkiran, H. Morton, P.H. Reddy, A partial reduction of Drp1 improves cognitive behavior and enhances mitophagy, autophagy and dendritic spines in a transgenic tau mouse model of Alzheimer disease, Hum. Mol. Genet. 31 (2022) 1788–1805.

[24] R.J. Youle, A.M. van der Bliek, Mitochondrial fission, fusion, and stress, Science 337 (2012) 1062–1065.
[25] Y.W. Ruan, X.J. Han, Z.S. Shi, Z.G. Lei, Z.C. Xu, Remodeling of synapses in the CA1 area of the hippocampus after transient global ischemia, Neuroscience 218 (2012) 268–277.
[26] S. Nair, A.L. Leverin, E. Rocha-Ferreira, K.S. Sobotka, C. Thornton, C. Mallard, H. Hagberg, Induction of mitochondrial fragmentation and mitophagy after neonatal hypoxia-ischemia, Cells 11 (2022).
[27] Y. Yuan, X. Zhang, Y. Zheng, Z. Chen, Regulation of mitophagy in ischemic brain injury, Neurosci.Bull. 31 (2015) 395–406.
[28] L. Jia, J. Wang, H. Cao, X. Zhang, W. Rong, Z. Xu, Activation of PGC-1α and mitochondrial biogenesis protects against prenatal hypoxic-ischemic brain injury, Neuroscience 432 (2020) 63–72.
[29] S. Sun, T. Jiang, N. Duan, M. Wu, C. Yan, Y. Li, M. Cai, Q. Wang, Activation of CB1R-dependent PGC-1α is involved in the improved mitochondrial biogenesis induced by electroacupuncture pretreatment, Rejuvenation Res. 24 (2021) 104–119.
[30] M. Al Rahim, S. Thatipamula, G.M. Pasinetti, M.A. Hossain, Neuronal pentraxin 1 promotes hypoxic-ischemic neuronal injury by impairing mitochondrial biogenesis via interactions with active Bax[6A7] and mitochondrial hexokinase II, ASN Neuro 13 (2021), 17590914211012888.
[31] J. Dluzniewska, A. Sarnowska, M. Beresewicz, I. Johnson, S.K. Srai, B. Ramesh, G. Goldspink, D.C. Górecki, B. Zablocka, A strong neuroprotective effect of the autonomous C-terminal peptide of IGF-1 Ec (MGF) in brain ischemia, FASEB J. 19 (2005) 1896–1898.
[32] T. Kirino, K. Sano, Selective vulnerability in the gerbil hippocampus following transient ischemia, Acta Neuropathol. 62 (1984) 201–208.
[33] O. Krupska, A. Sarnowska, B. Fedorczyk, M. Gewartowska, A. Misicka, B. Zablocka, M. Beresewicz, Ischemia/Reperfusion-induced translocation of PKCβII to mitochondria as an important mediator of a protective signaling mechanism in an ischemia-resistant region of the hippocampus, Neurochem. Res. 42 (2017) 2392–2403.
[34] O. Krupska, T. Kowalczyk, M. Beresewicz-Haller, P. Samczuk, K. Pietrowska, K. Zablocki, A. Kretowski, M. Ciborowski, B. Zablocka, Hippocampal sector-specific metabolic profiles reflect endogenous strategy for ischemia-reperfusion insult resistance, Mol. Neurobiol. 58 (4) (2020) 1621–1633.
[35] R.K. Dagda, S.J. Cherra 3rd, S.M. Kulich, A. Tandon, D. Park, C.T. Chu, Loss of PINK1 function promotes mitophagy through effects on oxidative stress and mitochondrial fission, J. Biol. Chem. 284 (2009) 13843–13855.
[36] J. Lam, P. Katti, M. Biete, M. Mungai, S. AshShareef, K. Neikirk, E. Garza Lopez, Z. Vue, T.A. Christensen, H.K. Beasley, T.A. Rodman, S.A. Murray, J.L. Salisbury, B. Glancy, J. Shao, R.O. Pereira, E.D. Abel, A. Hinton Jr., A universal approach to analyzing transmission electron microscopy with ImageJ, Cells 10 (2021).
[37] D. Narendra, A. Tanaka, D.F. Suen, R.J. Youle, Parkin is recruited selectively to impaired mitochondria and promotes their autophagy, J. Cell Biol. 183 (2008) 795–803.
[38] U.K. Laemmli, Cleavage of structural proteins during the assembly of the head of bacteriophage T4, Nature 227 (1970) 680–685.
[39] J.S. Thacker, D.H. Yeung, W.R. Staines, J.G. Mielke, Total protein or high-abundance protein: which offers the best loading control for Western blotting? Anal. Biochem. 496 (2016) 76–78.
[40] C.P. Moritz, Tubulin or not tubulin: heading toward Total protein staining as loading control in Western blots, Proteomics 17 (2017).
[41] A. Untergasser, I. Cutcutache, T. Koressaar, J. Ye, B.C. Faircloth, M. Remm, S. G. Rozen, Primer3-new capabilities and interfaces, Nucleic Acids Res. 40 (2012), e115.
[42] K.J. Livak, T.D. Schmittgen, Analysis of relative gene expression data using real-time quantitative PCR and the 2(-Delta Delta C(T)) method, Methods 25 (2001) 402–408.
[43] R. Gadamski, M.J. Mossakowski, Asymatic demage of the CA1 sector of ammon's horn after short-term forebrain ischemia in Mongolian gerbils, Neropatol. Polska 30 (1992) 209–219.
[44] K. Domanska-Janik, P. Bong, A. Bronisz-Kowalczyk, H. Zajac, B. Zablocka, AP1 transcriptional factor activation and its relation to apoptosis of hippocampal CA1 pyramidal neurons after transient ischemia in gerbils, J. Neurosci.Res. 57 (1999) 840–846.
[45] T. Kirino, Delayed neuronal death in the gerbil hippocampus following ischemia, Brain Res. 239 (1982) 57–69.
[46] P.A. Figueiredo, R.M. Ferreira, H.J. Appell, J.A. Duarte, Age-induced morphological, biochemical, and functional alterations in isolated mitochondria from murine skeletal muscle, J. Gerontol. A Biol. Sci. Med. Sci. 63 (2008) 350–359.
[47] H. Lee, S.B. Smith, Y. Yoon, The short variant of the mitochondrial dynamin OPA1 maintains mitochondrial energetics and cristae structure, J. Biol. Chem. 292 (2017) 7115–7130.
[48] T. MacVicar, T. Langer, OPA1 processing in cell death and disease - the long and short of it, J. Cell Sci. 129 (2016) 2297–2306.
[49] F.J. Antonawich, S. Krajewski, J.C. Reed, J.N. Davis, Bcl-x(l) bax interaction after transient global ischemia, J.Cereb.Blood Flow Metab. 18 (1998) 882–886.
[50] M. Beręsewicz-Haller, O. Krupska, P. Bochomulski, D. Dudzik, A. Chęcińska, W. Hilgier, C. Barbas, K. Zablocki, B. Zablocka, Mitochondrial metabolism behind region-specific resistance to ischemia-reperfusion injury in gerbil hippocampus. Role of PKCβII and phosphate-activated glutaminase, Int. J. Mol. Sci. 22 (2021).
[51] D. Corbett, J. Larsen, K.D. Langdon, Diazepam delays the death of hippocampal CA1 neurons following global ischemia, Exp.Neurol. 214 (2008) 309–314.
[52] L. Radenovic, A. Korenic, G. Maleeva, I. Osadchenko, T. Kovalenko, G. Skibo, Comparative ultrastructural analysis of mitochondria in the CA1 and CA3 hippocampal pyramidal cells following global ischemia in mongolian gerbils, Anat. Rec. (Hoboken) 294 (2011) 1057–1065.
[53] N.A. Datson, M.C. Morsink, P.J. Steenbergen, Y. Aubert, C. Schlumbohm, E. Fuchs, E.R. de Kloet, A molecular blueprint of gene expression in hippocampal subregions CA1, CA3, and DG is conserved in the brain of the common marmoset, Hippocampus 19 (2009) 739–752.
[54] S. Farris, J.M. Ward, K.E. Carstens, M. Samadi, Y. Wang, S.M. Dudek, Hippocampal subregions express distinct dendritic transcriptomes that reveal differences in mitochondrial function in CA2, Cell Rep. 29 (2019) 522–539.e6.
[55] H. Zhu, T. Yoshimoto, S. Imajo-Ohmi, M. Dazortsava, A. Mathivanan, T. Yamashima, Why are hippocampal CA1 neurons vulnerable but motor cortex neurons resistant to transient ischemia? J. Neurochem. 120 (2012) 574–585.
[56] V.L. Nemeth, A. Must, S. Horvath, A. Király, Z.T. Kincses, L. Vécsei, Gender-specific degeneration of dementia-related subcortical structures throughout the lifespan, J. Alzheimer's Dis. 55 (2017) 865–880.
[57] D.R. Spiegel, J. Smith, R.R. Wade, N. Cherukuru, A. Ursani, Y. Dobruskina, T. Crist, R.F. Busch, R.M. Dhanani, N. Dreyer, Transient global amnesia: current perspectives, Neuropsychiatr. Dis. Treat. 13 (2017) 2691–2703.
[58] H.B. Sarnat, J. Marín-García, Pathology of mitochondrial encephalomyopathies, Can. J. Neurol. Sci. 32 (2005) 152–166.
[59] D.H. Cho, T. Nakamura, S.A. Lipton, Mitochondrial dynamics in cell death and neurodegeneration, Cell Mol.Life Sci. 67 (2010) 3435–3447.
[60] J. Kim, J.P. Moody, C.K. Edgerly, O.L. Bordiuk, K. Cormier, K. Smith, M.F. Beal, R. J. Ferrante, Mitochondrial loss, dysfunction and altered dynamics in Huntington's disease, Hum.Mol.Genet. 19 (2010) 3919–3935.
[61] K. Owens, J.H. Park, S. Gourley, H. Jones, T. Kristian, Mitochondrial dynamics: cell-type and hippocampal region specific changes following global cerebral ischemia, J. Bioenerg.Biomembr. 47 (2015) 13–31.
[62] M. Manczak, R. Kandimalla, X. Yin, P.H. Reddy, Hippocampal mutant APP and amyloid beta-induced cognitive decline, dendritic spine loss, defective autophagy, mitophagy and mitochondrial abnormalities in a mouse model of Alzheimer's disease, Hum. Mol. Genet. 27 (2018) 1332–1342.
[63] B. Ongnok, T. Khuanjing, T. Chunchai, S. Kerdphoo, T. Jaiwongkam, N. Chattipakorn, S.C. Chattipakorn, Donepezil provides neuroprotective effects against brain injury and Alzheimer's pathology under conditions of cardiac ischemia/reperfusion injury, Biochim. Biophys. Acta Mol. basis Dis. 1867 (2021), 165975.
[64] V.K. Medala, B. Gollapelli, S. Dewanjee, G. Ogunmokun, R. Kandimalla, J. Vallamkondu, Mitochondrial dysfunction, mitophagy, and role of dynamin-related protein 1 in Alzheimer's disease, J. Neurosci. Res. 99 (2021) 1120–1135.
[65] X. Zhang, H. Yan, Y. Yuan, J. Gao, Z. Shen, Y. Cheng, Y. Shen, R.R. Wang, X. Wang, W.W. Hu, G. Wang, Z. Chen, Cerebral ischemia-reperfusion-induced autophagy protects against neuronal injury by mitochondrial clearance, Autophagy 9 (2013) 1321–1333.
[66] Q. Shi, Q. Cheng, C. Chen, The role of autophagy in the pathogenesis of ischemic stroke, Curr. Neuropharmacol. 19 (2021) 629–640.
[67] T. Jiang, J.T. Yu, X.C. Zhu, H.F. Wang, M.S. Tan, L. Cao, Q.Q. Zhang, L. Gao, J. Q. Shi, Y.D. Zhang, L. Tan, Acute metformin preconditioning confers neuroprotection against focal cerebral ischaemia by pre-activation of AMPK-dependent autophagy, Br. J. Pharmacol. 171 (2014) 3146–3157.
[68] J.Y. Hwang, J. Gertner, F. Pontarelli, B. Court-Vazquez, M.V. Bennett, D. Ofengeim, R.S. Zukin, Global ischemia induces lysosomal-mediated degradation of mTOR and activation of autophagy in hippocampal neurons destined to die, Cell Death Differ. 24 (2017) 317–329.
[69] M. Wu, H. Zhang, J. Kai, F. Zhu, J. Dong, Z. Xu, M. Wong, L.H. Zeng, Rapamycin prevents cerebral stroke by modulating apoptosis and autophagy in penumbra in rats, Ann. Clin. Transl. Neurol. 5 (2018) 138–146.
[70] D.J. Klionsky, A.K. Abdel-Aziz, S. Abdelfatah, M. Abdellatif, A. Abdoli, S. Abel, H. Abeliovich, M.H. Abildgaard, Y.P. Abudu, A. Acevedo-Arozena, I. E. Adamopoulos, K. Adeli, T.E. Adolph, A. Adornetto, E. Aflaki, G. Agam, A. Agarwal, B.B. Aggarwal, M. Agnello, P. Agostinis, et al., Guidelines for the use and interpretation of assays for monitoring autophagy, Autophagy 17 (2021) 1–382.
[71] W.H. Shin, J.H. Park, K.C. Chung, The central regulator p62 between ubiquitin proteasome system and autophagy and its role in the mitophagy and Parkinson's disease, BMB Rep. 53 (2020) 56–63.
[72] D.A. Stevens, Y. Lee, H.C. Kang, B.D. Lee, Y.I. Lee, A. Bower, H. Jiang, S.U. Kang, S. A. Andrabi, V.L. Dawson, J.H. Shin, T.M. Dawson, Parkin loss leads to PARIS-dependent declines in mitochondrial mass and respiration, Proc. Natl. Acad. Sci. U. S. A. 112 (2015) 11696–11701.
[73] D.P. Narendra, S.M. Jin, A. Tanaka, D.F. Suen, C.A. Gautier, J. Shen, M.R. Cookson, R.J. Youle, PINK1 is selectively stabilized on impaired mitochondria to activate Parkin, PLoS Biol. 8 (2010), e1000298.
[74] S.D. Chen, T.K. Lin, D.I. Yang, S.Y. Lee, F.Z. Shaw, C.W. Liou, Y.C. Chuang, Roles of PTEN-induced putative kinase 1 and dynamin-related protein 1 in transient global ischemia-induced hippocampal neuronal injury, Biochem. Biophys. Res. Commun. 460 (2015) 397–403.
[75] W. Qasim, Y. Li, R.M. Sun, D.C. Feng, Z.Y. Wang, D.S. Liu, J.H. Yao, X.F. Tian, PTEN-induced kinase 1-induced dynamin-related protein 1 Ser637 phosphorylation reduces mitochondrial fission and protects against intestinal ischemia reperfusion injury, World J. Gastroenterol. 26 (2020) 1758–1774.
[76] L.L. Clay Montier, J.Z. Deng, Y. Bai, Number matters: control of mammalian mitochondrial DNA copy number, J. Genet. Genomics 36 (2009) 125–131.
[77] R.J. Wiesner, J.C. Rüegg, I. Morano, Counting target molecules by exponential polymerase chain reaction: copy number of mitochondrial DNA in rat tissues, Biochem. Biophys. Res. Commun. 183 (1992) 553–559.

65

[78] F.N. Ashar, Y. Zhang, R.J. Longchamps, J. Lane, A. Moes, M.L. Grove, J. C. Mychaleckyj, K.D. Taylor, J. Coresh, J.I. Rotter, E. Boerwinkle, N. Pankratz, E. Guallar, D.E. Arking, Association of Mitochondrial DNA copy number with cardiovascular disease, JAMA Cardiol. 2 (2017) 1247–1255.

[79] L. Song, T. Liu, Y. Song, Y. Sun, H. Li, N. Xiao, H. Xu, J. Ge, C. Bai, H. Wen, Y. Zhang, R. Hui, J. Chen, mtDNA copy number contributes to all-cause mortality of lacunar infarct in a chinese prospective stroke population, J. Cardiovasc. Transl. Res. 13 (2020) 783–789.

[80] M. Baron, A.P. Kudin, W.S. Kunz, Mitochondrial dysfunction in neurodegenerative disorders, Biochem. Soc. Trans. 35 (2007) 1228–1231.

[81] A. Bender, K.J. Krishnan, C.M. Morris, G.A. Taylor, A.K. Reeve, R.H. Perry, E. Jaros, J.S. Hersheson, J. Betts, T. Klopstock, R.W. Taylor, D.M. Turnbull, High levels of mitochondrial DNA deletions in substantia nigra neurons in aging and Parkinson disease, Nat. Genet. 38 (2006) 515–517.

[82] K. Chew, L. Zhao, Interactions of mitochondrial transcription factor A with DNA damage: mechanistic insights and functional implications, Genes (Basel) 12 (2021).

[83] W. Yin, A.P. Signore, M. Iwai, G. Cao, Y. Gao, J. Chen, Rapidly increased neuronal mitochondrial biogenesis after hypoxic-ischemic brain injury, Stroke 39 (2008) 3057–3063.

[84] J. St-Pierre, S. Drori, M. Uldry, J.M. Silvaggi, J. Rhee, S. Jäger, C. Handschin, K. Zheng, J. Lin, W. Yang, D.K. Simon, R. Bachoo, B.M. Spiegelman, Suppression of reactive oxygen species and neurodegeneration by the PGC-1 transcriptional coactivators, Cell 127 (2006) 397–408.

[85] P.S. Vosler, S.H. Graham, L.R. Wechsler, J. Chen, Mitochondrial targets for stroke: focusing basic science research toward development of clinically translatable therapeutics, Stroke 40 (2009) 3149–3155.

[86] E. Trushina, S. Trushin, M.F. Hasan, Mitochondrial complex I as a therapeutic target for Alzheimer's disease, Acta Pharm. Sin. B 12 (2022) 483–495.

[87] W. Zuo, S. Zhang, C.Y. Xia, X.F. Guo, W.B. He, N.H. Chen, Mitochondria autophagy is induced after hypoxic/ischemic stress in a Drp1 dependent manner: the role of inhibition of Drp1 in ischemic brain damage, Neuropharmacology 86 (2014) 103–115.

PUBLIKACJA II

Wojtyniak P., Boratynska-Jasinska A., Serwach K., Gruszczynska-Biegala J., Zablocka B., Jaworski J., Kawalec K. Mitofusin 2 Integrates Mitochondrial Network Remodelling, Mitophagy and Renewal of Respiratory Chain Proteins in Neurons after Oxygen and Glucose Deprivation. *Mol Neurobiol* 59, 6502–6518 (2022). doi: 10.1007/s12035-022-02981-6.

Mitofusin 2 Integrates Mitochondrial Network Remodelling, Mitophagy and Renewal of Respiratory Chain Proteins in Neurons after Oxygen and Glucose Deprivation

Piotr Wojtyniak[1] · Anna Boratynska-Jasinska[1] · Karolina Serwach[1] · Joanna Gruszczynska-Biegala[1] ·
Barbara Zablocka[1] · Jacek Jaworski[2] · Maria Kawalec[1]

Abstract

In attempts to develop effective therapeutic strategies to limit post-ischemic injury, mitochondria emerge as a key element determining neuronal fate. Mitochondrial damage can be alleviated by various mechanisms including mitochondrial network remodelling, mitochondrial elimination and mitochondrial protein biogenesis. However, the mechanisms regulating relationships between these phenomena are poorly understood. We hypothesized that mitofusin 2 (Mfn2), a mitochondrial GTPase involved in mitochondrial fusion, mitochondria trafficking and mitochondria and endoplasmic reticulum (ER) tethering, may act as one of linking and regulatory factors in neurons following ischemic insult. To verify this assumption, we performed temporal oxygen and glucose deprivation (OGD/R) on rat cortical primary culture to determine whether Mfn2 protein reduction affected the onset of mitophagy, subsequent mitochondrial biogenesis and thus neuronal survival. We found that Mfn2 knockdown increased neuronal susceptibility to OGD/R, prevented mitochondrial network remodelling and resulted in prolonged mitophagosomes formation in response to the insult. Next, Mfn2 knockdown was observed to be accompanied by reduced Parkin protein levels and increased Parkin accumulation on mitochondria. As for wild-type neurons, OGD/R insult was followed by an elevated mtDNA content and an increase in respiratory chain proteins. Neither of these phenomena were observed for Mfn2 knockdown neurons. Collectively, our findings showed that Mfn2 in neurons affected their response to mild and transient OGD stress, balancing the extent of defective mitochondria elimination and positively influencing mitochondrial respiratory protein levels. Our study suggests that Mfn2 is one of essential elements for neuronal response to ischemic insult, necessary for neuronal survival.

Keywords Mitochondria · Mitophagy · Mitofusin 2 · Primary neurons · Mitochondrial biogenesis · Mitochondrial DNA · Brain ischemia

Introduction

Mitochondria are a key determinant in proper neuronal functioning. Mitochondrial dynamics include mitochondrial fission, fusion and motility. The molecular mechanisms and

critical mediators in mitochondrial dynamism have been discussed in minute detail and have been the subject of many detailed reviews [1–3]. The disturbances in the mitochondrial quality control mechanisms which affect the elimination of impaired mitochondria and consequently, mitochondrial turnover, are implicated in various neurodegenerative conditions, like Parkinson's and Alzheimer's Disease [4]. Mitochondria are also involved in neuronal response to the brain ischemia [5]. The precise mechanisms conditioning neuronal survival under ischemic stress are not entirely clear yet. To date, considerable effort has been put into better understanding of the role of mitochondria in neuronal response to the ischemic insult in order to find potential therapeutic targets to limit post-ischemic neuronal damage.

Piotr Wojtyniak and Anna Boratynska-Jasinska contributed equally to this work.

✉ Maria Kawalec
  mkawalec@imdik.pan.pl

[1] Mossakowski Medical Research Institute, Polish Academy of Sciences, Warsaw, Poland

[2] International Institute of Molecular and Cell Biology, Warsaw, Poland

🖉 Springer

69

Impaired mitochondria become the source of pro-apoptotic stimuli, therefore, various endogenous mechanisms can occur to alleviate mitochondrial damage. An increased mitochondrial fusion and fission events have been shown to facilitate mixing of the mitochondria content thereby preventing the accumulation of mitochondrial defects [1], while severely damaged mitochondria were reported to be eliminated by mitophagy [6]. Finally, the activation of mitochondrial biogenesis was shown to restore mitochondrial content and bioenergetic abilities of the neurons [7, 8]. However, the mechanisms orchestrating mitochondrial dynamics, mitophagy and mitochondrial biogenesis are still poorly understood.

Among the variety of mitochondrial proteins, an outer mitochondrial membrane GTPase, mitofusin 2 (Mfn2), emerges as a unique player which integrates various functions, particularly mitochondrial fusion, mitochondrial movement, the tethering of mitochondria to the endoplasmic reticulum (ER) and, presumably, mitophagy.

Two mitofusins, Mfn1 and Mfn2, are known as mammalian homologues of yeast Fzo fusion protein [9]. Mfn1 and Mfn2 share high similarity in their molecular structures and, partly, their functions. By forming homo- and heterodimers, they juxtapose mitochondria and facilitate the outer mitochondrial membrane (OMM) fusion [10]. However, Mfn2 homodimers alone are weakly efficient to induce OMM fusion thereby making Mfn1 participation an obligatory factor [11]. By contrast, it is Mfn2, not Mfn1, that is present at the endoplasmic reticulum conditioning mitochondria-ER tethering [12] and ER morphology [13].

Mfn2 participates in mitophagy by interacting with key proteins mediating mitochondria elimination. The selective elimination of mitochondria via mitophagy was first described by Kim et al. (2007) [14]. It was further demonstrated that the disruption of mitochondrial membrane potential resulted in the accumulation of PTEN-induced kinase 1, PINK1, in OMM [15] and the subsequent recruitment of E3 ubiquitin ligase Parkin into the impaired mitochondria. Parkin, in turn, by ubiquitination of OMM proteins, facilitates the attachment of autophagosome membranes to the damaged mitochondria that undergo degradation [16]. As shown by Chan et al. (2013), Mfn2 phosphorylation by PINK1 facilitates the translocation of Parkin from cytosol to the impaired mitochondria causing PINK1-phosphorylated Mfn2 to serve as a receptor for Parkin [17]. Mfn2 undergoes Parkin-mediated ubiquitination [18] but the precise role of this phenomenon is still under investigation. Nonetheless, what has already been proven is that Parkin-mediated Mfn2 ubiquitination affects mitochondria and ER contact sites [19] while Parkin-mediated Mfn2 degradation in proteasome facilitates the dissociation of mitochondria from the ER thereby enabling the onset of mitophagy [20]. Consequently, the maintenance of mitochondria-ER contacts suppresses

PINK1/Parkin-mediated mitophagy [21], which confirms the functional link between mitochondria-ER interaction and mitophagy.

At some point, the sites of mitochondria-ER contacts appear to be important for mitochondrial biogenesis as well. It was shown that Dynamin-related protein 1 (Drp1)-mediated mitochondrial division is crucial for appropriate mitochondrial nucleoid distribution during mitochondrial biogenesis [22] and that, at the same time, mitochondrial division preferentially occurs at mitochondria-ER contacts [23].

The role of other proteins mediating mitochondrial network remodelling after ischemic insult has been investigated before in in vitro and in vivo models. As shown by Wappler et al. (2013), the contribution of particular fusion and fission proteins, like Mfn1/2, Opa1, Drp1 and Fis1, varies depending on the duration of the insult, but the maintained fusion emerges as a predominant response of surviving neurons [24]. At the same time, in many experimental models the enhanced mitochondrial fission after ischemic insult was observed to precede apoptotic neuronal death [25], while the inhibition of Drp1-mediated mitochondrial fission turned out to be neuroprotective [26–28].

The precise molecular mechanism which regulates mitophagy and mitochondrial biogenesis has not yet been described, however, several links have already been observed. According to recent findings, the mutual antagonism between the PINK1/Parkin pathway and Peroxisome proliferator-activated receptor gamma coactivator 1-alpha (PGC-1α) expression can be detected [29]. PGC-1α is considered a master regulator for mitochondria biogenesis. PGC-1α works upstream of nuclear respiratory factor 1 (NRF-1), which is responsible for the expression of most respiratory complex proteins, and upstream of mitochondrial transcription factor A (TFAM), which is essential for mitochondrial DNA maintenance and replication [30]. It was further demonstrated that both Parkin and PINK1 deficiencies contribute to the accumulation of Parkin-interacting substrate (PARIS), which, in turn, inhibits PGC-1α expression [31, 32]. However, further research is needed to understand the complexity of this phenomenon.

In our study, we hypothesized that neuronal Mfn2 may act as a linking protein that integrates mitochondrial network remodelling with mitophagy and mitochondrial biogenesis. We further assumed that this interplay might be crucial for mitochondrial homeostasis and thus neuronal survival under ischemic insults. Our assumptions were based on the available scientific data on the role of Mfn2 in mitochondrial network dynamics (mitochondrial fusion and trafficking), the ability of Mfn2 to tether mitochondria and ER, and on the recorded fact that these Mfn2 functions can be modified by E3 ubiquitin ligases, such as Parkin, implicated in mitochondrial elimination.

70

To verify this concept, we performed a temporal oxygen and glucose deprivation (OGD), which is a well-established cellular model of ischemia-reperfusion injury [24, 33], on the primary culture of rat cortical neurons. We compared the effects of oxygen and glucose deprivation followed by reperfusion (OGD/R) on mitochondrial network morphology, mitophagosome formation as well as mitochondrial biogenesis markers in wild-type and Mfn2 knockdown neurons. In addition, we attempted to determine whether the knockdown of the Mfn2 may affect the onset of mitophagy and subsequent OGD/R-induced mitochondrial biogenesis, and eventually, the neuronal survival.

Materials and Methods

Primary Cell Cultures

Cortical neuronal cultures were prepared from Wistar rat brains on embryonic day 19 (E19). Pregnant female Wistar rats were provided by the Animal House of the Mossakowski Medical Research Institute, Polish Academy of Sciences (Warsaw, Poland). Animal care was provided in accordance with the European Communities Council Directive (86/609/EEC).

Embryo cortices were dissected and cut into 1-mm pieces on a 35-mm Petri dish in cold Ca^{2+}/Mg^{2+}-free HBSS (Gibco, Thermo Scientific, Grand Island, NY, USA). Then, the tissue was transferred to a 15-ml Falcon tube, rinsed twice with cold Ca^{2+}/Mg^{2+}-free HBSS and incubated for 10 min at 37 °C in Ca^{2+}/Mg^{2+}-free HBSS containing 0.2 % trypsin (Gibco). It was followed by double washing with cold HBSS in the presence of Ca^{2+}/Mg^{2+} (Gibco). Next, the cell suspension was generated by passaging 10 times through a fire-polished glass Pasteur pipette in cold Ca^{2+}/Mg^{2+} HBSS containing 1 mg/mL DNase I (Roche, Basel, Switzerland). The suspension was passed through a 70-μm cell strainer (Corning, USA) to eliminate tissue debris. For the immunoblotting, neurons were seeded on Poly-D-Lysine 6-well plates (Corning) at a density of 1×10^6 cells/well. For fluorescence measurements, cells were seeded on Poly-D-Lysine coated 24-well plates (Corning) at a density of 2.2×10^5 cells/well.

Neurons were seeded in a Neurobasal medium (Gibco) supplemented with 2% B-27 (Gibco), 0.5 mM GlutaMAX (Gibco), 12.5 μM glutamate (Merck/Sigma-Aldrich, Poznan, Poland), and 1% Antibiotic-Antimycotic (Gibco) at 37 °C in a humidified atmosphere with 5% CO_2. On day in vitro (DIV) 2 half of the medium was replaced with glutamate-free growth medium containing non-neuronal cell proliferation inhibitor CultureOne Supplement (Gibco). Such neuronal culture was found to consist of more than 90% of neurons with a minimum number of non-neuronal cells, based on MAP2/GFAP immunofluorescence staining.

Lentiviral Production and Cell Transduction

To induce Mfn2 knockdown, commercially available 29mer short-hairpin RNA (shRNA) constructs in lentiviral GFP vector (Origene, Rockville, USA, TL712567) were used. Two constructs, sh-Mfn2 B and sh-Mfn2 D, were selected for the experiments, based on satisfactory efficiency in Mfn2 reduction with a relatively low toxicity. As a negative control, a non-effective 29-mer scrambled shRNA cassette in pGFP-C-shLenti Vector was used (scrRNA; Origene). Viral production was performed as described in Gruszczynska-Biegala et al. (2020) [34]. Neurons were infected with sh-Mfn2 and scrRNA- carrying lentiviruses on DIV4 with a viral infection efficiency exceeding 90%. The experiments were performed 6 days post transduction (DIV 10).

Oxygen–glucose Deprivation and Reoxygenation (OGD/R)

OGD/R was performed on DIV 10. For OGD/R treatment, OGD media, composed of 130 mM NaCl (Sigma-Aldrich, Saint Louis, USA), 2.5 mM KCl (Sigma-Aldrich), 2.2 mM $CaCl_2$ (AppliChem GmbH, Darmstadt, Germany), 1.5 mM $MgCl_2$ x $6H_2O$ (AppliChem GmbH), 10 mM Hepes (AppliChem GmbH), pH 7.3–7.4, was bubbled with 95% N_2/5% CO_2 for 15 min.

The cells were washed twice with OGD media, then immediately transferred into the Modular Incubator Chamber (Billups-Rothenberg, San Diego, USA) filled with mixed gas containing 95% N_2/5% CO_2 for 15 min at 15–20 L/min. Thereafter, the sealed chamber was incubated at 37°C for 45 min reaching the total time of OGD as 1 h. Neurons in the control group were maintained under normoxic incubation conditions. After OGD, the cells were removed from the chamber, refreshed with previously collected conditioned culture medium and incubated at 37°C in 5% CO_2 for 3 h or 24 h of the reperfusion phase.

Immunoblotting

For western blotting, neurons were washed with PBS (Sigma-Aldrich) and lysed with Cell Lysis Buffer (Cell Signaling Technology, Danvers, USA) containing 1 mM PMSF (Sigma-Aldrich) for 5 min on ice. The samples were sonicated and centrifuged at $14,000 \times g$ for 10 min at 4°C. The supernatant was collected, and a Modified Lowry Protein Assay (Thermo Scientific, Grand Island, NY, USA) was performed to determine the total protein concentration. The samples were diluted in a reducing sample buffer and boiled at 100°C for 5 min. For western blotting with anti-OXPHOS

antibody cocktail (Abcam, Cambridge, UK), samples were not boiled, following the manufacturer's guidelines.

Equal amounts of protein (20–35 µg) were analyzed by 10–12% SDS-PAGE, electro-transferred onto nitrocellulose (Amersham; Cytiva, USA) or Immobilon-P PVDF (Merck Millipore, Burlington, USA) membrane and stained for the total protein (Ponceau S staining). Following imaging of the total protein, the membranes were blocked with 5% non-fat milk in Tris-buffered saline (TBS) with 0.1% Tween 20 (TBST) for 1 h at room temperature. Thereafter, the membranes were incubated with the appropriate primary antibodies diluted in TBST or 2.5% milk/TBST at 4°C overnight, including anti-Mfn1 (1:1000, 11E9-1H12, Novus Biologicals, USA, NBP1-71775), anti-Mfn2 (1:1000, Sigma-Aldrich, M6319), anti-Opa1 (1:1000, D6U6N, Cell Signaling, 80471), anti-Drp1 (1:1000, 4E11B1, Cell Signaling, 14647), anti-TOM20 (1:500, Cell Signaling, Danvers, USA, 42406), anti-HSP60 (1:1000, Cell Signaling, 12165) anti-PRK-8 (1:250, Santa Cruz Biotechnology, Dallas, USA, sc-32282), anti-PGC-1α (1:250, Santa Cruz Biotechnology, sc-518025), anti-NRF1 (1:500; Proteintech, UK, 12482-1-AP), anti-NRF1 (1:250; Santa Cruz Biotechnology, sc-28379), anti-OXPHOS (1:500; Abcam, Cambridge, UK, ab110413). The membranes were washed three times for 5 min in TBST and incubated with the following peroxidase-conjugated secondary antibodies: anti-mouse (Sigma-Aldrich, A9044) or anti-rabbit (Sigma-Aldrich, A0545) diluted in 5% non-fat milk in TBST for 30 min at room temperature, and again washed for 5 min in the TBST. Bound antibodies were visualized by Amersham ECL or Amersham ECL Select detection reagent (Cytiva, USA). Blots were imaged and quantified using the Fusion FX imaging system (Vilber Lourmat, Marne-la-Vallée, France). The band intensities of the proteins of interest were normalized to the total protein densities corresponding to the same lane and quantified using ImageJ software with gel analyzer feature (NIH, Bethesda, MD, USA) as shown by Thacker et al. (2016) [35].

Immunofluorescence and Image Acquisition

Neuronal cultures were seeded at a density of 7.9×10^4/cm^2 on 1.5 laminin coated coverslips (Neuvitro Corporation, Vancouver, WA, USA). The cells were stained with 100 nM Mitotracker Red CMXRos (Thermo Scientific) in preconditioned culture medium for 45 min., fixed with 4% paraformaldehyde (AppliChem, Darmstadt, Germany) in PBS (Sigma-Aldrich) followed by permeabilization with 0.25% Triton-X (Carl Roth, Karlsruhe, Germany) in PBS. The cells were stained with primary antibodies: mouse anti-Parkin (1:50; Santa Cruz Biotechnology, Santa Cruz, CA, sc-32282), mouse anti-MAP2 clone AP20 (1:250; EMD Millipore Corporation, Temecula, CA, USA, MAB3418) or rabbit anti-GFAP (1:1000; Abcam, Cambridge, UK, ab7260),

detected by secondary antibodies: goat anti-mouse CF 633 (1:400; Sigma-Aldrich, SAB4600333), donkey anti-mouse Alexa Fluor 488 (1:400; Jackson ImmunoResearch, West Grove, PA, USA, cat. 715-545-150) or donkey anti-rabbit RR-X (1:400; Jackson ImmunoResearch, cat. 711-295-152). The nuclei were visualized with Hoechst 33342 (8 µM, Thermo Scientific). The samples were mounted in the ProLong Glass Antifade Mountant (Thermo Scientific).

The immunostained cultures were viewed under Zeiss LSM780 Axio Observer confocal microscope (Carl Zeiss AG, Oberkochen, Germany). Images were acquired using a 100× Alpha Plan-Apochromat oil immersion objective (1.46 NA). The unidirectional scanning mode was used and the image resolution was 1024 × 1024 pixels. When needed, at least 9 z-sections of 290–300 nm size per image were taken. Laser power and detector gain values were set once and repeated throughout the experiments.

Quantitative Image Analysis of Mitochondrial Morphology and Parkin Accumulation

The acquired images were analyzed using the Mito-Morphology macro by Dagda et al. (2009) [36] created for ImageJ software (NIH, Bethesda, MD, USA). GFP fluorescence or MAP2 staining images were used to help draw outlines of the cell bodies, and these selections were copied into images with Mitotracker Red-stained mitochondria and processed by the Mito-Morphology macro. The method described by Van Laar et al. (2015) [37] was adapted to assess cells positive for Parkin accumulation on mitochondria. To confirm that Parkin colocalized with mitochondria in observed puncta, a line was drawn across the punctum and a plot of the fluorescence intensity along the line was examined, as shown previously [38]. Sites of Parkin accumulation displayed overlapping signals of high intensity both for Mitotracker and anti-Parkin channels. The neurons which exhibited at least one such punctum were considered positive, counted and related to the total number of imaged neurons in particular experimental time. The obtained data are the average of at least three independent experiments. The minimal number of cells analyzed for each experimental point was 20.

Mitophagy Assay

Mitophagy Dye (Dojindo EU GmbH., Munich, Germany) [39] was used to visualize mitophagosomes in live cells according to the manufacturer's instructions with minor modifications. In brief, the cells were plated on Ibidi µ-slide 8 Well plates (Ibidi GmbH, Germany) at a density of 8×10^4 cells/well. On DIV 10, the neurons were incubated with 200 nM Mitophagy dye at 37 °C for 30 min, washed twice and subjected to OGD/R experiment. At the appropriate time

before microscopic analysis, the cells were stained for 30 min with 1:1000 Lysoview 633 (Biotium, Inc., Fremont, CA, USA) and 8 μM Hoechst 33342 (Thermo Scientific) diluted in culture medium. The cells were washed twice and imaged using a Zeiss spinning disk Axio Observer Z1 confocal microscope (Carl Zeiss AG, Oberkochen, Germany) equipped with an incubation chamber with the 37°C temperature and humidified 5% CO_2 atmosphere. The images were acquired as Z-stacks with 240 nm spacing using a 63× Plan Apo 1.4 objective. The image processing was performed with ImageJ software (NIH, Bethesda, MD, USA). The selection of Mitophagy dye- and LysoView-positive objects was made with Colocalization Highlighter plugin, which resulted in an 8-bit colocalized point images, further transformed into a binary images. The number of colocalized puncta was quantified by Analyze Particles feature, using the Size and Circularity parameters to exclude noise and occasional aggregates.

DNA Isolation

Total cellular DNA was purified using E.Z.N.A. MicroElute Genomic DNA Kit (Omega Bio-tek, Norcross, GA, USA). In brief, at the indicated time points, the cells were washed twice, scraped from the plates, centrifuged at $1000 \times g$, suspended in PBS (Sigma-Aldrich) and processed according to the manufacturer's protocol. The purity (absorbance ratio at 260/280) and concentration of DNA samples were determined spectroscopically using DeNovix DS-11 FX+ (DeNovix Inc., Wilmington, DE, USA).

mtDNA Copy Number Quantitation

A singleplex real-time PCR assay was established for measuring the amount of rat mtDNA relative to the nuclear DNA. This assay targets the mitochondrial ND1 gene (26193) and the nuclear single-copy gene [40], β-actin (V01217.1) Primers and probes were designed using the Primer3web (https://primer3.ut.ee/) [41]. The probes were labeled at the 5′-end with FAM. A quencher dye, 6-carboxytetramethylrhodamine (TAMRA), was linked to the 3′-end of both probes. Primers and probes were synthesized by DNA Sequencing and Synthesis Facility IBB PAS, Warsaw, Poland. We used the following primers and probes: mtDNA forward primer, ND1226F: ACCCTCTCCCTTACACTAGC; mtDNA reverse primer, ND1405: AAGAGATGGTTTGGGCAACG; TaqMan probe, ND1_380TM: 5′-ACTCCCTATTCGGAG CCCTACGAGC; nuclear DNA forward primer, ACTB_F: GGGATGTTTGCTCCAACCAA; nuclear DNA reverse primer, ACT_R: GCGCTTTTGACTCAAGGATTTAA; TaqMan probe, ACTB_TM: 5′-CGGTCGCCTTCACCG TTCCAGTT. Real-time PCR was performed in a Micro-Amp EnduraPlate optical 96-well reaction plate (Applied

Biosystems, Foster City, CA, USA) sealed with MicroAmp optical adhesive film (Applied Biosystems) on the ABI 7500 FAST Real-time PCR System (Applied Biosystems). The reaction mix (total volume 20 μL) consisted of: 10 μL TaqMan Fast Advanced Master Mix (Applied Biosystems), 4 μL Nuclease-Free Water (Applied Biosystems), 2 μl mtDNA or nDNA primers (900 nM each), 2 μl mtDNA or nDNA probe (250 nM), 2 μl DNA (50 ng). The real-time PCR reactions were performed in triplicate for both genes. The temperature program was initiated with a polymerase activation at 95 °C for 2 min, followed by 40 cycles at 95 °C for 3 s and 60 °C for 30 s. The cycle threshold (Ct) values were determined using SDS 2.3 software (Applied Biosystems). Relative copy number was calculated using analysis of the difference in Ct between mtDNA and nuclear DNA. Relative quantification was performed by the $\Delta\Delta$Ct method [42] and expressing the ratio as a percentage of the calibrator — untreated control cells — set as 100%.

RNA Extraction and RT-qPCR

Total RNA was extracted from cells using Total RNA Mini Plus Concentrator kit (A&A Biotechnology, Gdansk, Poland). For assessing RNA quality and yield, A260/A280 and A260/A230 ratios for RNA preparation samples were analyzed with a DeNovix DS-11 FX+ spectrophotometer (DeNovix Inc., Wilmington, DE, USA). To determine Parkin mRNA expression, reverse transcription was carried out using High-Capacity RNA-to-cDNA Kit (Applied Biosystems) with total RNA (2 μg) according to the manufacturer's instructions. Real-time PCR was performed in triplicates using TaqMan Gene Expression Assay probes for Parkin (Rn00571787_m1), Gapdh (Rn01775763_g1) and β-actin (Rn01412977_g1) with TaqMan Fast Advanced Master Mix (Applied Biosystems) in the ABI 7500 FAST Real-time PCR System (Applied Biosystems). The thermal cycling was initiated by the polymerase activation step for 2 min at 95 °C, followed by 40 cycles at 95 °C for 3 s and 60 °C for 30 s. mRNA levels of β-actin or Gapdh were used as an internal control to normalize the mRNA levels of Parkin. The expression levels for Parkin were assessed in relation to Gapdh and β-actin expression ($\Delta\Delta$Ct method, according to Livak and Schmittgen (2001) [42]).

Lactate Dehydrogenase (LDH) Assay

Neuronal death was examined by measuring LDH release into the culture medium, using CytoTox-ONE Homogenous Membrane Integrity Assay (Promega, Madison, WI, USA), according to the manufacturer's manual. LDH levels for samples were normalized to Maximum LDH Release control.

Pyknotic Nuclei Count

Control and OGD/R-subjected live neurons were incubated on DIV 10 and DIV 11 respectively, with 8 μM Hoechst 33342 (Thermo Scientific) in culture medium. After 30 min, the staining solution was replaced with HBSS (Gibco) and images were taken using Olympus IX71 fluorescence microscope equipped with Olympus Colorview III camera (Olympus, Tokyo, Japan) and dedicated Cell^F software. Nucleus counting was performed using the Cell Counter plugin for ImageJ (NIH, Bethesda, MD, USA).

Mitochondrial Membrane Potential

Mitochondrial membrane potential was measured fluorometrically using JC-1 dye (5,5′,6,6-tetrachloro-1,1′,3,3-tetraethylbenzimidazolylcarbocyanine iodide; Sigma-Aldrich/Merck), according to Cossarizza et al. (2001) [43]. JC-1 fluorescence was measured at Ex/Em: 475/530 nm for green and at 475/590 nm for the red channel using monochromator-based microplate reader, Tecan INFINITE M1000 PRO with dedicated software (Tecan Group Ltd, Mannedorf, Switzerland). In brief, the neurons were cultured on 24-well BioCoat plates (Corning). On DIV 10, directly after the OGD experiment, control and OGD-treated neurons were incubated for 10 min with 1 uM JC-1. After washing, the fluorescence was measured in PhenolRed-free Ca^{2+}/ Mg^{2+} HBSS (Thermofisher Scientific, USA). In parallel, JC-1 measurement was performed on neurons treated for 1 h with 5–10 μM mitochondrial uncoupler CCCP (Carbonyl cyanide 3-chlorophenylhydrazone; Sigma-Aldrich) to further diminish the mitochondrial membrane potential.

Statistical Analysis

The results are presented as mean ± standard deviation. Statistical analysis was performed using one-way analysis of variance (ANOVA) followed by the Bonferroni's multiple comparison test. For data sets that did not meet the normal distribution, the Kruskal-Wallis test was used followed by Dunn's multiple comparison test. All calculations were performed using GraphPad Prism 5.0 (GraphPad Software, San Diego, CA, USA).

Results

Mfn2 Knockdown Results in Increased Neuronal Damage 24 h after Oxygen and Glucose Deprivation

The in vitro experiments were performed on primary cultures of rat cortical neurons with reduced numbers of glial cells. To mimic ischemic insult, neurons were subjected to the temporal deprivation of oxygen and glucose performed according to the scheme shown in Fig. 1A. After 10 days of culturing, the culture medium was replaced by deoxygenated glucose-free buffer and culture plates were placed in an oxygen-free chamber at 37°C. After 1 h, the culture medium was restored and neurons were returned to normoxic conditions (reoxygenation). The samples were collected at 3 h and 24 h. The controls were obtained from the neurons that were kept under normoxic condition throughout the experiment.

The duration of oxygen and glucose deprivation was optimised to avoid significant cell death 24 h later to allow for the observation of long-time effects of the insult. In our study, 1 h OGD reduced the mitochondrial membrane potential in wild-type (wt) neurons by almost 20 %, as shown by changes in JC-1 probe fluorescence (Fig. 1B). In comparison, 1-h treatment with the mitochondrial uncoupler, 5 μM CCCP, reduced the mitochondrial membrane potential in wt neurons by half, confirming the moderate character of the OGD insult (Fig. 1B). Also, for such a subtle insult, we did not observe an increase in LDH release in wt neurons (Fig. 1C).

As demonstrated by western blot, 1-h OGD significantly and constantly reduced the Mfn2 level in total cell lysates of wt neurons. The reduction of the Mfn2 protein was observed as early as 3 h after the insult, while the Mfn1 and Hsp60 proteins were unaltered and Opa1, Drp1 and TOM22 temporarily dropped at 3 h after the OGD (Fig. 1D and Supplementary Fig. 1).

To determine whether Mfn2 protein affects neuronal damage after OGD, first, we validated the knockdown constructs for Mfn2 (sh-Mfn2 B and sh-Mfn2 D), as demonstrated at Fig. 2A–B. As shown by western blot, both shRNA constructs significantly reduced the level of Mfn2, while the level of the Mfn1 did not diminish. As measured on DIV10, the sh-Mfn2 B and sh-Mfn2 D constructs reduced Mfn2 protein level by 86% and 89%, respectively, relative to scrRNA-transduced neurons. Meanwhile, Mfn1 protein was unaltered by scrRNA and OGD, while in sh-Mfn2 neurons Mfn1 was elevated by 23% (sh-Mfn2 B) or 54% (sh-Mfn2 D) before the insult, and up to 33% (sh-Mfn2 B) and 56% (sh-Mfn2 D) after the insult (Fig. 2B).

The reduction in the mitochondrial membrane potential caused by 1 h OGD in shRNA-transduced neurons was comparable to those observed for wt neurons (Fig. 2C).

To verify whether Mfn2 deficiency can affect neuronal viability, we measured lactate dehydrogenase (LDH) release (Fig. 2D) and the number of pyknotic nuclei in the total cell population (Fig. 2E). In scrRNA-treated neurons, the reduction in mitochondrial membrane potential caused by 1 h OGD was not followed by a significant decrease in neuronal viability even after 24 h (Fig. 2D). In contrast, LDH release in Mfn2 knockdown neurons was significantly increased 24 h after OGD and exceeded 50% of the maximum possible
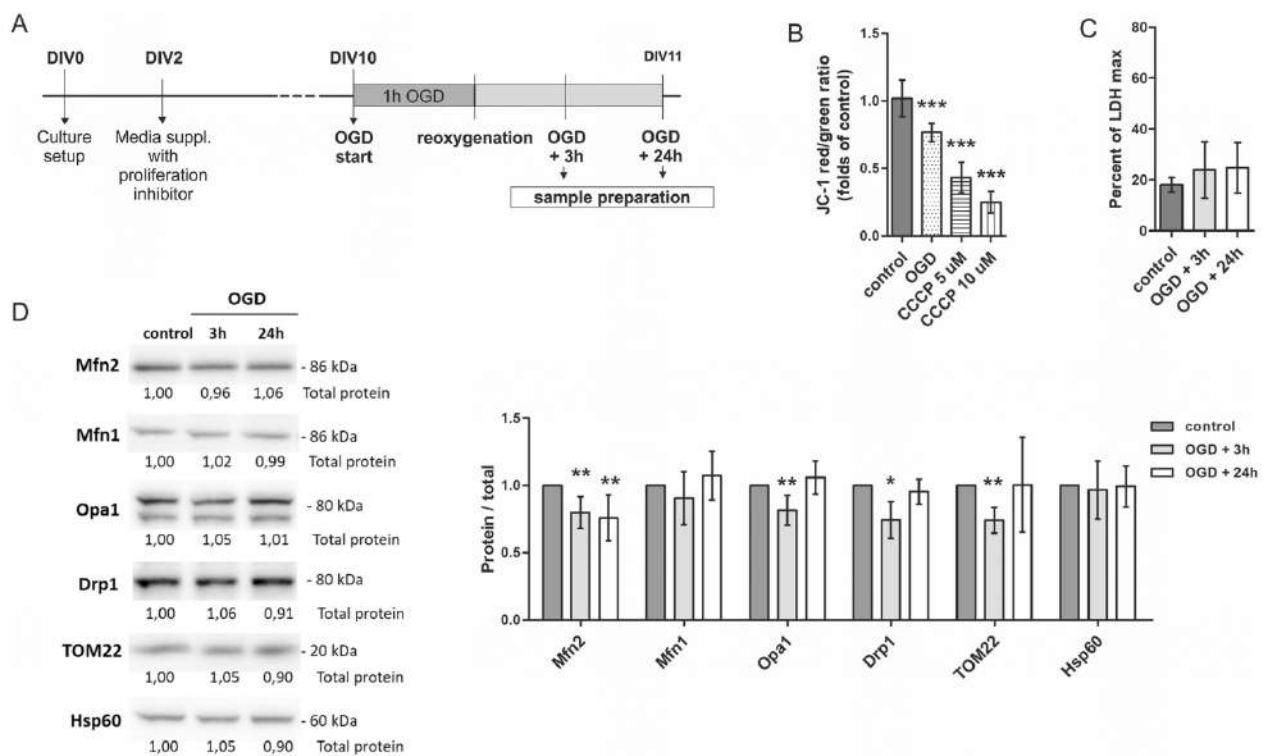
⍣ Springer

Fig. 1 Mfn2 protein level is reduced after mild OGD in rat cortical neurons. (A) Experimental design. OGD — oxygen and glucose deprivation. DIV — day in vitro; (B) Effects of 1 h OGD on mitochondrial membrane potential in wild-type (wt) neurons expressed as relative red to green fluorescence ratio of JC-1 probe, directly after the insult. CCCP was used as a control of $\Delta\psi$ reduction. Mean ± SD; n = 4. ***p < 0.001 vs wt control; (C) Effects of OGD/R on cell sur-

vival in wt neurons measured as LDH release. Mean ± SD; n = 6. (D) Representative western blots and densitometric analysis of Mfn2, Mfn1, Opa1, Drp1, TOM22 and Hsp60 in cell lysates of wt neurons after OGD/R. n = 4. *p < 0.05, **p < 0.01, vs wt control. The optical density of the particular bands was normalized to the total protein in line stained with Ponceau S. Normalization factors are shown under representative western blot image (Supplementary Fig. 1)

LDH release. (Fig. 2D). The percentage of pyknotic nuclei in Mfn2 knockdown neurons 24 h after the OGD reached over 50% which was also significantly higher than in wt and scrRNA-transduced neurons (Fig. 2E).

Admittedly, the Mfn2 knockdown alone did not affect the viability of neurons during the culturing but it increased neuronal sensitivity to oxygen and glucose deprivation observed 24 h after the insult.

Mfn2 is Necessary for the proper Mitochondrial Network Morphology and Recovery after OGD and Reoxygenation

Considering the role of Mfn2 in mitochondrial fusion and trafficking, we next analyzed the differences in the morphology of the mitochondrial network in Mfn2 knockdown neurons in response to OGD/R insult.

Mitochondria were labelled with Mitotracker Red probe and mitochondrial morphology analysis in the soma of rat cortical neurons was performed using 2D confocal images (Fig. 3A, G). To characterize the mitochondrial network

morphology, the following parameters were used: mito-count (Fig. 3B, H), mitochondrial content (Fig. 3C, I), average mitochondrial size (Fig. 3D, J), mitochondrial interconnectivity (Fig. 3E, K) and mitochondrial elongation (Fig. 3F, L) according to Dagda et al. (2009) [36].

A rapid drop in the mito-count parameter was observed in wt neurons in response to OGD/R (Fig. 3B). It was accompanied by a significant increase in mitochondrial content (Fig. 3C) and mitochondrial average size (Fig. 3D). A mito-count parameter represents the number of closely connected mitochondria recognized by the software as separate objects. A mito-count decrease, together with an elevated average mitochondria size indicates an intensified mitochondrial fusion induced by OGD/R. This is further supported by a significant increase in mitochondrial interconnectivity (Fig. 3E) and mitochondrial elongation parameters (Fig. 3F), which is initiated soon after the insult. As the reduced number of mito-objects was accompanied by the increased mitochondrial content, the flux of mitochondria to the soma in response to OGD/R may be considered.
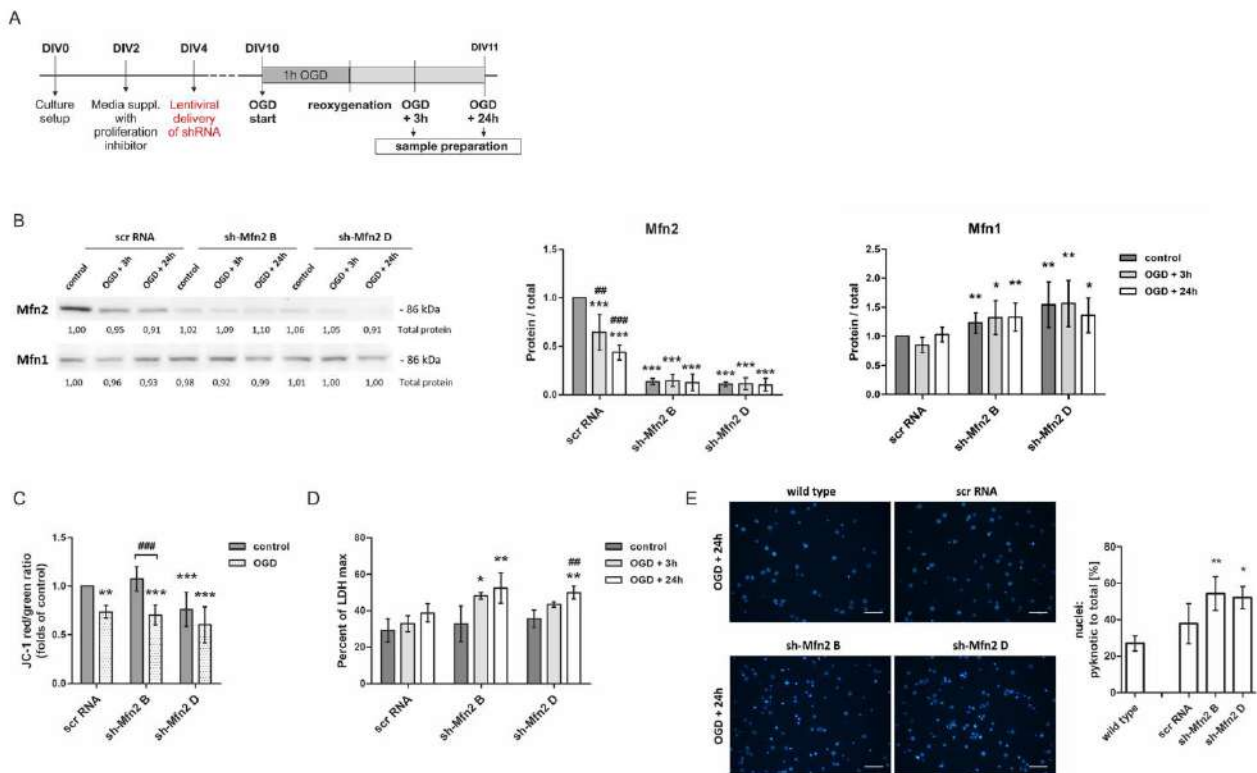
Fig. 2 Mfn2 knockdown increases the susceptibility of neurons to OGD/R. (A) Experimental design. OGD — oxygen and glucose deprivation. DIV — day in vitro; (B) Representative western blot and densitometric analysis of Mfn1 and Mfn2 in cell lysates of shRNA-transduced neurons after OGD/R. $n = 4$. $* p < 0.05$, $**p < 0.01$, $***p < 0.001$ vs scrRNA control; $\#\#p < 0.01$; $\#\#\#p < 0.001$ vs shRNA control; the optical density of the particular bands was normalized to the total protein in line stained with Ponceau S. Normalization factors are shown under representative western blot images. (C) Effects of 1 h OGD on mitochondrial membrane potential in shRNA-transduced neurons expressed as relative red to green fluorescence ratio of JC-1 probe, directly after the insult. Mean ± SD; $n = 4$. $**p < 0.01$, $***p < 0.001$ vs scrRNA control; $\#\#\#p < 0.001$ vs sh-Mfn2 control; (D) Effects of OGD/R on cell survival measured as LDH release. Mean ± SD; $n = 6$. $*p < 0.05$; $**p < 0.01$ vs scrRNA control. $\#\#p < 0.01$ vs sh-Mfn2 control; (E) Effect of OGD/R on the percentage of pyknotic nuclei in the total number of nuclei in wt and shRNA-transduced neurons, 24 h after OGD. Nuclei were stained with Hoechst 33342; chart and representative images. Scale bars: 50 μm, $n = 4$. $*p < 0.05$, $**p < 0.01$ vs scrRNA control

Similar alterations in mitochondrial morphology were observed for scrRNA-transduced neurons after OGD/R (Fig. 3G). The number of mito-objects represented by the mito-count parameter was slightly reduced by the OGD/R (Fig. 3H). It was accompanied by a higher content of mitochondria (Fig. 3I) and an increased mitochondrial elongation parameter at 3 h and 24 h after the insult (Fig. 3L). However, the mitochondrial interconnectivity parameter in scrRNA control was only slightly elevated when compared to wt neurons. Such an increase was sustained after OGD/R (Fig. 3K).

By contrast, in sh-Mfn2 controls, the mito-count parameter demonstrated a significantly greater number of mito-objects than in scrRNA neurons (Fig. 3H), while the average size of mitochondria in sh-Mfn2 controls was significantly diminished (Fig. 3J). It was accompanied by a decreased mitochondrial elongation parameter (Fig. 3L) and mitochondrial interconnectivity (Fig. 3K). Therefore, the mitochondrial network in Mfn2 knockdown neurons

was much more dispersed and fragmented into smaller mitochondria in comparison to scrRNA neurons, even before the insult.

Furthermore, neither the average mitochondrial size (Fig. 3J) nor the mitochondrial content (Fig. 3I) was observed to increase in Mfn2 knockdown neurons in response to OGD/R. The mitochondrial elongation parameter was lowered even more by OGD/R (Fig. 3L). Thus, the Mfn2 knockdown prevented the OGD/R-induced mitochondria gathering in the soma and mitochondria elongation observed for wt and scrRNA-transduced neurons.

As shown by the mito-count parameter, the number of identified separate mito-objects in sh-Mfn2 B neurons decreased 3 h after OGD/R, but returned to the control value 24 h later (Fig. 3H). This was followed by a transient and slight increase in the average mitochondrial size in sh-Mfn2 B neurons, as a significant decrease in this parameter was observed 24 h after OGD/R (Fig. 3J). These observations
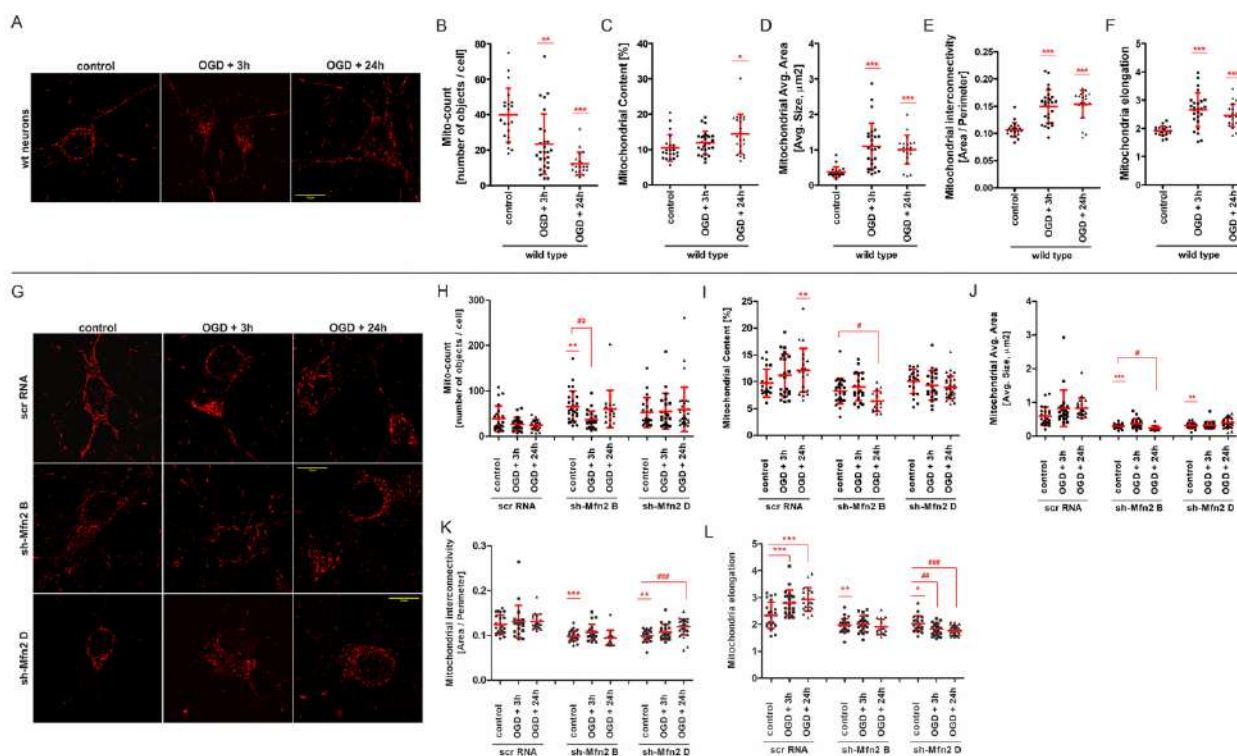
Fig. 3 Mfn2 knockdown affects the mitochondrial network in control neurons and prevents the remodelling of mitochondrial network after OGD. (A) Representative images of mitochondria in wild-type (wt) neurons, visualized with Mitotracker Red probe, before and after OGD/R. Scale bars represent 10 μm. (B–F) Quantitative image analysis of mitochondrial network parameters in wt neurons, $n = 3$. A number of cells analyzed for each experimental point: 21–27. * $p < 0.05$, **$p < 0.01$, ***$p < 0.001$ vs wt control. (G) Representative images of mitochondria in shRNA-transduced neurons, visual- ized with Mitotracker Red probe, before and after OGD/R. Scale bars represent 10 μm. (H–L) Quantitative image analysis of mitochondrial network parameters in shRNA-transduced neurons, $n = 3$. A number of cells analyzed for each experimental point: 21–27. * $p < 0.05$, **$p < 0.01$, ***$p < 0.001$ vs scrRNA control; #$p < 0.05$, ##$p < 0.01$, ###$p < 0.001$ vs sh-Mfn2 control. For the image analysis, the following parameters were used: mito-count (B, H), mitochondrial content (C, I), average mitochondrial size (D, J), mitochondrial interconnectivity (E, K) and mitochondrial elongation (F, L)

might indicate an ineffective attempt at the mitochondrial fusion in response to OGD.

All in all, wt neurons demonstrated an increased mitochondrial fusion and an enhanced mitochondrial network branching in response to OGD. The changes in the mitochondrial network started shortly after the insult and lasted up to 24 h. In sh-Mfn2 neurons, in turn, the Mfn2 knockdown altered the mitochondrial network morphology, favouring its fragmentation and preventing the post-insult remodelling of the mitochondrial network.

Mfn2 Knockdown Enhances Mitophagy in Primary Rat Cortical Neurons

Having regard to recent reports on the relationship between mitochondrial network dynamics and mitophagy, we further examined the effect of Mfn2 knockdown on the onset of mitophagy after OGD/R.

We used the mitochondrial-specific fluorescent probe, Mitophagy Dye, which is characterized by the shift in fluorescence intensity in response to the change in pH caused by the fusion of mitochondria-containing autophagosomes and lysosomes (Fig. 4A). To support the recognition of late mitophagosomes, lysosomes were also visualized. In the merged images, the mitochondria-lysosomes colocalization points were observed as bright orange dots in wt neurons (Fig. 4B) and shRNA-transduced neurons (Fig. 4C).

The quantitative analysis of mitophagosomes showed an increased number of late mitophagosomes in all types of neurons, shortly after OGD/R (Fig. 4D, E). However, in wt and scrRNA-transduced neurons, the number of mitophagosomes returned to control values within 24 h, indicating a transient activation of mitochondrial degradation. In Mfn2 knockdown neurons, the number of late mitophagosomes was still elevated 24 h after OGD/R (Fig. 4E).

The study on mitophagosomes formation was followed by an analysis of E3-ubiquitin ligase Parkin accumulation on mitochondria. An increased recruitment of Parkin to mitochondria is considered as one of the hallmarks of mitochondria damage and a crucial step in selective
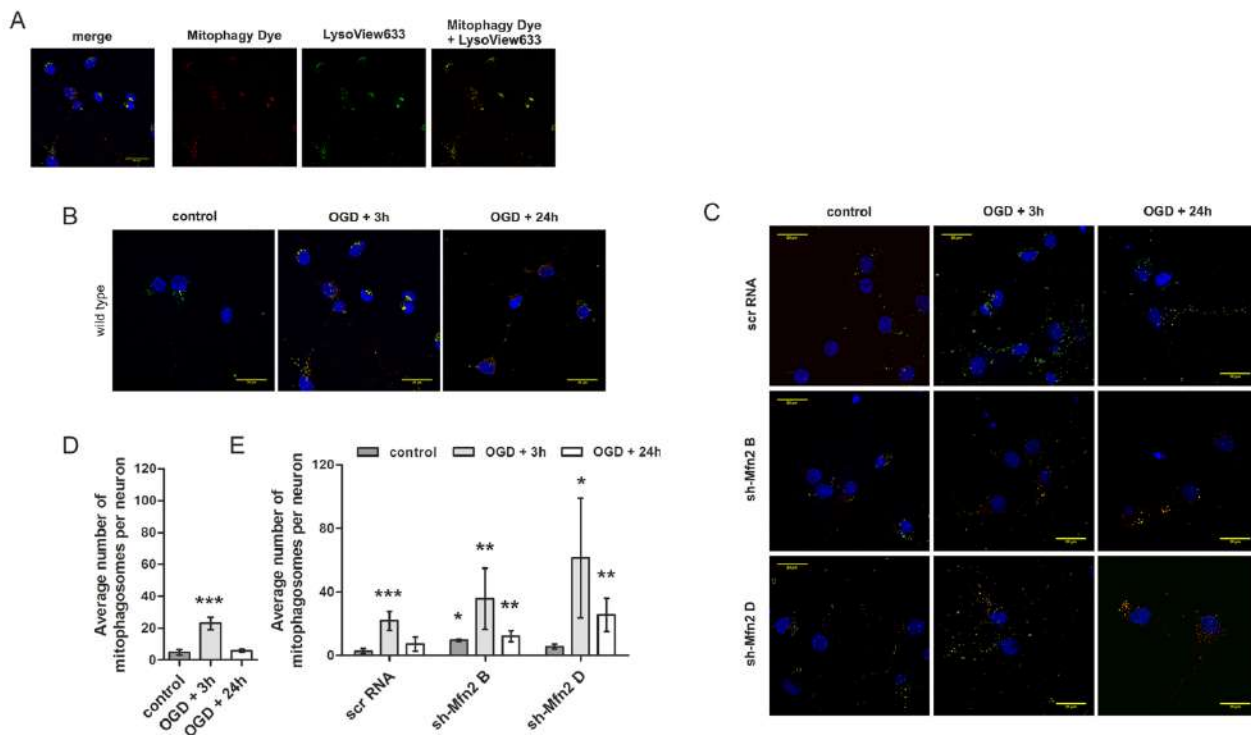
Fig. 4 Mfn2 knockdown in primary neurons enhances late mitophagosomes formation in response to OGD/R. (A) Representative images of mitophagosomes visualized with Mitophagy Dye (red) and LysoView 633 (green) in wild-type (wt) neurons subjected to OGD/R. Representative images present: mitochondria/mitophagosomes (red), lysosomes (green) and nuclei (blue) followed by merged image. Bar: 20 μm. (B, C) Representative merged images of mitophagosomes in wt and shRNA-transduced neurons subjected to OGD/R, respectively. Mitophagosomes are seen as bright orange dots. Bar: 20 μm. (D, E) Average number of mitophagosomes per neuron in wt and shRNA neurons respectively; the number of cells in each time point = 13–32; n = 3–5; *p < 0.05, **p < 0.01, ***p < 0.001 vs control or scrRNA control

mitochondria elimination. Immunocytochemical staining was performed for Parkin along with mitochondria labelling with Mitotracker Red probe. Confocal images were taken for wt and shRNA-transduced neurons (Fig. 5A).

The quantitative analysis of merged confocal images revealed an increase in the percentage of neurons with Parkin accumulation on mitochondria in wt and scrRNA neurons 3 h after the OGD/R (Fig. 5B, C). It was accompanied by a drop in Parkin protein levels in total cell lysates of wt (Fig. 5D) and scrRNA neurons (Fig. 5E). However, in Mfn2 knockdown neurons, Parkin accumulation on mitochondria was significantly elevated even before OGD (Fig. 5C) and it was accompanied by a decreased Parkin protein level in sh-Mfn2 controls, reaching only 53% and 39% (for shMfn2 B and shMfn2 D respectively) of wt controls (Fig. 5E, F). Further analysis by quantitative RT-PCR confirmed an equal expression of Parkin mRNA in scrRNA and sh-Mfn2 neurons, which excluded the presumption that the differences in Parkin protein levels between the controls might result from shRNA off-target effects (Fig. 5G).

Summing up, an increased Parkin localisation on mitochondria along with decreased Parkin protein levels in sh-Mfn2 control neurons suggest a mitochondrial dysfunction induced by Mfn2 knockdown (Fig. 5). Moreover, the Mfn2 knockdown resulted in a prolonged mitochondrial elimination in response to OGD/R, as evidenced by the increased number of mitophagosomes in sh-Mfn2 neurons 24 h after the insult (Fig. 4).

Mfn2 Knockdown Impairs Compensatory Mitochondrial Biogenesis in Rat Cortical Neurons Subjected to OGD/R

Since mitochondria are the main source of energy in neurons, further investigation was aimed at establishing whether mitochondrial damage caused by OGD/R could be alleviated by compensatory mitochondrial biogenesis also in Mfn2 knockdown neurons.

As shown by western blot analysis, the level of PGC-1α, the upstream regulator of mitochondrial biogenesis, was significantly increased in all the considered types of neurons 24

h after the insult (Fig. 6A, D). The downstream factor NRF-1 was significantly increased in sh-Mfn2 neurons (Fig. 6D), while in wt and scrRNA neurons, the level of NRF-1 was transiently decreased (Fig. 6A, D).

Western blot analysis was supported by the measurement of mitochondrial DNA content (Fig. 6B, E). An increased mitochondrial to nuclear DNA ratio (mtDNA/nDNA) was observed in wt neurons shortly after the insult (Fig. 6B). It was followed by a significant rise in the protein level of the representative subunits of the respiratory chain complexes 24 h after the insult (Fig. 6C). A similar relationship was observed for scrRNA neurons. However, an increase in mtDNA/nDNA ratio was transient (Fig. 6E) and the following increases of particular respiratory chain subunits were also present, yet not as pronounced as for wt neurons (Fig. 6F).

In contrast to control neurons, no increase in the mtDNA/nDNA ratio after the insult (Fig. 6E) and no rise in protein levels in any of the respiratory chain subunits considered (Fig. 6F) were observed in Mfn2 knockdown neurons.

Thus, Mfn2 knockdown appeared to supress the respiratory chain protein biogenesis in neurons after OGD/R.

Discussion

In this paper, we hypothesized that Mfn2 may act as a regulatory factor which integrates mitochondrial network dynamics with mitophagy and mitochondrial biogenesis in neurons following a transient ischemic insult.

We showed that in response to OGD/R, the dynamics of the mitochondrial network in wt neurons was increased to ameliorate the mitochondrial damage caused by the lack of oxygen and glucose. In addition, to prevent the bioenergy failure, compensatory biosynthesis of the respiratory chain proteins was initiated. However, in Mfn2 knockdown neurons, mitochondrial damage was not repaired by mitochondrial network dynamics. We demonstrated that Mfn2 knockdown prevented the remodelling of the mitochondrial network favouring the fragmentation of the mitochondria, intensified mitochondrial elimination and prevented the biosynthesis of respiratory complexes following OGD/R. Consequently, an increased neuronal death after OGD/R was observed for Mfn2 knockdown neurons, strongly suggesting that Mfn2 is one of the essential elements of the neuronal response to ischemic insult, necessary for the neuronal survival.

Alterations in mitochondrial dynamics have been implicated in many neurodegenerative diseases [1, 44]. Previous studies showed that Mfn2 was involved in mitochondrial trafficking in axons [45] and the abolition of this function of Mfn2 by genetic mutations or knockout changed mitochondrial movement and lead to axonal degeneration as

a consequence [46]. Moreover, a considerable number of experimental models have observed a link between mitochondrial fusion and fission and the onset of mitophagy [47, 48]. Multiple studies demonstrated Drp1-driven mitochondrial fission as a frequent consequence of ischemic injury [6]. According to Zuo et al. (2014), Drp1-driven mitochondrial fission contributed to neuronal survival by supporting the elimination of damaged mitochondria [47], while Kumar et al. (2016) indicated the biphasic mitochondrial fragmentation profile. In their study, OGD was followed by an extensive mitochondrial fragmentation which preceded apoptosis and neuronal death or by a moderate mitochondrial fragmentation followed by an increase in mitochondrial fusion during the re-oxygenation phase, resulting in neuronal survival [49]. In primary neurons, Nair et al. (2022) found a primary mitochondria fission wave immediately after 90-min OGD with a significant increase in mitophagy followed by a secondary phase of fission at 24 h following recovery [50]. Although it was hypothesised that excessive mitophagy in the early phase was a pathologic response which may contribute to secondary energy depletion, secondary mitophagy may be involved in regeneration and repair [50]. Further studies reported that increased events of mitochondrial fusion and fission supported the maintenance of mitochondrial function and thus cell survival by enhanced mixing of mitochondrial content [51]. The post-OGD intensified mitochondrial fusion in wt neurons observed in our model is consistent with the previous findings as it also seemed to contribute to neuronal survival.

In our study, the mitochondria in Mfn2 knockdown neurons showed a decreased size followed by reduced mitochondrial interconnectivity and elongation. As mentioned earlier, mitochondrial fusion and trafficking may also be mediated by Mfn2 homologue, Mfn1, which has been recorded to show even greater fusion activity [11]. However, in our model, selective Mfn2 knockdown was sufficient to alter mitochondrial morphology before the insult and to suppress mitochondrial network remodelling in response to OGD/R. Meanwhile, the protein levels of other agents mediating mitochondrial dynamics, Opa1 and Drp1, were not changed by shRNA transduction (data not shown) and Mfn1 was elevated (Fig. 2B). This was followed by prolonged mitophagy and increased neuronal death, as demonstrated by the increased LDH release and a higher number of pyknotic nuclei. Our data show that Mfn2 is required in the reoxygenation phase for the proper mitochondrial recovery. We suggest that Mfn2 is necessary for mitochondrial network post-insult remodelling which serves as an early quality control mechanism, and thus prevents over-elimination of mitochondria. These observations are consistent with the report by Puri et al. (2019), who demonstrated that mitochondrial elimination in neurons was secondary towards mitochondria repair [21].
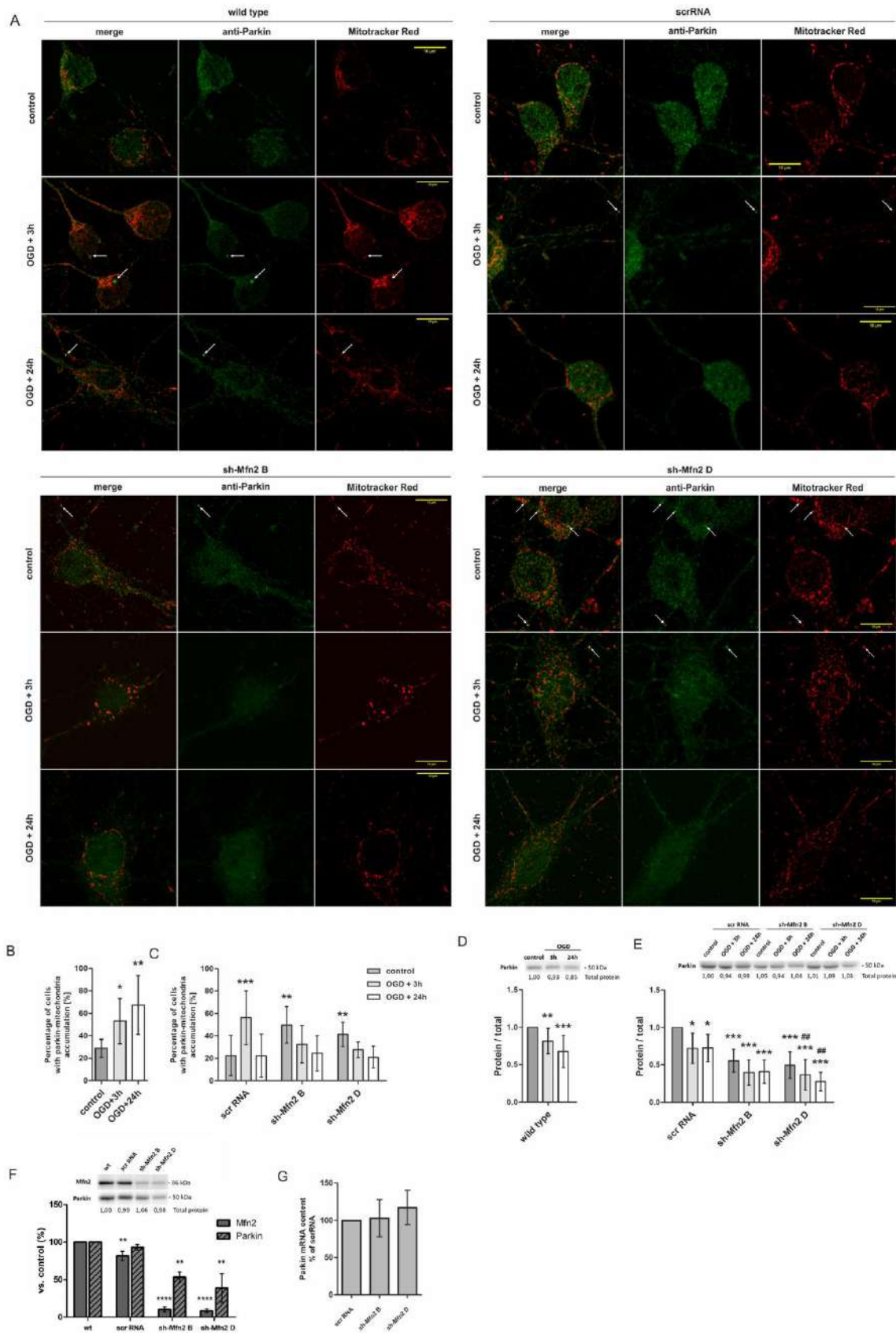
◄**Fig. 5.** Mfn2 knockdown in neurons is accompanied by increased Parkin accumulation on mitochondria. A. Representative images of wild-type (wt), scrRNA and sh-Mfn2 neurons presenting mitochondria and Parkin accumulation (bright dots indicated by arrows). Mitochondria visualized in red (Mitotracker Red) and Parkin (anti-Parkin) pseudocoloured in green. Bar = 10 μm. (B, C) Average percentage of wt and shRNA-transduced neurons positive for Parkin and mitochondria accumulation in controls and after OGD/R, $n = 3$. $*p < 0.05$, $**p < 0.01$, $***p < 0.001$ vs wt or scrRNA controls. (D, E) Representative western blots and densitometric analysis of Parkin in cell lysates of wt and shRNA-transduced neurons, respectively, after OGD/R, $n = 5$. (F) Representative western blot and densitometric analysis of Parkin level in cell lysates of control wt, scrRNA- and sh-Mfn2 neurons on DIV10; $n = 4$–6. (G) Quantitative Real-Time PCR for Parkin in scrRNA- and sh-Mfn2 neurons on DIV10; $n = 3$, $n = 3$. The optical density of the particular bands on western blots was normalized to total protein in line stained with Ponceau S and is presented relative to wt or scrRNA controls as mean $\pm$ SD; Normalization factors are shown under representative western blot images. $*p < 0.05$; $**p < 0.01$, $****p < 0.0001$ vs wt (B, D, F) or scrRNA control (C, E). $\#p < 0.05$, $\#\#p < 0.01$, vs sh-Mfn2 control (E)

In our model, Mfn2 protein level in wt and scrRNA neurons was significantly reduced after the OGD/R. As previously shown by Wappler et al. (2013), the duration of OGD, thus the severity of the insult, resulted in different involvement of key proteins mediating mitochondrial fusion and fission. In their model, 1 h OGD did not alter the protein level of pro-fusion (Mfn1/2 and Opa1) and pro-fission (Drp1, Fis1) proteins although some alteration in mitochondrial shape and mitochondrial network were observed [24]. However, in our experimental conditions, 1 h OGD proved to be sufficient to cause mitochondrial network remodelling that was accompanied by a significant reduction of Mfn2 protein. The discrepancy may potentially result from minor differences in the experimental and culturing conditions, e.g. a different ratio between neurons and glia causing different susceptibility towards the insults.

The observed constant reduction of Mfn2 after OGD/R in wt neurons appeared to be specific for this protein, as we did not observe similar changes for its homolog, Mfn1, and the mitochondrial matrix marker, Hsp60. We did, however, observe a transient drop in Opa1, Drp1 and TOM22 immunoreactivity at 3 h. This may imply the participation of enhanced mitophagy or other cellular processes, such as e.g. proteasomal degradation of OMM proteins which may not necessarily lead to the elimination of whole mitochondria but might be involved in endogenous mechanisms regulating mitochondria elimination [52].

OGD-induced reduction of Mfn2, as was observed here, is in line with the outcomes obtained in previous studies in in vitro and in vivo models [53]. As demonstrated by McLelland et al. (2018), Mfn2 proteasomal degradation facilitated the dissociation of mitochondria from ER thereby enabling mitophagy [20]. In our model, the number of mitophagosomes in Mfn2 knockdown neurons outranked their number

in wt and scrRNA neurons after OGD/R (3 h and 24 h), indicating intensified mitophagy in comparison to wt neurons. However, the increased mitochondrial elimination in Mfn2 knockdown neurons did not support cells survival. Therefore, our conclusion is that increased mitophagy alone does not contribute to neuroprotection and that Mfn2 knockdown may disrupt the balance between mitochondrial recovery and mitochondrial elimination, increasing the neuronal susceptibility towards ischemic insult.

According to recent studies, Mfn2 degradation after ischemic insult is mediated by E3 ubiquitin ligase, Parkin [18, 54]. As shown by Chen et al. (2013), PINK1 phosphorylates Mfn2 to facilitate the accumulation of Parkin on damaged mitochondria [17]. Simultaneously, Parkin mediates Mfn2 ubiquitination and degradation, which has an impact on mitochondria-ER tethering [18, 20]. Considering the above, the mutual relation between Mfn2 and Parkin seems to link mitochondrial dynamics with mitochondrial elimination. Here, we have shown that Mfn2 knockdown was accompanied by a decrease of Parkin and the reduction did not result from altered mRNA expression. It seems to support the thesis on Mfn2-Parkin relationship in mitophagy coordination. Enhanced Parkin localisation on mitochondria in sh-Mfn2 neurons together with a decreased mitochondrial membrane potential, as observed for sh-Mfn2 D neurons, may additionally indicate that Mfn2 knockdown causes mild mitochondrial dysfunction, which does not affect neuronal survival in control conditions but contributes to increased susceptibility towards OGD. The exact mechanism of this phenomenon, however, requires further investigation.

In our model, OGD/R was observed to induce an increase in PGC-1α protein level. In wt neurons, it was followed by an increase in mtDNA content and the biosynthesis of representative proteins for respiratory complexes, revealing a mitochondrial biogenesis as an integral element of pro-surviving response to OGD/R. This phenomenon was not observed in Mfn2 knockdown neurons. The mechanism is not fully understood, but several considerations have already emerged. The mtDNA particles in cells are packed into mtDNA-protein complexes, nucleoids [55], and can be passively transferred between mitochondria during mitochondrial fusion and fission events [56]. Considering the above, Mfn2 deficiency may affect mtDNA synthesis and segregation by impairing mitochondrial fusion and trafficking. It has also been demonstrated that for proper mtDNA distribution, especially in peripheral zones of the cell, nucleoids have to be actively transported via Kinesin Family Member (KIF5B)-driven mitochondrial dynamic tubulation activities (Miro) that occur predominantly at the ER-mitochondria contact sites [57]. ER-mitochondria contacts are the main location of distribution of newly synthetized mtDNA to daughter mitochondria. It can therefore be assumed that the proper mitochondria-ER positioning, as also determined by Mfn2, may be crucial for mtDNA synthesis in
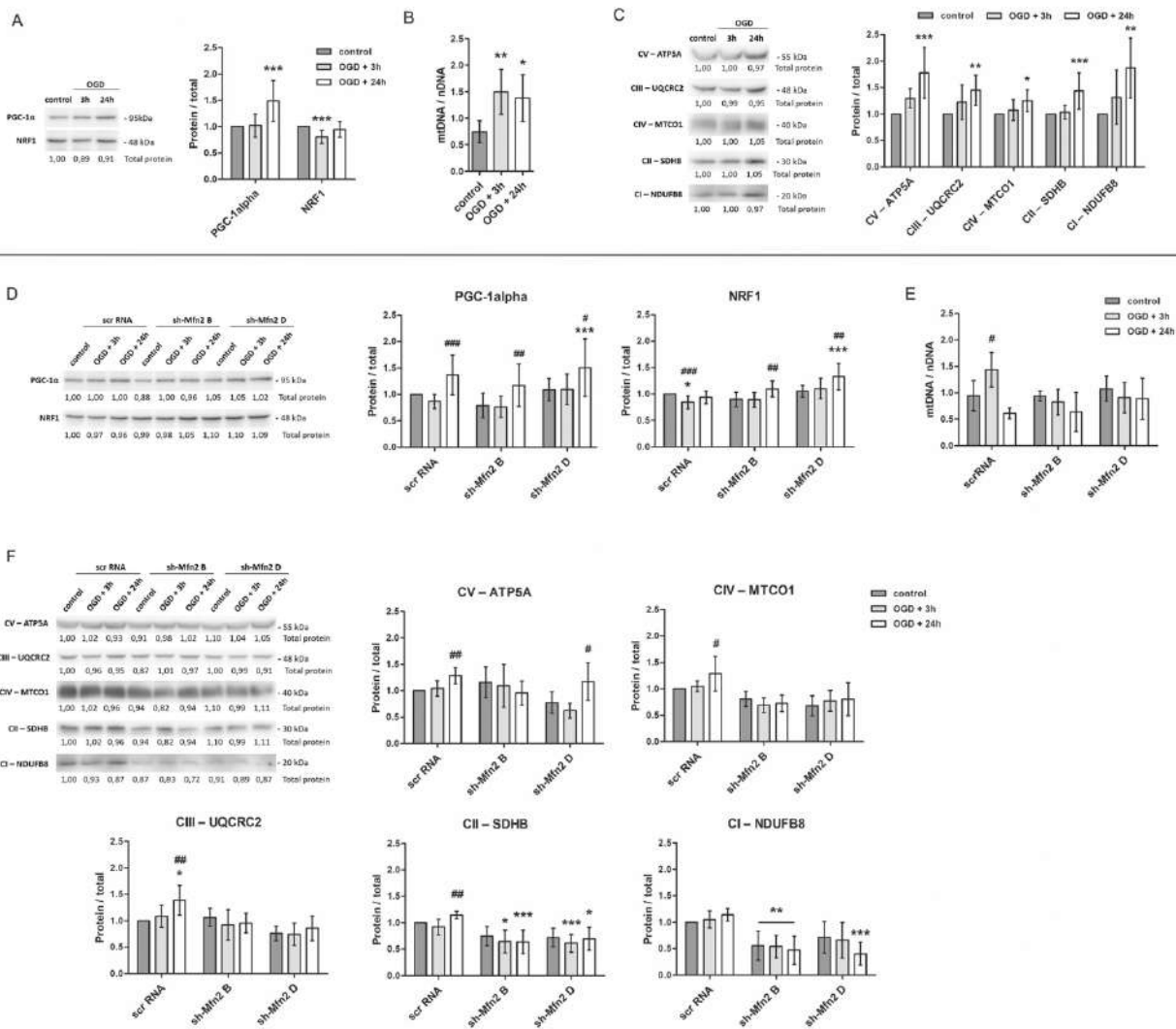
Fig. 6 Mfn2 knockdown supresses biosynthesis of respiratory chain proteins in neurons after OGD/R. (A, D) Representative western blots and densitometric analysis of mitochondria biogenesis key proteins: PGC-1α and NRF-1 in cell lysates of wild-type (wt) and shRNA-transduced neurons, respectively, $n = 5$. (B, E) Average mitochondrial to nuclear DNA ratio (mtDNA/nDNA) in wt and shRNA neurons, respectively, before and after OGD/R; Data are expressed as mean ± SD, $n = 5$. (C, F) Representative western blots and densitometric analysis of representative respiratory chain subunits in cell lysates of wt and shRNA neurons, respectively, $n = 5$. Western blot data are shown as the fold change over control of the protein of interest. Optical density of particular bands was normalized to total protein in line stained with Ponceau S and presented as mean ± SD. The normalization factors are shown under representative western blot images. * $p < 0.05$, **$p < 0.01$, ***$p < 0.001$ vs wt control or scrRNA control; #$p < 0.05$, ##$p < 0.01$, ###$p < 0.001$ vs sh-Mfn2 control

response to ischemic insult. More research is needed to elucidate the molecular mechanism describing how Mfn2 knockdown affects not only the mtDNA biosynthesis and distribution but also mitochondrial biogenesis in general.

Conclusion

Our data support the hypothesis that Mfn2 in neurons is involved in their response to mild and transient OGD/R stress by balancing the rate of elimination of defective mitochondria. In addition, Mfn2 has a positive influence on the mitochondrial restoration expressed as mtDNA and proteins in the respiratory chain content. In Mfn2 knockdown neurons, stress recovery is not as efficient as in wt cells. This may potentially be caused by mitochondrial impairment which is not effectively repaired by restoration of mitochondrial network dynamics and respiratory chain protein content while mitochondria elimination is enhanced after the insult. Consequently, Mfn2 knockdown results in increased neuronal death following OGD/R stress, confirming that Mfn2 is one of essential elements

Springer

of neuronal response to ischemic insult, crucial for neuronal survival.

Data Availability The datasets generated during and/or analysed during the current study are available from the corresponding author on reasonable request.

Declarations

All procedures involving animals were performed in accordance with the ethical standards of the institution or practice at which the studies were conducted.

Conflict of Interest The authors declare no competing interests.

References

1. Chen H, Chan DC (2009) Mitochondrial dynamics--fusion, fission, movement, and mitophagy--in neurodegenerative diseases. Hum Mol Genet 18:R169–R176. https://doi.org/10.1093/hmg/ddp326
2. Dorn GW (2019) Evolving concepts of mitochondrial dynamics. Annu Rev Physiol 81:1–17. https://doi.org/10.1146/annurev-physiol-020518-114358
3. Giacomello M, Pyakurel A, Glytsou C, Scorrano L (2020) The cell biology of mitochondrial membrane dynamics. Nat Rev Mol Cell Biol 21:204–224. https://doi.org/10.1038/s41580-020-0210-7
4. Anzell AR, Maizy R, Przyklenk K, Sanderson TH (2018) Mitochondrial quality control and disease: insights into ischemia-reperfusion injury. Mol Neurobiol 55:2547–2564. https://doi.org/10.1007/s12035-017-0503-9
5. He Z, Ning N, Zhou Q, Khoshnam SE, Farzaneh M (2020) Mitochondria as a therapeutic target for ischemic stroke. Free Radic Biol Med 146:45–58. https://doi.org/10.1016/j.freeradbiomed.2019.11.005
6. Zhang X, Yan H, Yuan Y, Gao J, Shen Z, Cheng Y, Shen Y, Wang RR et al (2013) Cerebral ischemia-reperfusion-induced autophagy protects against neuronal injury by mitochondrial clearance. Autophagy 9:1321–1333. https://doi.org/10.4161/auto.25132
7. Yin W, Signore AP, Iwai M, Cao G, Gao Y, Chen J (2008) Rapidly increased neuronal mitochondrial biogenesis after hypoxic-ischemic brain injury. Stroke 39:3057–3063. https://doi.org/10.1161/STROKEAHA.108.520114
8. Xie Y, Li J, Fan G, Qi S, Li B (2014) Reperfusion promotes mitochondrial biogenesis following focal cerebral ischemia in rats. PLoS One 9:e92443. https://doi.org/10.1371/journal.pone.0092443
9. Santel A, Fuller MT (2001) Control of mitochondrial morphology by a human mitofusin. J Cell Sci 114:867–874
10. Chen H, Detmer SA, Ewald AJ, Griffin EE, Fraser SE, Chan DC (2003) Mitofusins Mfn1 and Mfn2 coordinately regulate mitochondrial fusion and are essential for embryonic development. J Cell Biol 160:189–200. https://doi.org/10.1083/jcb.200211046
11. Ishihara N, Eura Y, Mihara K (2004) Mitofusin 1 and 2 play distinct roles in mitochondrial fusion reactions via GTPase activity. J Cell Sci 117:6535–6546. https://doi.org/10.1242/jcs.01565
12. de Brito OM, Scorrano L (2008) Mitofusin 2 tethers endoplasmic reticulum to mitochondria. Nature 456:605–610. https://doi.org/10.1038/nature07534
13. de Brito OM, Scorrano L (2009) Mitofusin-2 regulates mitochondrial and endoplasmic reticulum morphology and tethering: the role of Ras. Mitochondrion 9:222–226. https://doi.org/10.1016/j.mito.2009.02.005
14. Kim I, Rodriguez-Enriquez S, Lemasters JJ (2007) Selective degradation of mitochondria by mitophagy. Arch Biochem Biophys 462:245–253. https://doi.org/10.1016/j.abb.2007.03.034
15. Narendra DP, Jin SM, Tanaka A, Suen DF, Gautier CA, Shen J, Cookson MR, Youle RJ (2010) PINK1 is selectively stabilized on impaired mitochondria to activate Parkin. PLoS Biol 8:e1000298. https://doi.org/10.1371/journal.pbio.1000298
16. Narendra D, Tanaka A, Suen DF, Youle RJ (2008) Parkin is recruited selectively to impaired mitochondria and promotes their autophagy. J Cell Biol 183:795–803. https://doi.org/10.1083/jcb.200809125
17. Chen Y, Dorn GW (2013) PINK1-phosphorylated mitofusin 2 is a Parkin receptor for culling damaged mitochondria. Science 340:471–475. https://doi.org/10.1126/science.1231031
18. Gegg ME, Cooper JM, Chau KY, Rojo M, Schapira AH, Taanman JW (2010) Mitofusin 1 and mitofusin 2 are ubiquitinated in a PINK1/parkin-dependent manner upon induction of mitophagy. Hum Mol Genet 19:4861–4870. https://doi.org/10.1093/hmg/ddq419
19. Basso V, Marchesan E, Peggion C, Chakraborty J, von Stockum S, Giacomello M, Ottolini D, Debattisti V et al (2018) Regulation of ER-mitochondria contacts by Parkin via Mfn2. Pharmacol Res 138:43–56. https://doi.org/10.1016/j.phrs.2018.09.006
20. McLelland GL, Goiran T, Yi W, Dorval G, Chen CX, Lauinger ND, Krahn AI, Valimehr S et al (2018) Mfn2 ubiquitination by PINK1/parkin gates the p97-dependent release of ER from

mitochondria to drive mitophagy. Elife 7. https://doi.org/10.7554/eLife.32866

21. Puri R, Cheng XT, Lin MY, Huang N, Sheng ZH (2019) Mul1 restrains Parkin-mediated mitophagy in mature neurons by maintaining ER-mitochondrial contacts. Nat Commun 10:3645. https://doi.org/10.1038/s41467-019-11636-5

22. Lewis SC, Uchiyama LF, Nunnari J (2016) ER-mitochondria contacts couple mtDNA synthesis with mitochondrial division in human cells. Science 353:aaf5549. https://doi.org/10.1126/science.aaf5549

23. Friedman JR, Lackner LL, West M, DiBenedetto JR, Nunnari J, Voeltz GK (2011) ER tubules mark sites of mitochondrial division. Science 334:358–362. https://doi.org/10.1126/science.1207385

24. Wappler EA, Institoris A, Dutta S, Katakam PV, Busija DW (2013) Mitochondrial dynamics associated with oxygen-glucose deprivation in rat primary neuronal cultures. PLoS One 8:e63206. https://doi.org/10.1371/journal.pone.0063206

25. Yang JL, Mukda S, Chen SD (2018) Diverse roles of mitochondria in ischemic stroke. Redox Biol 16:263–275. https://doi.org/10.1016/j.redox.2018.03.002

26. Grohm J, Kim SW, Mamrak U, Tobaben S, Cassidy-Stone A, Nunnari J, Plesnila N, Culmsee C (2012) Inhibition of Drp1 provides neuroprotection in vitro and in vivo. Cell Death Differ 19:1446–1458. https://doi.org/10.1038/cdd.2012.18

27. Zhao YX, Cui M, Chen SF, Dong Q, Liu XY (2014) Amelioration of ischemic mitochondrial injury and Bax-dependent outer membrane permeabilization by Mdivi-1. CNS Neurosci Ther 20:528–538. https://doi.org/10.1111/cns.12266

28. Li Y, Wang M, Wang S (2016) Effect of inhibiting mitochondrial fission on energy metabolism in rat hippocampal neurons during ischemia/reperfusion injury. Neurol Res 38:1027–1034. https://doi.org/10.1080/01616412.2016.1215050

29. Peng K, Xiao J, Yang L, Ye F, Cao J, Sai Y (2019) Mutual antagonism of PINK1/Parkin and PGC-1α contributes to maintenance of mitochondrial homeostasis in rotenone-induced neurotoxicity. Neurotox Res 35:331–343. https://doi.org/10.1007/s12640-018-9957-4

30. Wu Z, Puigserver P, Andersson U, Zhang C, Adelmant G, Mootha V, Troy A, Cinti S et al (1999) Mechanisms controlling mitochondrial biogenesis and respiration through the thermogenic coactivator PGC-1. Cell 98:115–124. https://doi.org/10.1016/S0092-8674(00)80611-X

31. Lee Y, Stevens DA, Kang SU, Jiang H, Lee YI, Ko HS, Scarffe LA, Umanah GE et al (2017) PINK1 primes Parkin-mediated ubiquitination of PARIS in dopaminergic neuronal survival. Cell Rep 18:918–932. https://doi.org/10.1016/j.celrep.2016.12.090

32. Stevens DA, Lee Y, Kang HC, Lee BD, Lee YI, Bower A, Jiang H, Kang SU et al (2015) Parkin loss leads to PARIS-dependent declines in mitochondrial mass and respiration. Proc Natl Acad Sci U S A 112:11696–11701. https://doi.org/10.1073/pnas.1500624112

33. Ryou MG, Mallet RT (2018) An in vitro oxygen-glucose deprivation model for studying ischemia-reperfusion injury of neuronal cells. Methods Mol Biol 1717:229–235. https://doi.org/10.1007/978-1-4939-7526-6_18

34. Gruszczynska-Biegala J, Strucinska K, Maciag F, Majewski L, Sladowska M, Kuznicki J (2020) STIM protein-NMDA2 receptor interaction decreases NMDA-dependent calcium levels in cortical neurons. Cells 9. https://doi.org/10.3390/cells9010160

35. Thacker JS, Yeung DH, Staines WR, Mielke JG (2016) Total protein or high-abundance protein: which offers the best loading control for Western blotting? Anal Biochem 496:76–78. https://doi.org/10.1016/j.ab.2015.11.022

36. Dagda RK, Cherra SJ, Kulich SM, Tandon A, Park D, Chu CT (2009) Loss of PINK1 function promotes mitophagy through effects on oxidative stress and mitochondrial fission. J Biol Chem 284:13843–13855. https://doi.org/10.1074/jbc.M808515200

37. Van Laar VS, Roy N, Liu A, Rajprohat S, Arnold B, Dukes AA, Holbein CD, Berman SB (2015) Glutamate excitotoxicity in neurons triggers mitochondrial and endoplasmic reticulum accumulation of Parkin, and, in the presence of N-acetyl cysteine, mitophagy. Neurobiol Dis 74:180–193. https://doi.org/10.1016/j.nbd.2014.11.015

38. Szulc-Dabrowska L, Gregorczyk KP, Struzik J, Boratynska-Jasinska A, Szczepanowska J, Wyzewski Z, Toka FN, Gierynska M et al (2016) Remodeling of the fibroblast cytoskeletal architecture during the replication cycle of Ectromelia virus: a morphological in vitro study in a murine cell line. Cytoskeleton (Hoboken) 73:396–417. https://doi.org/10.1002/cm.21308

39. Iwashita H, Torii S, Nagahora N, Ishiyama M, Shioji K, Sasamoto K, Shimizu S, Okuma K (2017) Live cell imaging of mitochondrial autophagy with a novel fluorescent small molecule. ACS Chem Biol 12:2546–2551. https://doi.org/10.1021/acschembio.7b00647

40. Nicklas JA, Brooks EM, Hunter TC, Single R, Branda RF (2004) Development of a quantitative PCR (TaqMan) assay for relative mitochondrial DNA copy number and the common mitochondrial DNA deletion in the rat. Environ Mol Mutagen 44:313–320. https://doi.org/10.1002/em.20050

41. Untergasser A, Cutcutache I, Koressaar T, Ye J, Faircloth BC, Remm M, Rozen SG (2012) Primer3--new capabilities and interfaces. Nucleic Acids Res 40:e115. https://doi.org/10.1093/nar/gks596

42. Livak KJ, Schmittgen TD (2001) Analysis of relative gene expression data using real-time quantitative PCR and the 2(-Delta Delta C(T)) Method. Methods 25:402–408. https://doi.org/10.1006/meth.2001.1262

43. Cossarizza A, Salvioli S (2001) Flow cytometric analysis of mitochondrial membrane potential using JC-1. Curr Protoc Cytom:Chapter 9–Unit 9.14. https://doi.org/10.1002/0471142956.cy0914s13

44. Chan DC (2020) Mitochondrial dynamics and its involvement in disease. Annu Rev Pathol 15:235–259. https://doi.org/10.1146/annurev-pathmechdis-012419-032711

45. Misko A, Jiang S, Wegorzewska I, Milbrandt J, Baloh RH (2010) Mitofusin 2 is necessary for transport of axonal mitochondria and interacts with the Miro/Milton complex. J Neurosci 30:4232–4240. https://doi.org/10.1523/JNEUROSCI.6248-09.2010

46. Misko AL, Sasaki Y, Tuck E, Milbrandt J, Baloh RH (2012) Mitofusin2 mutations disrupt axonal mitochondrial positioning and promote axon degeneration. J Neurosci 32:4145–4155. https://doi.org/10.1523/JNEUROSCI.6338-11.2012

47. Zuo W, Zhang S, Xia CY, Guo XF, He WB, Chen NH (2014) Mitochondria autophagy is induced after hypoxic/ischemic stress in a Drp1 dependent manner: the role of inhibition of Drp1 in ischemic brain damage. Neuropharmacology 86:103–115. https://doi.org/10.1016/j.neuropharm.2014.07.002

48. Chen M, Chen Z, Wang Y, Tan Z, Zhu C, Li Y, Han Z, Chen L et al (2016) Mitophagy receptor FUNDC1 regulates mitochondrial dynamics and mitophagy. Autophagy 12:689–702. https://doi.org/10.1080/15548627.2016.1151580

49. Kumar R, Bukowski MJ, Wider JM, Reynolds CA, Calo L, Lepore B, Tousignant R, Jones M et al (2016) Mitochondrial dynamics following global cerebral ischemia. Mol Cell Neurosci 76:68–75. https://doi.org/10.1016/j.mcn.2016.08.010

50. Nair S, Leverin AL, Rocha-Ferreira E, Sobotka KS, Thornton C, Mallard C, Hagberg H (2022) Induction of mitochondrial

fragmentation and mitophagy after neonatal hypoxia-ischemia. Cells 11:doi:10.3390/cells11071193

51. Chan DC (2006) Mitochondrial fusion and fission in mammals. Annu Rev Cell Dev Biol 22:79–99. https://doi.org/10.1146/annurev.cellbio.22.010305.104638

52. Chan NC, Salazar AM, Pham AH, Sweredoski MJ, Kolawa NJ, Graham RL, Hess S, Chan DC (2011) Broad activation of the ubiquitin-proteasome system by Parkin is critical for mitophagy. Hum Mol Genet 20:1726–1737. https://doi.org/10.1093/hmg/ddr048

53. Martorell-Riera A, Segarra-Mondejar M, Muñoz JP, Ginet V, Olloquequi J, Pérez-Clausell J, Palacín M, Reina M et al (2014) Mfn2 downregulation in excitotoxicity causes mitochondrial dysfunction and delayed neuronal death. EMBO J 33:2388–2407. https://doi.org/10.15252/embj.201488327

54. Tanaka A, Cleland MM, Xu S, Narendra DP, Suen DF, Karbowski M, Youle RJ (2010) Proteasome and p97 mediate mitophagy and degradation of mitofusins induced by Parkin. J Cell Biol 191:1367–1380. https://doi.org/10.1083/jcb.201007013

55. Satoh M, Kuroiwa T (1991) Organization of multiple nucleoids and DNA molecules in mitochondria of a human cell. Exp Cell Res 196:137–140. https://doi.org/10.1016/0014-4827(91)90467-9

56. Yan C, Duanmu X, Zeng L, Liu B, Song Z (2019) Mitochondrial DNA: distribution, mutations, and elimination. Cells 8. https://doi.org/10.3390/cells8040379

57. Qin J, Guo Y, Xue B, Shi P, Chen Y, Su QP, Hao H, Zhao S et al (2020) ER-mitochondria contacts promote mtDNA nucleoids active transportation via mitochondrial dynamic tubulation. Nat Commun 11:4471. https://doi.org/10.1038/s41467-020-18202-4

http://rcin.org.pl

OŚWIADCZENIA WSPÓŁAUTORÓW

Pracownia Biologii Molekularnej
Instytut Medycyny Doświadczalnej i Klinicznej
Im. M. Mossakowskiego PAN
02-106 Warszawa ul. Adolfa Pawińskiego 5

Mgr Piotr Wojtyniak
E-mail: pwojtyniak@imdik.pan.pl

Warszawa, 03.01.2023

Oświadczenie kandydata

Niniejszym poświadczam swój wkład w powstanie następujących publikacji:

1. Kawalec M, Wojtyniak P, Bielska E, Lewczuk A, Boratyńska-Jasińska A, Beręsewicz-Haller M, Frontczak-Baniewicz M, Gewartowska M, Zabłocka B. Mitochondrial dynamics, elimination and biogenesis during post-ischemic recovery in ischemia-resistant and ischemia-vulnerable gerbil hippocampal regions. Biochim Biophys Acta Mol Basis Dis. 2022 Dec 22:166633. doi: 10.1016/j.bbadis.2022.166633

Wkład obejmuje:
Wykonywanie większości doświadczeń biochemicznych i analiz statystycznych. Analizę wyników, analizę obrazów TEM, pisanie manuskryptu (materiały i metody) oraz przygotowywanie wykresów i paneli zdjęć do rycin w publikacji. Poprawianie manuskryptu.

2. Wojtyniak P., Boratynska-Jasinska A., Serwach K., Gruszczynska-Biegala J., Zablocka B., Jaworski J., Kawalec K. Mitofusin 2 Integrates Mitochondrial Network Remodelling, Mitophagy and Renewal of Respiratory Chain Proteins in Neurons after Oxygen and Glucose Deprivation. Mol Neurobiol 59, 6502–6518 (2022). doi: 10.1007/s12035-022-02981-6

Wkład obejmuje:
Przygotowywanie konstruktów lentiwirusowych oraz komórek o zmienionej ekspresji Mfn2 do doświadczeń. Zakładanie i prowadzenie hodowli komórek *in vitro* oraz przeprowadzanie procedury OGD. Wykonywanie większości doświadczeń biochemicznych, analiza wyników oraz analiza statystyczna. Pisanie manuskryptu (materiały i metody) oraz przygotowywanie wykresów do rycin w publikacji.

Piotr Wojtyniak

87

Pracownia Biologii Molekularnej
Instytut Medycyny Doświadczalnej i Klinicznej
Im. M. Mossakowskiego PAN
02-106 Warszawa ul. Adolfa Pawińskiego 5

Dr Maria Kawalec
E-mail: mkawalec@imdik.pan.pl

Warszawa, 02.01.2023

Oświadczenie współautora

Niniejszym poświadczam swój wkład w powstanie następujących publikacji:

1. Kawalec M, Wojtyniak P, Bielska E, Lewczuk A, Boratyńska-Jasińska A, Beręsewicz-Haller M, Frontczak-Baniewicz M, Gewartowska M, Zabłocka B. Mitochondrial dynamics, elimination and biogenesis during post-ischemic recovery in ischemia-resistant and ischemia-vulnerable gerbil hippocampal regions. Biochim Biophys Acta Mol Basis Dis. 2022 Dec 22:166633. doi: 10.1016/j.bbadis.2022.166633

2. Wojtyniak P., Boratynska-Jasinska A., Serwach K., Gruszczynska-Biegala J., Zablocka B., Jaworski J., Kawalec K. Mitofusin 2 Integrates Mitochondrial Network Remodelling, Mitophagy and Renewal of Respiratory Chain Proteins in Neurons after Oxygen and Glucose Deprivation. Mol Neurobiol 59, 6502–6518 (2022). doi: 10.1007/s12035-022-02981-6

Wkład obejmuje:
Planowanie doświadczeń, nadzór nad realizacją działań badawczych i analiza wyników. Udział w wykonywaniu doświadczeń biochemicznych. Sformułowanie koncepcji pracy (publikacja 2), udział w sformułowaniu koncepcji pracy (publikacja 1), napisanie manuskryptu (oprócz materiałów i metod) i przygotowanie rycin, odpowiedzi na uwagi recenzentów, prowadzenie korespondencji z redaktorem. Pozyskiwanie środków na badania.

Maria Kawalec

Maria Kawalec

Pracownia Biologii Molekularnej
Instytut Medycyny Doświadczalnej i Klinicznej
Im. M. Mossakowskiego PAN
02-106 Warszawa ul. Adolfa Pawińskiego 5

Prof. dr hab. Barbara Zabłocka
E-mail: bzablocka@imdik.pan.pl

Warszawa, 02.01.2023

Oświadczenie współautora

Niniejszym poświadczam swój wkład w powstanie następujących publikacji:

1. Kawalec M, Wojtyniak P, Bielska E, Lewczuk A, Boratyńska-Jasińska A, Beręsewicz-Haller M, Frontczak-Baniewicz M, Gewartowska M, Zabłocka B. Mitochondrial dynamics, elimination and biogenesis during post-ischemic recovery in ischemia-resistant and ischemia-vulnerable gerbil hippocampal regions. Biochim Biophys Acta Mol Basis Dis. 2022 Dec 22:166633. doi: 10.1016/j.bbadis.2022.166633

2. Wojtyniak P., Boratynska-Jasinska A., Serwach K., Gruszczynska-Biegala J., Zablocka B., Jaworski J., Kawalec K. Mitofusin 2 Integrates Mitochondrial Network Remodelling, Mitophagy and Renewal of Respiratory Chain Proteins in Neurons after Oxygen and Glucose Deprivation. Mol Neurobiol 59, 6502–6518 (2022). doi: 10.1007/s12035-022-02981-6

Wkład obejmuje:
Opiekę merytoryczną i nadzór nad realizacją działań badawczych. Udział w planowaniu badań, analizie wyników, sformułowanie koncepcji pracy (publikacja 1), udział w sformułowaniu koncepcji pracy (publikacja 2), przygotowaniu manuskryptu i odpowiedzi na uwagi recenzentów. Pozyskiwanie środków na badania.

Barbara Zabłocka

Pracownia Biologii Molekularnej
Instytut Medycyny Doświadczalnej i Klinicznej
Im. M. Mossakowskiego PAN
02-106 Warszawa ul. Adolfa Pawińskiego 5

Dr Anna Boratyńska-Jasińska
E-mail: aboratynska@imdik.pan.pl

Warszawa, 02.01.2023

Oświadczenie współautora

Niniejszym poświadczam swój wkład w powstanie następujących publikacji:

1. Kawalec M, Wojtyniak P, Bielska E, Lewczuk A, Boratyńska-Jasińska A, Beręsewicz-Haller M, Frontczak-Baniewicz M, Gewartowska M, Zabłocka B. Mitochondrial dynamics, elimination and biogenesis during post-ischemic recovery in ischemia-resistant and ischemia-vulnerable gerbil hippocampal regions. Biochim Biophys Acta Mol Basis Dis. 2022 Dec 22:166633. doi: 10.1016/j.bbadis.2022.166633
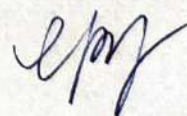
Wkład obejmuje:
Udział w wykonywaniu doświadczeń: pomiar ilości mtDNA. Analizę ilościowa obrazów TEM i udział w przygotowywaniu rycin do publikacji. Pisanie (materiały i metody) i poprawianie manuskryptu.

2. Wojtyniak P., Boratynska-Jasinska A., Serwach K., Gruszczynska-Biegala J., Zabłocka B., Jaworski J., Kawalec K. Mitofusin 2 Integrates Mitochondrial Network Remodelling, Mitophagy and Renewal of Respiratory Chain Proteins in Neurons after Oxygen and Glucose Deprivation. Mol Neurobiol 59, 6502–6518 (2022). doi: 10.1007/s12035-022-02981-6

Wkład obejmuje:
Udział w prowadzeniu hodowli *in vitro* oraz wykonywaniu doświadczeń: pomiar ilości mtDNA oraz techniki mikroskopii fluorescencyjnej. Udział w wykonywaniu analizy statystycznej i przygotowywaniu rycin do publikacji. Pisanie (materiały i metody) i poprawianie manuskryptu.

Anna Boratyńska-Jasińska

90

Pracownia Biologii Molekularnej
Instytut Medycyny Doświadczalnej i Klinicznej
Im. M. Mossakowskiego PAN
02-106 Warszawa ul. Adolfa Pawińskiego 5

Mgr Ewelina Bielska
E-mail: bielska.ewelina@gmail.com

Warszawa, 30.12.2022

Oświadczenie współautora

Niniejszym poświadczam swój wkład w powstanie następującej publikacji:

Kawalec M, Wojtyniak P, Bielska E, Lewczuk A, Boratyńska-Jasińska A, Beręsewicz-Haller M, Frontczak-Baniewicz M, Gewartowska M, Zabłocka B. Mitochondrial dynamics, elimination and biogenesis during post-ischemic recovery in ischemia-resistant and ischemia-vulnerable gerbil hippocampal regions. Biochim Biophys Acta Mol Basis Dis. 2022 Dec 22:166633. doi: 10.1016/j.bbadis.2022.166633

Wkład obejmuje:
Udział w doświadczeniach biochemicznych.

Ewelina Bielska

Pracownia Biologii Molekularnej
Instytut Medycyny Doświadczalnej i Klinicznej
Im. M. Mossakowskiego PAN
02-106 Warszawa ul. Adolfa Pawińskiego 5

Lek. wet. Anita Lewczuk
E-mail: alewczuk@imdik.pan.pl

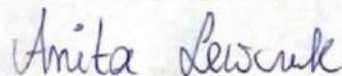Warszawa, 30.12.2022

Oświadczenie współautora

Niniejszym poświadczam swój wkład w powstanie następującej publikacji:

Kawalec M, Wojtyniak P, Bielska E, Lewczuk A, Boratyńska-Jasińska A, Beręsewicz-Haller M, Frontczak-Baniewicz M, Gewartowska M, Zabłocka B. Mitochondrial dynamics, elimination and biogenesis during post-ischemic recovery in ischemia-resistant and ischemia-vulnerable gerbil hippocampal regions. Biochim Biophys Acta Mol Basis Dis. 2022 Dec 22:166633. doi: 10.1016/j.bbadis.2022.166633

Wkład obejmuje:
Przeprowadzanie zabiegu ischemii i reperfuzji u zwierząt doświadczalnych, izolacja hipokampów, analiza histopatologiczna, pisanie manuskryptu (materiały i metody).

Anita Lewczuk

Anita Lewczuk

92

Pracownia Biologii Molekularnej
Instytut Medycyny Doświadczalnej i Klinicznej
Im. M. Mossakowskiego PAN
02-106 Warszawa ul. Adolfa Pawińskiego 5

Dr Małgorzata Beręsewicz-Haller
E-mail: mberesewicz@imdik.pan.pl

<div align="right">Warszawa, 02.01.2023</div>

Oświadczenie współautora

Niniejszym poświadczam swój wkład w powstanie następującej publikacji:

Kawalec M, Wojtyniak P, Bielska E, Lewczuk A, Boratyńska-Jasińska A, Beręsewicz-Haller M, Frontczak-Baniewicz M, Gewartowska M, Zabłocka B. Mitochondrial dynamics, elimination and biogenesis during post-ischemic recovery in ischemia-resistant and ischemia-vulnerable gerbil hippocampal regions. Biochim Biophys Acta Mol Basis Dis. 2022 Dec 22:166633. doi: 10.1016/j.bbadis.2022.166633

Wkład obejmuje:
Przeprowadzanie zabiegu ischemii i reperfuzji u zwierząt doświadczalnych, izolacja hipokampów, udział w korekcie manuskryptu.

<div align="right">
Małgorzata Beręsewicz-Haller
</div>

Pracownia Badań Mikroskopowo – Elektronowych
Instytut Medycyny Doświadczalnej i Klinicznej
Im. M. Mossakowskiego PAN
02-106 Warszawa ul. Adolfa Pawińskiego 5

Dr Magdalena Gewartowska
E-mail: mgewartowska@imdik.pan.pl

Warszawa, 03.01.2023

Oświadczenie współautora

Niniejszym poświadczam swój wkład w powstanie następującej publikacji:

Kawalec M, Wojtyniak P, Bielska E, Lewczuk A, Boratyńska-Jasińska A, Beręsewicz-Haller M, Frontczak-Baniewicz M, Gewartowska M, Zabłocka B. Mitochondrial dynamics, elimination and biogenesis during post-ischemic recovery in ischemia-resistant and ischemia-vulnerable gerbil hippocampal regions. Biochim Biophys Acta Mol Basis Dis. 2022 Dec 22:166633. doi: 10.1016/j.bbadis.2022.166633

Wkład obejmuje:
Wykonywanie i analiza zdjęć TEM oraz przygotowanie opisu wykorzystanych metod.

Magdalena Gewartowska

94

Pracownia Badań Mikroskopowo – Elektronowych
Instytut Medycyny Doświadczalnej i Klinicznej
Im. M. Mossakowskiego PAN
02-106 Warszawa ul. Adolfa Pawińskiego 5

Dr hab. Małgorzata Frontczak-Baniewicz
E-mail: mbaniewicz@imdik.pan.pl

Warszawa, 03.01.2023

Oświadczenie współautora

Niniejszym poświadczam swój wkład w powstanie następującej publikacji:

Kawalec M, Wojtyniak P, Bielska E, Lewczuk A, Boratyńska-Jasińska A, Beręsewicz-Haller M, Frontczak-Baniewicz M, Gewartowska M, Zabłocka B. Mitochondrial dynamics, elimination and biogenesis during post-ischemic recovery in ischemia-resistant and ischemia-vulnerable gerbil hippocampal regions. Biochim Biophys Acta Mol Basis Dis. 2022 Dec 22:166633. doi: 10.1016/j.bbadis.2022.166633

Wkład obejmuje:
Analizę zdjęć TEM.

Małgorzata Frontczak-Baniewicz

95

Pracownia Biologii Molekularnej
Instytut Medycyny Doświadczalnej i Klinicznej
Im. M. Mossakowskiego PAN
02-106 Warszawa ul. Adolfa Pawińskiego 5

Mgr Karolina Serwach
E-mail: kserwach@imdik.pan.pl

Warszawa, 29.12.2022

Oświadczenie współautora

Niniejszym poświadczam swój wkład w powstanie następującej publikacji:

Wojtyniak P., Boratynska-Jasinska A., Serwach K., Gruszczynska-Biegala J., Zablocka B., Jaworski J., Kawalec K. Mitofusin 2 Integrates Mitochondrial Network Remodelling, Mitophagy and Renewal of Respiratory Chain Proteins in Neurons after Oxygen and Glucose Deprivation. Mol Neurobiol 59, 6502–6518 (2022). doi: 10.1007/s12035-022-02981-6

Wkład obejmuje:
Uśmiercanie zwierząt i izolacja kory mózgu z embrionów. Zgłaszanie uwag do manuskryptu.

Karolina Serwach

Pracownia Biologii Molekularnej
Instytut Medycyny Doświadczalnej i Klinicznej
Im. M. Mossakowskiego PAN
02-106 Warszawa ul. Adolfa Pawińskiego 5

Dr hab. Joanna Gruszczyńska-Biegała
E-mail: jgruszczynska@imdik.pan.pl

Warszawa, 19.10.2022
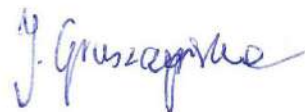
Oświadczenie współautora

Niniejszym poświadczam swój wkład w powstanie następującej publikacji:

Wojtyniak P., Boratynska-Jasinska A., Serwach K., Gruszczynska-Biegala J., Zablocka B., Jaworski J., Kawalec K. Mitofusin 2 Integrates Mitochondrial Network Remodelling, Mitophagy and Renewal of Respiratory Chain Proteins in Neurons after Oxygen and Glucose Deprivation. Mol Neurobiol 59, 6502–6518 (2022). https://doi.org/10.1007/s12035-022-02981-6.

Wkład obejmuje:

Użyczenie: plazmidów do konstrukcji wektorów lentiwirusowych, linii komórek HEK 293T, bakterii TOP10 E. coli, protokołów doświadczalnych. Zgłaszanie uwag do manuskryptu.

Joanna Gruszczyńska-Biegała

97

Laboratorium Neurobiologii Molekularnej i Komórkowej
Międzynarodowy Instytut Biologii
Molekularnej i Komórkowej
02-109 Warszawa ul. Ks. Trojdena 3

Prof. dr hab. Jacek Jaworski
E-mail: jaworski@iimcb.gov.pl

Warszawa, 12.12.2022

Oświadczenie współautora

Niniejszym poświadczam swój wkład w powstanie następującej publikacji:

Wojtyniak P., Boratynska-Jasinska A., Serwach K., Gruszczynska-Biegala J., Zablocka B., Jaworski J., Kawalec K. Mitofusin 2 Integrates Mitochondrial Network Remodelling, Mitophagy and Renewal of Respiratory Chain Proteins in Neurons after Oxygen and Glucose Deprivation. Mol Neurobiol 59, 6502–6518 (2022). https://doi.org/10.1007/s12035-022-02981-6.

Wkład obejmuje:

Konsultacje metodyczne i merytoryczne oraz udział w przygotowaniu manuskryptu.

Jacek Jaworski